MECHANICAL AND MICROSCOPIC INVESTIGATION OF WHISKER-REINFORCED SILICONE RUBBER

by

© Mark Weber

A thesis submitted to the Faculty of Graduate Studies in partial fulfillment of the requirements for the degree of Master of Engineering

Department of Chemical Engineering
McGill University
Montreal, Canada

September, 1989

MECHANICAL AND MICROSCOPIC INVESTIGATION OF SILICONE RUBBER

ABSTRACT

The fiber orientation and mechanical properties of a Franklin Fiber whisker reinforced silicone rubber were studied. The composites were molded using both transfer and compression molding. Processing parameters, such as sprue design, milling procedure, and mold temperature were varied to determine their effects on the orientation of the fibers and the tensile properties of the composite.

A novel image analysis system is used to determine fiber orientation. The fiber orientation is anisotropic and independent of sprue design and temperature, but dependent on the milling procedure. The tensile strength and elongation at break are isotropic for each composite, while the Young's modulus and tensile set are affected by fiber orientation. All properties are temperature dependent. The experimental Young's moduli do not show agreement with theoretical predictions.

RESUME

L'orientation des fibres et les propriétés mécaniques d'un caoutchouc silicone, renforcé avec des fibres Franklin Fiber, ont été étudiés. Les composites ont été fabriques en utilisant le moulage par transfert et le moulage par compression. Les paramètres du proces, comme la conception des carottes, le procédé de mélangeage sur rouleaux, et la température ont été variés pour déterminer leur effet sur l'orientation des fibres et les propriétés en tension.

Un nouveau systeme d'analyse est utilisé pour déterminer l'orientation des fibres. L'orientation est anisotrope et indépendante de la conception des carottes et de la température, mais dépendante sur le procédé de mélangeage sur rouleaux. La résistance à la traction et l'allongement à la rupture sont isotropes pour chaque composite, mais le module d'Young et le recouvrement élastique sont affectés par l'orientation des fibres. Une élévation de température cause une réduction des propriétés en tension. Les résultats pour le module d'Young ne concordent pas avec les prédictions théoriques.

ACKNOWLEDGEMENTS

I would like to express my gratitude to my research supervisor, Prof. M.R. Kamal, for his guidance, support, and encouragement throughout this project.

In addition, I wish to thank:

- The Lord Corporation for their financial support and supply of materials and equipment used in this work, and especially Dr. K.K. Tay of Lord for his invaluable help and guidance.
- The machine shop personnel, both at McGill and at Lord, for the construction of several pieces of equipment used in the project.
- Dr. A. Turgut Mutel for his tremendous assistance and inspiration in all phases of the project, particularly with the computer programming.
- Mr. Guenter Lohfink for his helpful discussions on the theory of rubber and his photographic assistance.
- Messrs. Bryn Hird and Dimitri Kolovos for their performance of some of the experimental work.
- Messrs. Philip Bates, Taras Broadhead, Patrick Brousseau, Burke Nelson, and Tony Samurkas for their friendship.
- The Chemical Engineering Department, NSERC, and the Ministere de l'Education, Gouvernement du Quebec, for their financial assistance.
- My parents and family for being there.
- Miss Christine Bryce for her encouragement, support, and friendship.

TABLE OF CONTENTS

LIST OF FIGURES

LIST OF TABLES

1. INTRODUCTION

Reinforced rubber composites are of interest due to their combination of the elasticity of the rubber and the strength and stiffness of the reinforcement. These composites find use as automobile parts, tires, belts, hoses, and footwear. The reinforcement is either continuous cords, particulate fillers, or short fibers. Some background on both rubber and reinforcement will be given in this section.

1.1. Rubber

According to Flory (1), a rubber is capable of sustaining large deformations without rupture and of recovering spontaneously to very nearly its original dimensions after removal of the applied stress. Rubber consists of long polymer chains which normally exhibit a random configuration. When stress is applied, the chains change their configuration to accomodate the deformation. Rubber also exhibits a network structure which consists of physical and chemical crosslinks. The physical crosslinks are not permanent and allow chain slippage. The chemical crosslinks are a result of vulcanization, which leads to the formation of a permanent network structure. This structure contributes to rubber elasticity and to the tendency of rubber to recover its shape after deformation (2).

Many types of rubber are used as the matrix component in the composite system. The material of interest in this work is silicone rubber. Warrick et al. (3) have written an extensive review of silicone rubber, its composition, vulcanization, reinforcement, analysis, properties, and uses. The relevent properties of silicone rubber are discussed below.

1.1.1. Silicone Rubber (4)

Silicone rubber exhibits good thermal stability, resistance to ozone attack, and excellent flexibility. These properties are mainly due to its molecular structure, which is compared to the structure of natural rubber in Figure 1.1. Natural rubber has a backbone of carbon-carbon linkages, whereas the backbone of the silicone rubber consists of silicon-oxygen bonds. This silicon-oxygen bond is also found in materials such as quartz, glass, and sand, and gives the rubber its thermal stability. The organic side-chains, methyl groups in this case, provide the excellent flexibility found in silicone rubber. This type of silicone rubber with methyl side chains is designated MQ by the American Society for Testing and Materials (ASTM).

Natural rubber also contains double bonds within the backbone, whereas the silicon rubber backbone consists solely of single bonds. These sites of unsaturation in the natural rubber are susceptible to ozone attack, which can occur due to the

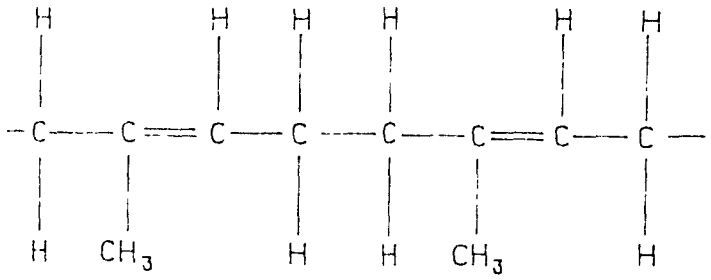

Natural Rubber

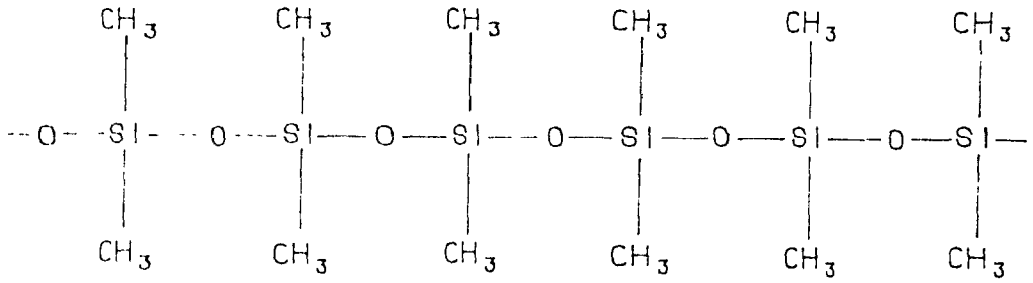

Silicone Rubber (MQ Type)

Figure 1.1. Comparison Between Natural and Silicone Rubber Structures.

environment or electrical fields. Since there are no double bonds in the silicone rubber chain, this rubber is extremely resistant to ozone.

Silicone rubber is known to contain a high free volume fraction and its crosslinked network is found to be relatively weak (3). Therefore, silicone polymers respond dramatically to reinforcement. For many commercial applications, the reinforcement of silicone rubber is a necessity.

1.2. Reinforcement

The reinforcement of both thermoplastics and rubber results in mechanical and thermal property improvement. Rubber possesses a low modulus and high elasticity, and these properties give rubber an advantage over thermoplastics in many instances. However, certain rubber applications require greater stiffness and less elasticity. Therefore, the rubber is reinforced to achieve these properties. Continuous cords, particulate fillers, and short fibers are commonly used as reinforcement.

The tensile modulus, tear strength, and compression set are all increased with the addition of either particulate fillers or short fibers. The tensile strength and elongation at break are enhanced by the addition of particulate filler, whereas the addition of short fibers has a detrimental effect on both

of these properties. The decrease in strength with short fiber reinforcement occurs due to the reduction in elongation at break, in spite of the substantial increase in tensile modulus. Short fiber composites are anisotropic, due to the anisotropic nature of the fibers, resulting in mechanical properties which are dependent on the orientation of the fibers. The properties are improved to a greater degree when the fibers are aligned in the test direction, rather than transverse to testing, although property enhancement is still realized in the transverse direction. Tables 1.1 (5) and 1.2 (6) demonstrate the effect of reinforcing natural rubber with particulate fillers and short fibers, respectively.

As mentioned previously, there exist three main types of rubber reinforcement. They are continuous cords, particulate fillers, and short fibers. Each is discussed in some detail below.

1.2.1. Continuous Cord Reinforcement

Continuous cords have been used extensively as a reinforcement, particularly for tires. Continuous cords absorb the loads applied to the composite efficiently, and the composite retains its flexibility, especially in the direction normal to the fibers, because the reinforcement does not alter the rubber properties on a microscopic scale. The cords can also be placed into any desired orientation pattern,

Table 1.1. The Reinforcement of Natural Rubber with Particulate Silica.

Silica, phr	0	20
Tensile strength, MPa	1.6	21.9
Modulus 300%, MPa	-	2.7
Elongation at break, %	230	640
Tear strength, kN/m	35.3	46.0
Compression set, %	35	42

Table 1.2. The Reinforcement of Natural Rubber with Silk Fiber.

Silk fiber, phr	Fiber orientation	0	20
Tensile strength, MPa	L	21.98	11.70
	T	21.21	6.99
Modulus 5%, MPa	L	0.10	2.35
	T	0.10	0.55
Elongation at break, %	L	660	30
	T	650	320
Tear strength, kN/m	L	31.1	57.5
	T	31.4	60.2
Compression set, %	L	38	63
	T	38	62

L = Longitude direction
T = Transverse direction

so as to optimize mechanical properties. Though continuous cords increase the strength and modulus, they impart significant anisotropy to the composite. This must be taken into account when using continuous cords as a reinforcement.

1.2.2. Particulate Fillers

The mechanical properties of rubber can be improved by the addition of particulate fillers, such as carbon black or silica. The fillers redistribute the stresses and form crosslinks via filler-elastomer bonds, thus causing increases in modulus and strength. Since fillers are essentially spherical, the filler-rubber composite is much more isotropic than either cord-rubber or short fiber-rubber composites. However, it cannot match these other composites in strength and modulus.

1.2.3. Short Fibers

Short fiber composites exhibit properties intermediate between continuous cord and particulate filler composites. Short fiber composites are weaker than continuous fiber composites, but stronger than filler-reinforced rubber (7). Although they are not as strong as cords, they allow easier composite fabrication and improved overall economics. Also, the properties of short fiber-reinforced materials are less anisotropic than cord composites, although not to the extent

of particulate composites (8).

1.2.3.1. Whiskers

There are a multitude of short fibers which have found use in short fiber-rubber composites. Glass, carbon, nylon, cellulose, aramid, and silk fibers are just a few examples. Another type of short fiber reinforcement is the whisker or microfiber. Whiskers are very small, smaller than a normal short fiber, but they possess equal or greater strength. This is due to the fact that whiskers are perfect single crystals and contain fewer defects than short fibers. A whisker would theoretically act as a combination of a particulate filler and a short fiber, giving the strength of a short fiber and the isotropic characteristics of a particulate filler, although a certain degree of anisotropy would still exist. It is this combination of strength and size that makes whiskers an attractive reinforcement for rubber.

2. OBJECTIVES

The present project represents an initial experimental effort to aid in the understanding of the processing and mechanical behavior of microfiber-reinforced rubber composites and to relate this behavior to the state of fiber orientation in the composites. More specifically, the objectives of this project are:

1. To produce composites consisting of silicone rubber and Franklin Fiber whiskers (microfibers) by both transfer and compression molding.
2. To evaluate the feasibility of controlling microfiber orientation by manipulating the sprue design in transfer molding or the milling procedure in compression molding.
3. To develop experimental and image analysis techniques for evaluation of microfiber orientation.
4. To evaluate the relationships between orientation of the microfibers, processing conditions, and mechanical behavior of the composites.

3. LITERATURE REVIEW

3.1. Reinforced Rubber

3.1.1. Theory of Reinforcement

The reinforcement of polymeric materials results in a partition of an applied stress between the matrix and the reinforcement. The properties of the composite can be predicted, given the properties of the constituents, by using theoretical relations. Such relations include the Halpin-Tsai equations (9), which predict the mechanical properties of cord, particulate, and short fiber reinforced polymers. For continuous cord reinforcement, the rule of mixtures applies, and the composite Young's modulus in the longitudinal direction is (10):

$$E_c = E_f \phi_f + E_m \phi_m \qquad (1)$$

where E is the Young's modulus, ϕ is the volume fraction of the specified phase, and c, f, and m refer to the composite, fiber phase, and matrix phase, respectively. In the transverse direction, the composite modulus is (10):

$$E_c = E_m (1 + 2\phi_f) / \phi_m \qquad (2)$$

For these equations, it is assumed that the cords are perfectly aligned, well bonded, regularly spaced, and unidirectional.

For particulate reinforced materials, one composite Young's modulus is predicted by the Halpin-Tsai equation, due to the isotropic nature of particulate fillers. For rigid, spherical, isotropic, and randomly dispersed particles, the predicted composite Young's modulus is (10):

$$E_c = E_m (1 + 2 C \phi_f) / (1 - C \phi_f) \quad (3)$$

where: $C = (E_f / E_m - 1) / (E_f / E_m + 2)$

The composite modulus for short fiber composites can also be predicted using the corresponding Halpin-Tsai equation. The anisotropy of the reinforcing fibers results in a direction-dependent composite modulus. The longitudinal Young's modulus is (10):

$$E_L = E_m (1 + 2 (L/D) n_L \phi_f) / (1 - n_L \phi_f) \quad (4)$$

where: $n_L = (E_f / E_m - 1) / ((E_f / E_m) + 2 (L/D))$

and L/D is the aspect ratio of the fibers. In the transverse direction, the Young's modulus is predicted to be (10):

$$E_T = E_m (1 + 2 n_T \phi_f) / (1 - n_T \phi_f) \quad (5)$$

where: $n_T = (E_f / E_m - 1) / ((E_f / E_m) + 2)$

The assumptions made in deriving the above equations are that the fibers are strongly aligned in the test direction, well bonded, regularly spaced, and have a uniform length.

For well-bonded short fibers strongly oriented in the direction of an applied stress, a tensile stress is generated in the fiber due to shear stresses applied through the matrix.

This transfer of the applied load to the fibers occurs at the fiber ends where the shear stresses are at a maximum. The matrix shear stresses decrease along the length of the fiber and are zero at the midlength. The tensile stresses in the fiber increase along the fiber length, starting from a small value at the end. They are given by the following relation (8):

$$\sigma_f (L) = 2/R \int_0^L \tau(s)\ ds \qquad (6)$$

where L and R are the length and radius of the fiber, respectively, and τ is the local position-dependent shear stress in the matrix. The fiber tensile stresses eventually either reach a peak when the fiber strength is reached, which causes fiber fracture and composite failure, or plateau when the matrix shear deformation becomes zero.

3.1.2. Whisker Composites

Whiskers combine strength and small size to offer good reinforcement and reduced anisotropy. One type of commercially available whiskers is Franklin Fiber. It is a calcium sulfate whisker fiber, available in either an anhydrous or hemi-hydrate form. Franklin Fiber is produced by hydrothermal synthesis, drying, and heating, whereby gypsum is converted to either the hemi-hydrate or anhydrous forms of calcium sulfate as single crystal whisker fibers. A typical chemical analysis of both forms of Franklin Fiber is given in

Table 3.1 (11).

Franklin Fiber whiskers have been used to reinforce plastics and show great promise. Table 3.2 demonstrates the effect of adding 30 % Franklin Fiber (FF) to both polypropylene (PP) and high density polyethylene (HDPE) (11). Improvements to properties under both tension and flexure were realized. Franklin Fibers were also used as a partial replacement for glass fiber. A bulk molding compound, whose composition is given in Table 3.3, was modified by replacing 25 % of the glass fibers with Franklin Fibers (11). As shown in Table 3.4, this modified composite was found to be superior to the 100 % glass fiber composite in tension and in flexure. Franklin Fiber has been found to be most effective when used in conjunction with another type of short fiber.

Although Franklin Fiber has been used to reinforce plastics, there is no published information on the reinforcement of rubber with Franklin Fiber. However, it has been recommended as a potentially advantageous reinforcing material for rubber for certain applications (12), especially when high heat resistance, low thermal conductivity, improved surface texture, lower cost, and improved fatigue and flex life are desired.

Table 3.1. Typical Chemical Analysis of Franklin Fiber.

Compound	Amount in Anhydrous Form (%)	Amount in Hemi-Hydrate Form (%)
$CaSO_4$	97.68	70-50
$CaSO_4$ -1/2 H_2O	-	30-50
$CaSO_4$ -2 H_2O	-	Negligible
$CaCO_3$ -$MgCO_3$	1.27	1.27
SiO_2 & insolubles	0.13	0.13
Fe_2O_3 & Al_2O_3	0.31	0.31
ph (10% slurry)	10.4	8.2

Table 3.2. The Reinforcement of Polyolefins with Franklin Fiber.

Sample	Tens. Str. (MPa)	Tens. Mod. (MPa)	Flex. Str. (MPa)	Flex. Mod. (MPa)
100% PP	35.7	1.37×10^3	46.9	1.58×10^3
30% FF/70% PP	31.6	2.36×10^3	51.6	3.93×10^3
100% HDPE	22.3	8.69×10^2	25.8	9.79×10^2
30% FF/70% HDPE	18.7	1.50×10^3	28.9	2.13×10^3

PP = Polypropylene
HDPE = High Density Polyethylene

Table 3.3. Composition of a Bulk Molding Compound.

Material	Weight %
Calcium Carbonate	55.0
Polyester Resin	28.1
Glass Fiber	15.6
Zinc Stearate	1.0
Other	0.3

Table 3.4. Replacement of Glass Fiber with Franklin Fiber in a Bulk Molding Compound.

Sample	Tens. Str. (MPa)	Tens. Mod. (MPa)	Flex. Str. (MPa)	Flex. Mod. (MPa)
100% Glass(G)	31.9	4.67×10^3	53.8	8.83×10^3
75% G/25% FF	40.1	5.13×10^3	70.5	9.65×10^3

G = Glass fiber
FF = Franklin Fiber

3.2. Processing and Molding of Rubber Composites

The fabrication of rubber composites is usually achieved by a combination of mixing and molding. For certain molding processes, a milling stage precedes the molding operation. Compression, injection, and transfer molding are all commonly used in the rubber industry, and the fundamental aspects of each of these will be presented in this section.

3.2.1. Compression Molding

Before a rubber composite can be compression molded, it must be roll milled. The milled sheet is then compression molded to the desired shape. The milling stage has a significant impact on the mechanical properties of the composite, due to its effects on orientation and breakage of the fibers. Milling causes uniaxial orientation due to extensional forces in the mill direction. Therefore, the orientation of the fibers in a composite may be increased by increasing the total strain. This may be achieved by decreasing the gap space between the rolls or increasing the thickness of the sheet. Changing the roll speed or increasing the number of passes of the sheet through a constant gap space has no effect (13).

The breakdown of fibers in the milling process has a large effect on the mechanical properties of the composite. The greater the aspect ratio of the fibers, the greater the effect

of the reinforcement. Flexible fibers with good fatigue strength, such as polyamide, undergo little breakdown, and retain a high aspect ratio. However, the flexibility of such fibers makes them difficult to orient. Rigid fibers with poor fatigue properties, such as glass, undergo significant breakdown; however, they can exhibit better orientation because of their rigidity (14).

After milling, the composite sheet is molded. The flow during compression molding can cause a change in the orientation of the fibers from that induced by milling (15). Also, residual stresses can be introduced into the part if complete relaxation of flow stresses is not achieved after closing of the mold (16). Therefore, flow in the mold must be minimized to avoid reorientation of the fibers and to reduce stresses resulting from flow.

3.2.2. Injection and Transfer Molding

Injection and transfer molding are very similar, as, in each case, the rubber is fed under pressure through a sprue into a heated and closed mold cavity. One significant difference between them is in the melting of the material. The melting is achieved in transfer molding solely by the heating of the material. In the injection molding process, both heating and shearing cause melting. The shearing is achieved with the use of a rotating screw. The combination of heating and shearing

is more effective in melting the material, giving injection molding a faster cycle than transfer molding, and reducing cure time considerably. However, the shearing induced by the screw results in increased fiber breakage, as compared to transfer molding.

Both injection and transfer molding cause significant anisotropy, much more than is caused by compression molding. This is due to the substantial flow induced by injection and transfer molding. The flow is non-uniform in injection and transfer molding, resulting in non-uniform fiber orientation and non-uniform mechanical properties. A typical example of the anisotropy in fiber orientation found in injection molded samples is shown in Figure 3.1 for a nylon fiber composite molded with a center gated disk mold (17). The fibers have a circumferential orientation due to compressional flow. As the melt enters the mold, it decelerates, creating a negative velocity gradient. This causes a compression in the radial direction and an extension in the hoop direction, rotating the fibers to create circumferential orientation (18).

3.3. Mechanical Properties of Molded Rubber Composites

The reinforcement of rubber with short fibers typically causes a decrease in elongation at break with an increase in fiber concentration. The initial decrease is nearly logarithmic until a certain fiber loading, after which the elongation at

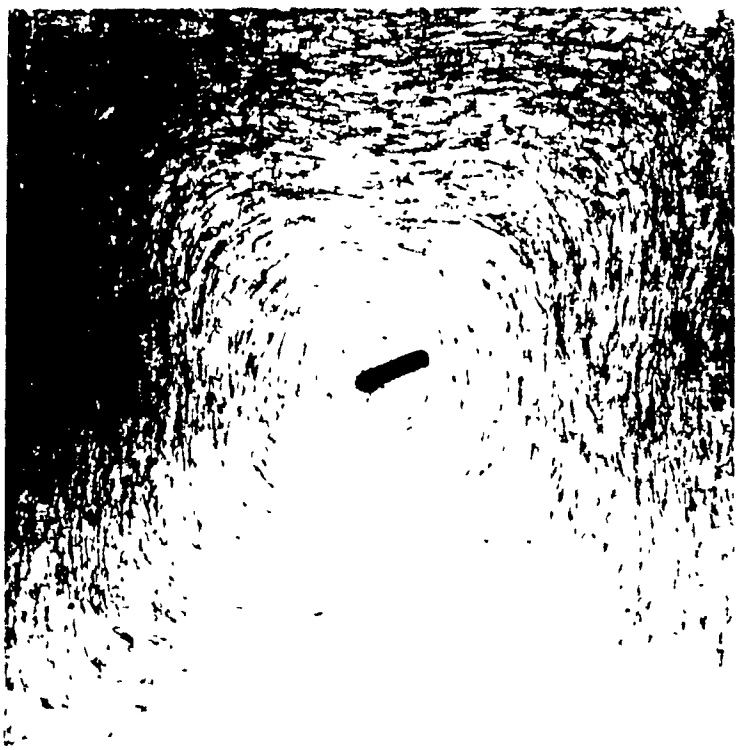

Figure 3.1. Orientation of Nylon Fibers in an Injection Molded Composite.

break decreases slowly, and then plateaus. These observations are shown in Figure 3.2 (19) for a cellulose fiber composite. The Young's modulus is increased as the concentration of fibers is increased. At low fiber loadings the increase is small, but, above some critical point, it increases almost linearly with concentration, as shown in Figure 3.2 (20) for a cellulose fiber composite. The tensile strength of a short fiber-rubber composite is influenced by the combined effect of the elongation at break and Young's modulus, as seen in Figure 3.3 (20) for a cellulose fiber composite. Initially, the sharp decline in elongation at break dominates over the slight increase in Young's modulus, and the tensile strength decreases until some critical concentration. As the fiber concentration is increased beyond this point, its effect on elongation at break decreases, while its relation with Young's modulus still follows an approximately linear increase. The combined effect of these leads to an increase in tensile strength with increasing fiber concentration. In general, the critical fiber concentration needed to obtain an initial increase in tensile strength is approximately 10% fibers by volume. A fiber concentration of at least 25% by volume is needed to achieve composite tensile strength equal to that of the matrix.

The orientation of the fibers in the composite has a significant impact on the mechanical properties. The variation of tensile strength and Young's modulus with fiber

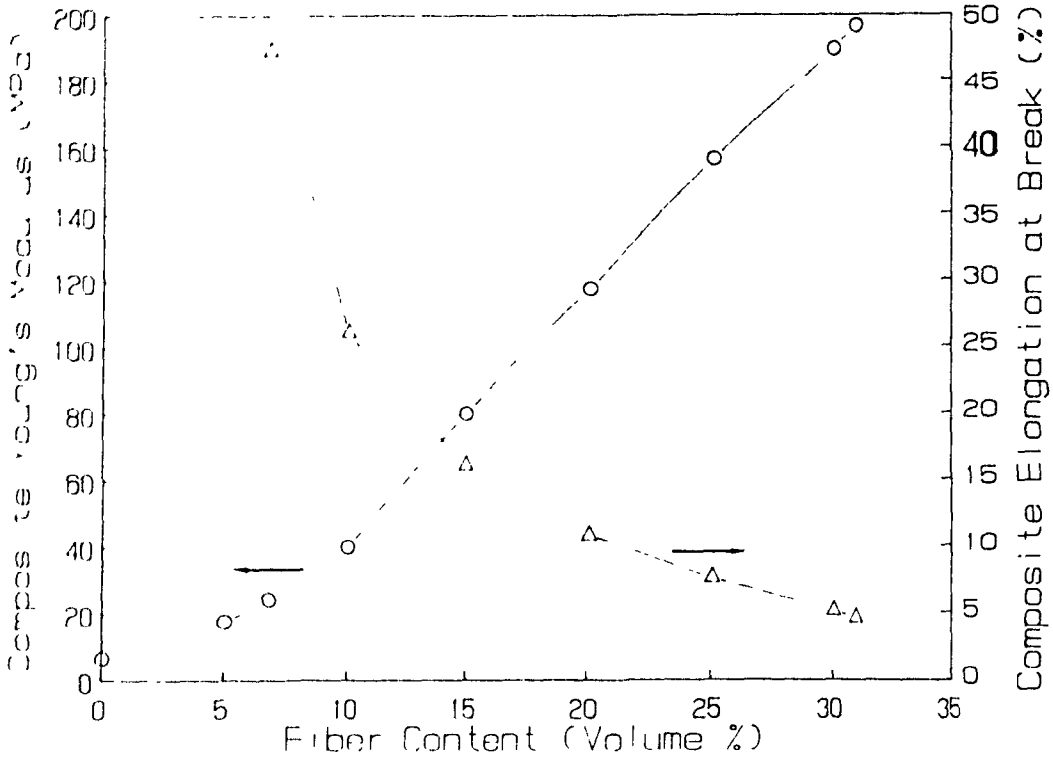

Figure 3.2. Effect of Fiber Concentration on Elongation at Break (Δ) and Young's Modulus (O).

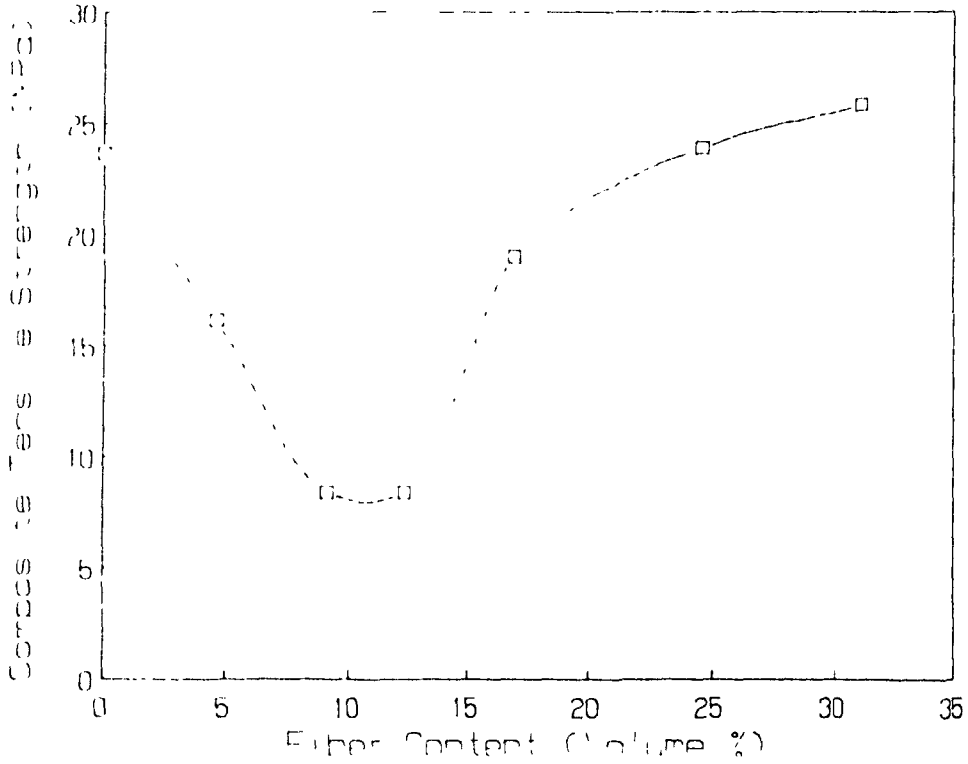

Figure 3.3. Effect of Fiber Concentration on Tensile Strength.

orientation is shown in Figures 3.4 (19) and 3.5 (19), respectively. The tensile strength and Young's modulus achieve their maximum values when the fibers are aligned parallel to the direction of testing. When the fibers are aligned perpendicular to the test direction, the strength and modulus values are at their lowest, since the fibers absorb less of the applied load when they are transversely oriented. When the fibers are aligned at an angle between these two extremes, the tensile modulus of the composite can be calculated using the following relation (21):

$$1/E_\theta = \cos^2 \theta \; / \; E_L \; + \sin^2 \theta \; / \; E_T \qquad (7)$$

where E_θ is the modulus of the composite wherein the fibers deviate from the test direction by the angle θ, E_L the longitudinal (test direction) composite modulus ($\theta = 0°$), and E_T the transverse composite modulus ($\theta = 90°$). Equation (7) is applicable for unidirectional composites. The tensile modulus is very sensitive to orientation, as shown in Figure 3.5, so it is often used as a means of determining anisotropy (22).

The milling stage in compression molding and the flow in injection and transfer molding cause fiber orientation. This results in anisotropic mechanical properties, especially for injection and transfer molded samples due to the strong alignment of the fibers. This anisotropy in mechanical properties is seen even in particulate filler composites, where the reinforcement is isotropic, due to the stretching

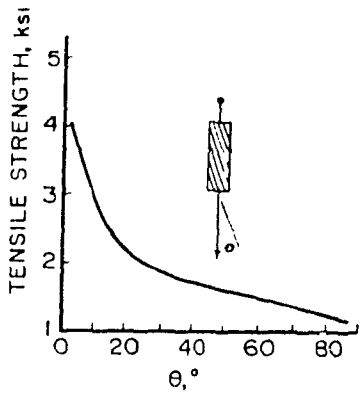

Figure 3.4. Effect of Fiber Orientation on Tensile Strength.

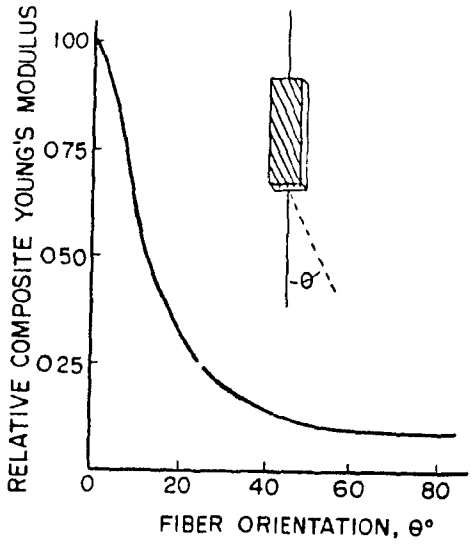

Figure 3.5. Effect of Fiber Orientation on Young's Modulus.

and alignment of the rubber chains (17, 23).

Figures 3.6 and 3.7 compare the effects of injection and compression molding on the 300% modulus and tensile strength, respectively, for a carbon black reinforced rubber (17). The anisotropy was greater for the injection molded samples as expected, although the difference between properties measured along the mold flow lines and transverse to the mold flow lines was only about 15%. The anisotropy is greater for short fiber composites than particulate composites, due to the anisotropy of the short fibers. However, the effect of short fiber orientation on the mechanical properties of injection or transfer molded rubber composites has not been studied extensively.

3.3.1. Effect of Processing Parameters

The processing parameter that has been extensively studied is the molding temperature. The efficiency of the molding process may be improved by increasing the molding temperature, which causes a reduction in the cure time, thereby reducing the cycle time. However, it also causes less efficient cross-linking. Since the time for cross-linking is decreased, fewer crosslinks are formed. When molding at high temperatures, care must be taken to avoid premature vulcanization, or scorch, of the material. When a material is scorched, it contains local strains due to insufficient relaxation time.

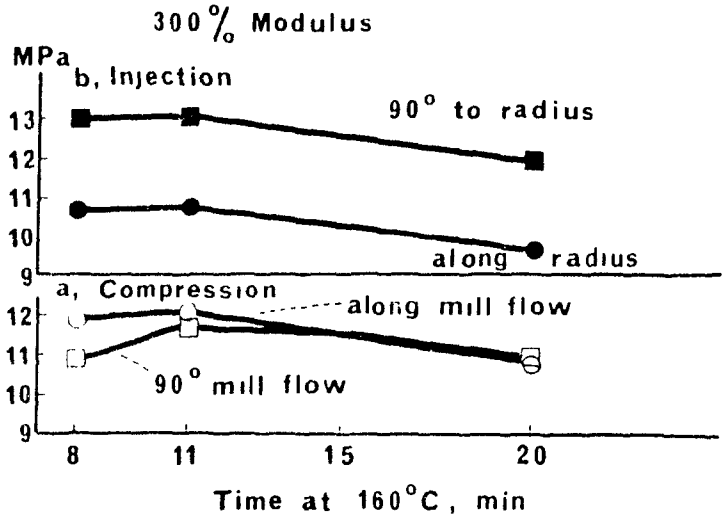

Figure 3.6. Comparison of 300% Modulus for Compression and Injection Molded Carbon Black Composites.

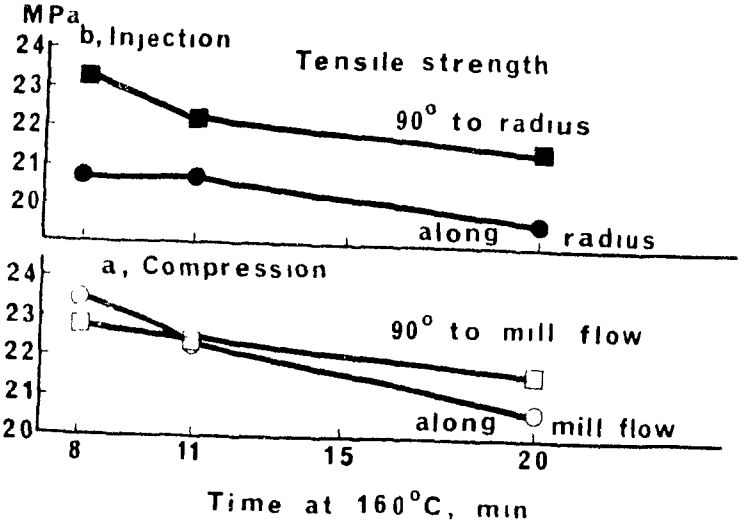

Figure 3.7. Comparison of Tensile Strength for Compression and Injection Molded Carbon Black Composites.

This results in a decrease in the elasticity of the rubber and causes poor mechanical properties.

The effect of an increase in mold temperature on mechanical properties of a carbon black reinforced rubber is shown in Figure 3.8 (17). The properties were rated at a maximum of 100 at 160°C and decreased as the temperature was increased. While the increase in mold temperature caused a decrease in mechanical properties, it did not significantly alter the anisotropy ratios of the injection and compression molded samples.

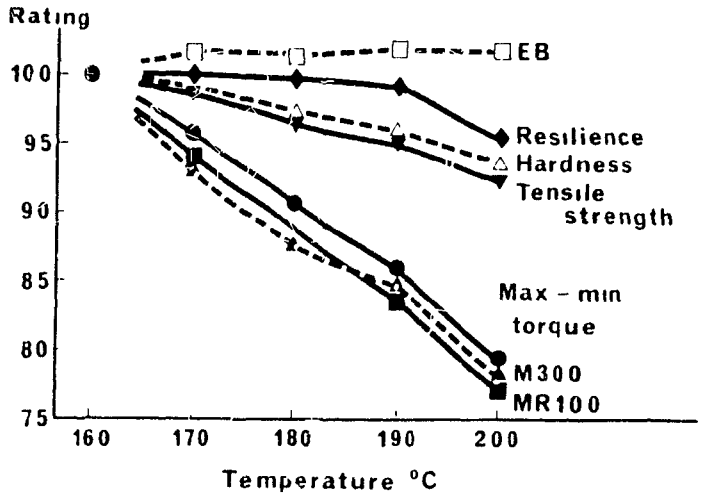

Figure 3.8. Dependence of Composite Physical Properties on Cure Temperature.

EB = Elongation at Break
M300 = 300% Modulus
MR100 = Relaxed Modulus (100%)

4. EXPERIMENTAL

For this project, a silicone rubber-whisker composite was studied to determine the effect of different molding operations and processing parameters on fiber orientation and mechanical properties. The experimental procedure used to accomplish this is given in this section.

4.1. Materials

The materials used in this project were Silastic 35U silicone rubber with methyl-vinyl side chains (VMQ type), manufactured by Dow Corning, and Franklin Fiber whiskers, manufactured by the United States Gypsum Company. The fibers had an aspect ratio of 30 (L = 60 microns, D = 2 microns), as specified by the manufacturer. The physical properties of the unreinforced rubber and the fibers are given in Tables 4.1 (24) and 4.2 (11), respectively. An epoxy silane coupling agent was used to improve the bond between the fibers and the rubber. The composition of the mix is shown in Table 4.3. The original mixing and milling of the rubber and fibers was carried out by the Lord Corporation at their plant in Erie, Pennsylvania. After mixing, the rubber-fiber composite was milled to ensure proper dispersion of the fibers. The mixed and milled composite was then shipped to the Lord Research Center in Cary, North Carolina in twenty kilogram blocks for molding.

Table 4.1. Silicone Rubber Properties.

Rubber	Spec. Gravity at 25°C	Tensile Strength (MPa)	Elongation at Break (%)	Modulus 100% (MPa)	Tear Strength (kN/m)
Silastic 35U	1.13	8.14	800	0.83	19.3

Table 4.2. Franklin Fiber Properties.

Fibers	L (μm)	D (μm)	Aspect Ratio	Spec. Gravity	Tensile Strength (MPa)	Elastic Modulus (MPa)
Franklin	60	2	30	2.96	2.07×10^3	1.79×10^5

Table 4.3. Composite Formulation.

Compound	phr	weight %
Silastic 35U rubber (VMQ type)	100	93.4
Franklin Fibers (anhydrous type)	6	5.6
Dicumyl peroxide (40% dispersion)	1.05	1.0

4.2. Molding Techniques

Two molding techniques were used for this project: transfer molding and compression molding. All molding was carried out at the Lord Research Center using their facilities.

4.2.1. Transfer Molding

An Injectamatic transfer molding machine, manufactured by Hydratecs Inc., was used. The mold was first allowed to heat to the desired temperature, which was measured by a thermocouple located at the outer surface of the mold. When the temperature was reached, a one hundred gram slab of the rubber-fiber mixture which had been cut from the block with scissors was inserted into the transfer pot. The press was closed until the force reached 8.24 - 8.93 MPa (1200 - 1300 psi). The rubber was then cured and a 15 cm x 15 cm (6 in x 6 in) sheet resulted. Miller-Stephenson MS 136 mold release agent was used to ensure that the cured sheet was easily removed from the mold. Ten samples were made for each molding condition.

4.2.1.1. Molding Conditions

The variables which were manipulated in the experiment were the mold temperature and the sprue design. Two different mold temperatures were used: 163°C (325°F) and 204°C (400°F). The

corresponding cure times were 25 minutes and 6 minutes, respectively. Three sprue designs were compared: converging sprues, diverging sprues, and straight sprues. These are shown in Figure 4.1. Molding was carried out at each temperature for the three geometries.

4.2.2. Compression Molding

Before the rubber-fiber mixture could be compression molded, it was milled in order to obtain sheets of approximately 2 mm thickness. The milling was carried out using a Nerpco Inc. roll mill, which was equipped with a Sterltronic temperature controller. For the milling, the roll temperature was 42°C, the front roll speed was 10 rpm, and the back roll speed was 17 rpm. The gap between the rolls was adjusted to approximately 2 mm.

Two procedures were followed in the milling of the samples, in order to obtain sheets with different levels of orientation. In an effort to obtain random fiber orientation, the rubber-fiber mixture was passed through the mill at least five times in the same direction. The sheet was removed from the mill and placed back between the rolls in exactly the same direction as in the previous pass. The sheet was not turned over or reversed, and the mill parameters were kept constant. This was repeated six to eight times per milled sheet. The samples were labelled "random milling". In the second

Converging Sprue

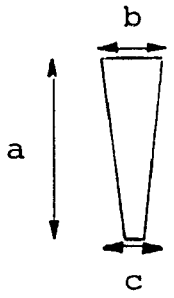

a = 2.38 cm (15/16 in)
b = 0.79 cm (5/16 in)
c = 0.24 cm (3/32 in)

Diverging Sprue

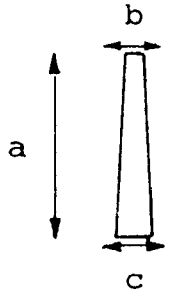

a = 2.38 cm (15/16 in)
b = 0.24 cm (3/32 in)
c = 0.48 cm (3/16 in)

Straight Sprue

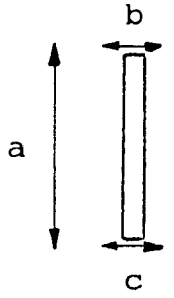

a = 2.38 cm (15/16 in)
b = 0.24 cm (3/32 in)
c = 0.24 cm (3/32 in)

Figure 4.1. Sprue dimensions.

milling procedure, an attempt was made to increase the level of orientation in the milling direction by increasing the strain. The sheet was milled, folded in half, and milled again. This was repeated two to four times per sheet. These samples were labelled "controlled milling".

For the compression molding, a Pasadena Hydraulics Inc. compression molding machine was used. The machine and the mold were heated electrically to the desired temperature which was measured by thermometers placed on the outer surface of the platens. The milled sheets were cut into 15 cm x 15 cm (6 in x 6 in) squares with scissors in order to fit exactly into the mold cavity. Once the temperature was attained, the mold was removed, and a square was placed in the mold cavity. The mold was closed and placed between the platens of the machine. The press was closed and opened three times to ensure that no air was trapped in the mold. Subsequently, the applied weight was increased to 6804 kg (7.5 tons) and the sheet was allowed to cure. A 15 cm x 15 cm (6 in x 6 in) sheet resulted. Ten samples were molded for each condition.

4.2.2.1. Molding Conditions

The variables that were investigated were the molding temperature and the orientation of the fibers, which was described above. Three different temperatures were used: 163°C (325°F), 180°C (356°F), and 204°C (400°F). The

corresponding cure times were 25 minutes, 7 minutes, and 6 minutes, respectively. At each temperature, samples with both controlled and random orientation were molded. Due to time constraints, only the sheets molded at 163°C and 204°C were studied.

4.3. Sample Analysis and Testing

4.3.1. Orientation Analysis

The orientation of the fibers in the molded samples was determined using microtoming and image analysis techniques. Each is discussed in detail in the following sections.

4.3.1.1. Microtome Specimen Preparation

The specimens that were to be microtomed were chosen from several positions in the sample so as to obtain a representative description of the fiber orientation throughout the sample. Figures 4.2 and 4.3 show the locations chosen for analysis of the transfer and compression molded samples, respectively. At each location, sections were cut in three planes: depth, longitude, and transverse. The longitudinal and transverse planes are shown in Figures 4.2 and 4.3, while the depth plane is in the sample thickness direction. The compression molded samples with controlled orientation were milled so as to obtain strong orientation in the mill

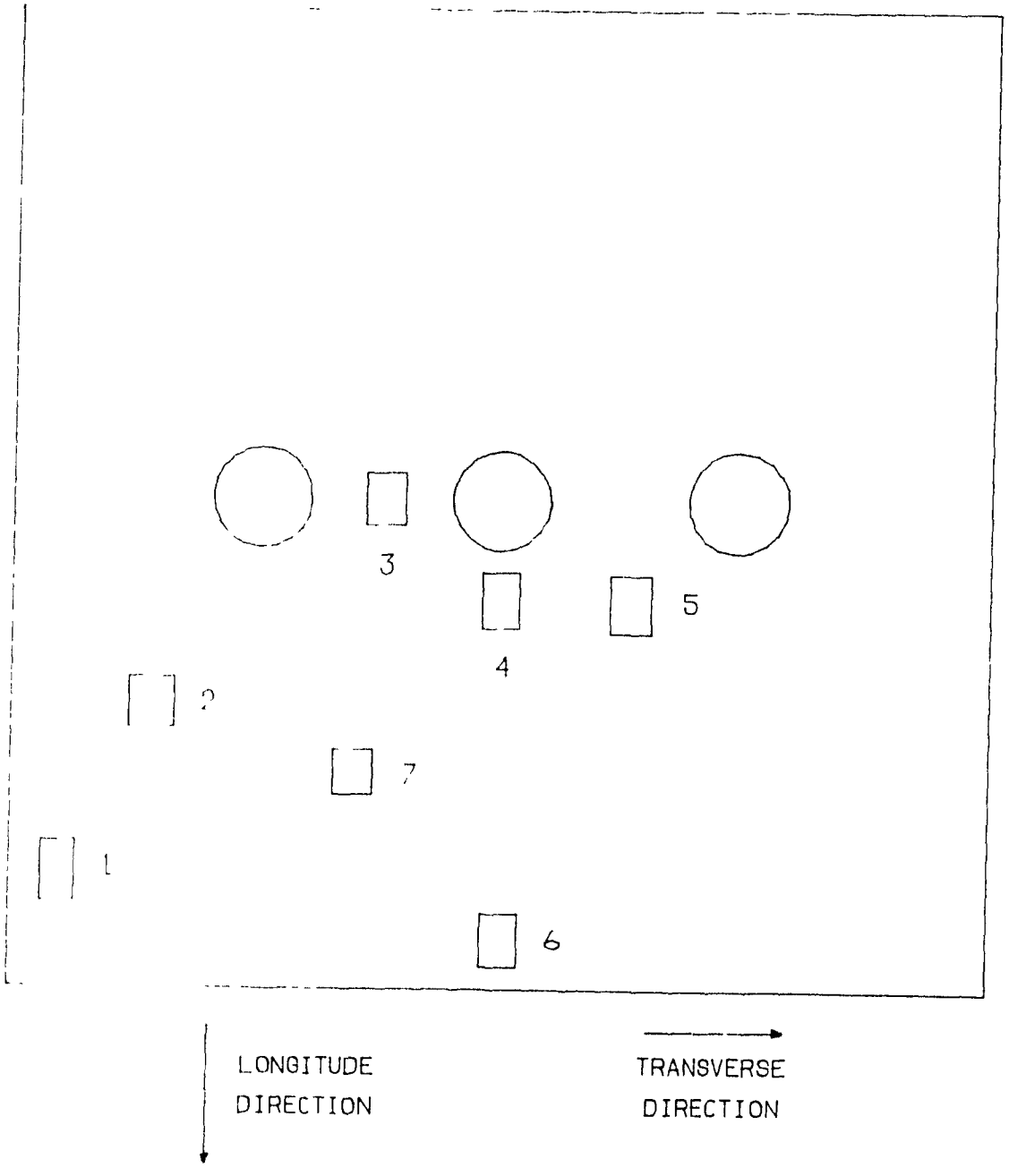

Figure 4.2. Microtome Locations for Transfer Molded Samples.

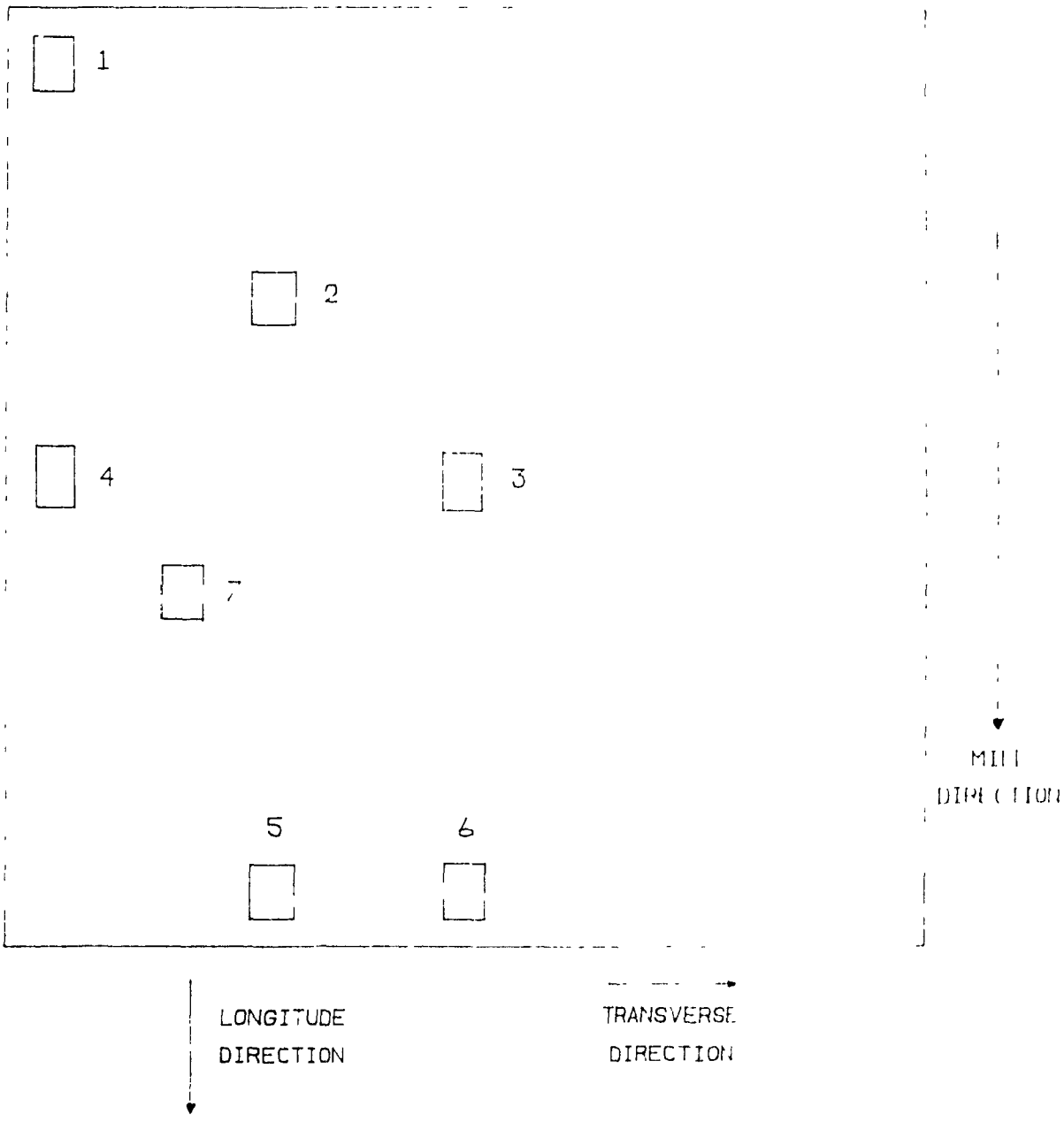

Figure 4.3. Microtome Locations for Compression Molded Samples.

direction. This direction is shown in Figure 4.3.

The sample sheets were placed on a flat surface and the sections were cut using a sharp blade. The sections were approximately 6 mm in length and 3-4 mm in width. The thickness of each cut specimen was measured using a Mitutoyo micrometer and recorded. Once the cutting was completed, the sections were bonded onto black pure gum rubber stoppers. The top and bottom surfaces of the stoppers were roughened with sand paper and cleaned with acetone. One section was bonded onto each surface using Silastic 732 RTV adhesive from Dow Corning. The stoppers were left at ambient conditions for 24 hours to ensure full curing of the adhesive. After this period, the samples were ready for microtoming.

4.3.1.2. Microtoming Procedure

The sections were microtomed using a sliding Reichert microtome, model OmE, and a Lipshaw surgical steel blade. Due to the rubbery nature of the samples, the microtoming was done under cryogenic conditions using liquid nitrogen. The rubber stopper was placed in a 15 cm x 15 cm two-ply sheet of aluminum foil and the foil was folded around the sides of the stopper to encase the stopper and leave only the specimen exposed. This arrangement was placed in the microtome assembly and the holding screw was tightened. The microtome blade was placed in its slot at a set angle of 15° and the

screws tightened. The stopper was then adjusted using the positioning screws so that the top surface of the specimen was parallel to the blade.

After the adjustments were completed, the aluminum foil was folded up so as to enclose the specimen in a "cup". The liquid nitrogen was poured out of a dewer and into the "cup", freezing the specimen. Once the liquid nitrogen evaporated below the upper surface of the specimen, the sides of the "cup" were folded down and the microtome blade was brought forward. After each pass of the blade the height of the specimen was raised by five microns using the dial on the side of the microtome until a slice of the specimen was obtained. The slice was placed on a microscope slide which was wetted with Resolve, a low viscosity microscope immersion oil from Stephens Scientific. The sides of the aluminum foil were folded up again and the process repeated. One slice was obtained per liquid nitrogen application and five slices were placed on each slide. After five slices, a cover glass was placed on the slide and taped down.

For the depth slices, ten layers, beginning at the skin layer and proceeding to the core, were cut in order to obtain as much information as possible about the samples using a reasonable number of slices. Since the samples were approximately 2 mm thick, the distance from skin to core was 1000 microns. The ten layers were therefore approximately

100 microns apart, so after the slices at one layer were obtained, a 100 micron thick section of material was cut off. The slices at the next layer were then microtomed. To ensure that each layer provided one good specimen, two consecutive slices were cut. In total, twenty slices, each with a thickness of 5 microns, were obtained for each microtome location. The thickness of the depth section was measured after microtoming was completed and subtracted from the thickness before microtoming. This figure was then compared to the amount that was assumed to be cut off for each layer to ensure that the thicknesses were as accurate as possible.

4.3.1.3. Image Analysis

The microstructure of the composites was observed and analyzed using an image analysis technique. The microscope slides were placed under a Leitz Laborlux S optical microscope which was equipped with a Sony XC-38 miniature video camera. The image seen by the camera was frame grabbed by a PIP 1024 video digitiser board from Matrox Electronic Systems Ltd. which was loaded into a Hewlett Packard Vectra microcomputer. The image was then displayed on a NEC Multisync monitor and enhanced and thresholded. A computer program was used to locate the fibers and analyze their length and orientation.

The accuracy of this image analysis system was tested by comparing photographs of the image seen through the microscope

with the image captured by the video camera and the digitized representation of the slice. Figure 4.4 shows the strongly oriented microtomed slice as seen through the microscope, Figure 4.5 shows the slice as seen on the video screen, and Figure 4.6 gives the digitized version of the image. There is good agreement between the Figures, demonstrating the accuracy of the image analysis system for a strongly oriented layer. The system was also tested using a section that had random orientation and a large number of fibers. The results are shown in Figures 4.7 through 4.9 in the same sequence as above. Even for a randomly oriented layer with a high concentration of fibers, the system proved accurate.

4.3.2. Tensile Tests

The Instron tensile tester was used to test the tensile strength, elongation at break, Young's modulus, and tensile set of the samples, as per ASTM test D 412-87. This is the standard test method for rubber properties in tension. Dumbbell sections were cut from the samples, but not according to the specifications of ASTM test D 412-87, due to the fact that only a limited amount of material was available for testing and it was desired to obtain as much information as possible.

It was decided to use specimens of the size given in ASTM test D 638-87b, which is the standard test method for tensile

Figure 4.4. Microtomed Slice as Seen Through the Microscope.

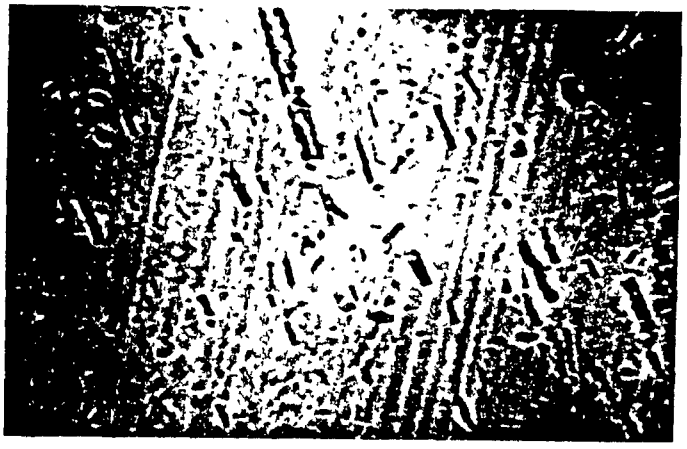

Figure 4.5. Microtomed Slice as Seen on the Video Screen.

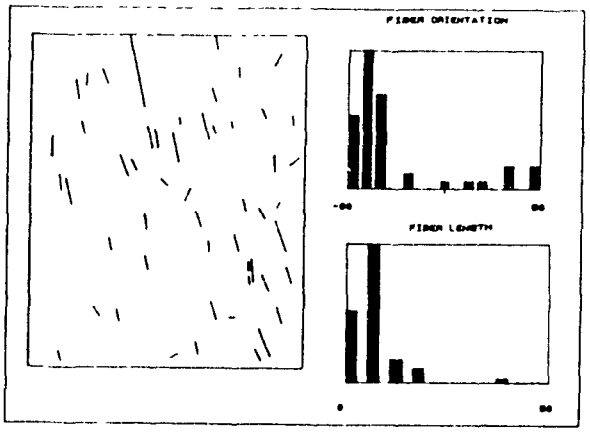

Figure 4.6. Digitized Representation of Microtomed Slice.

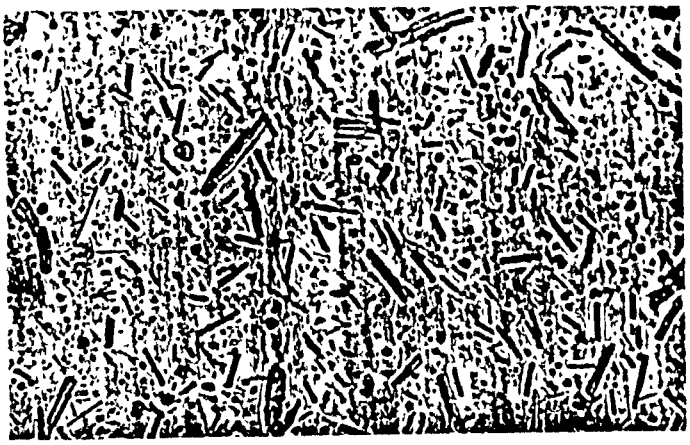

Figure 4.7. Microtomed Slice as Seen Through the Microscope.

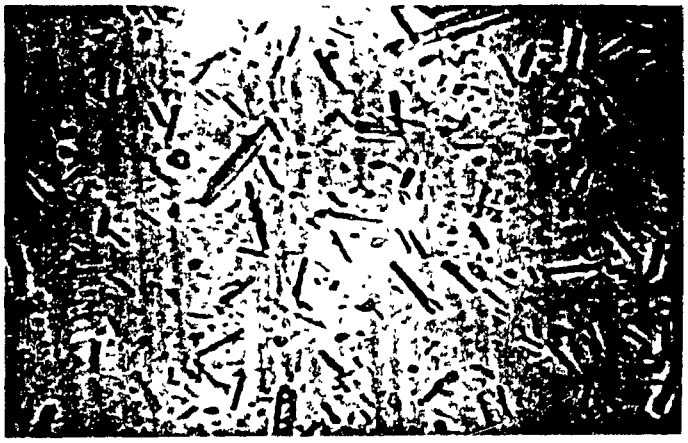

Figure 4.8. Microtomed Slice as Seen on the Video Screen.

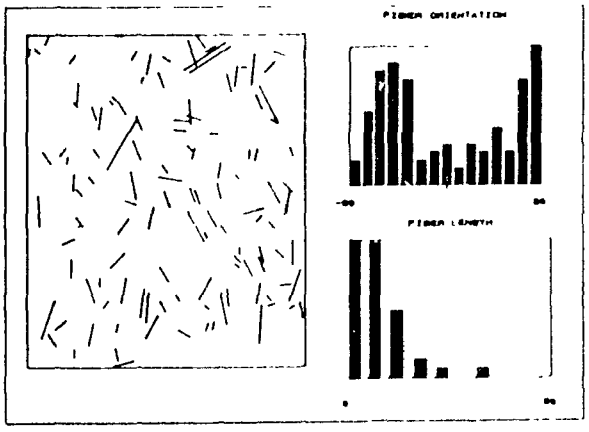

Figure 4.9. Digitized Representation of Microtomed Slice.

properties of plastics. The type V tension test specimen was selected. A sketch of this specimen is given in Figure 4.10. Specimens were cut from the molded samples at several locations, using a type V die made in the departmental workshop.

Testing was carried out as per ASTM D 412-87 using the Instron Mechanical Tester, model 1123. The cut specimens were conditioned at room temperature for at least three hours prior to testing. Test marks were drawn on the samples according to the gage length given in ASTM D 638-87b for die V. The crosshead speed for all tests was 500 mm/min. Pneumatic grips were used to prevent slippage of the sample during stretching. The elongation for the tensile set was 500 %.

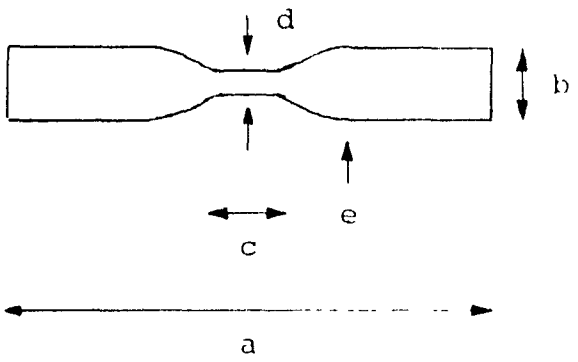

a (overall length) = 63.5 mm (2.5 in)

b (overall width) = 9.53 mm (0.375 in)

c (length of narrow section) = 9.53 mm (0.375 in)

d (width of narrow section) = 3.18 mm (0.125 in)

e (radius of fillet) = 12.7 mm (0.50 in)

Figure 4.10. Dimensions of ASTM D638-87b Die V Tensile Test Die.

5. EXPERIMENTAL RESULTS AND DISCUSSION

5.1. Fiber Orientation and Length Results

The fiber orientation and length distributions were determined by the use of the image analysis computer program. Five depth locations were studied for both the transfer and compression molded samples. These locations included the skin and core layers, as well as three intermediate layers. The three layers were chosen after viewing a longitudinal slice of the sample and noting the levels at which variations in fiber orientation occurred. An orientation function of the form (25):

$$f = 0.5 \left[3 < \cos^2 \theta > - 1 \right] \qquad (8)$$

was calculated for each layer. A value of 1.0 denotes longitudinal fiber orientation, while a value of -0.5 indicates transverse fiber orientation. Random fiber orientation is given by a value of 0.

5.1.1. Transfer Molded Samples

The results for the samples that were transfer molded with converging sprues at 163°C are given in Figures 5.1 through 5.7. These results indicate a circumferential fiber orientation within the sample at the core level. This was expected due to the decrease in velocity as the material travels downstream in the mold cavity. This negative velocity

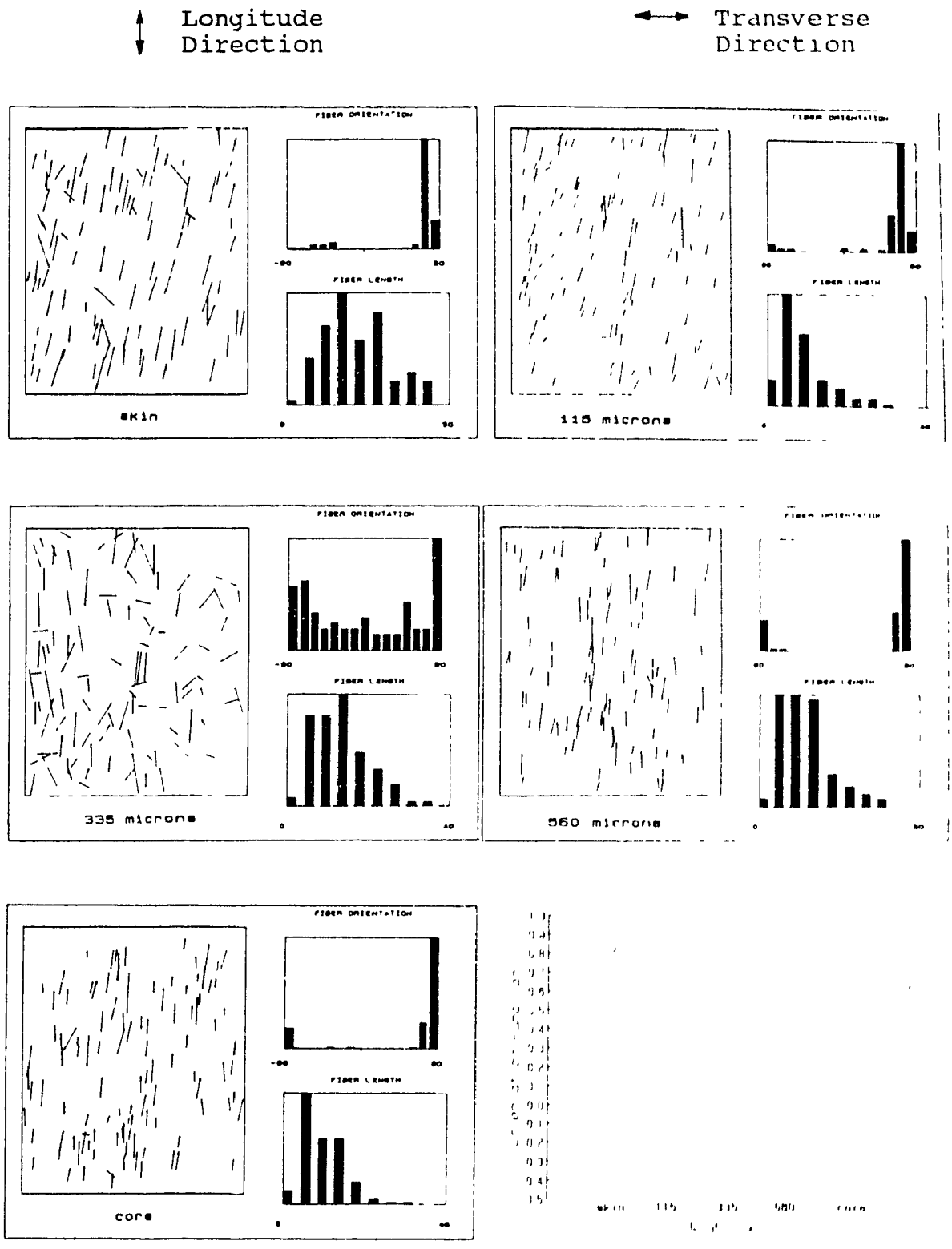

Figure 5.1. Orientation and Length Distributions for Samples Molded with Converging Sprues at 163 C (Microtome Location 1).

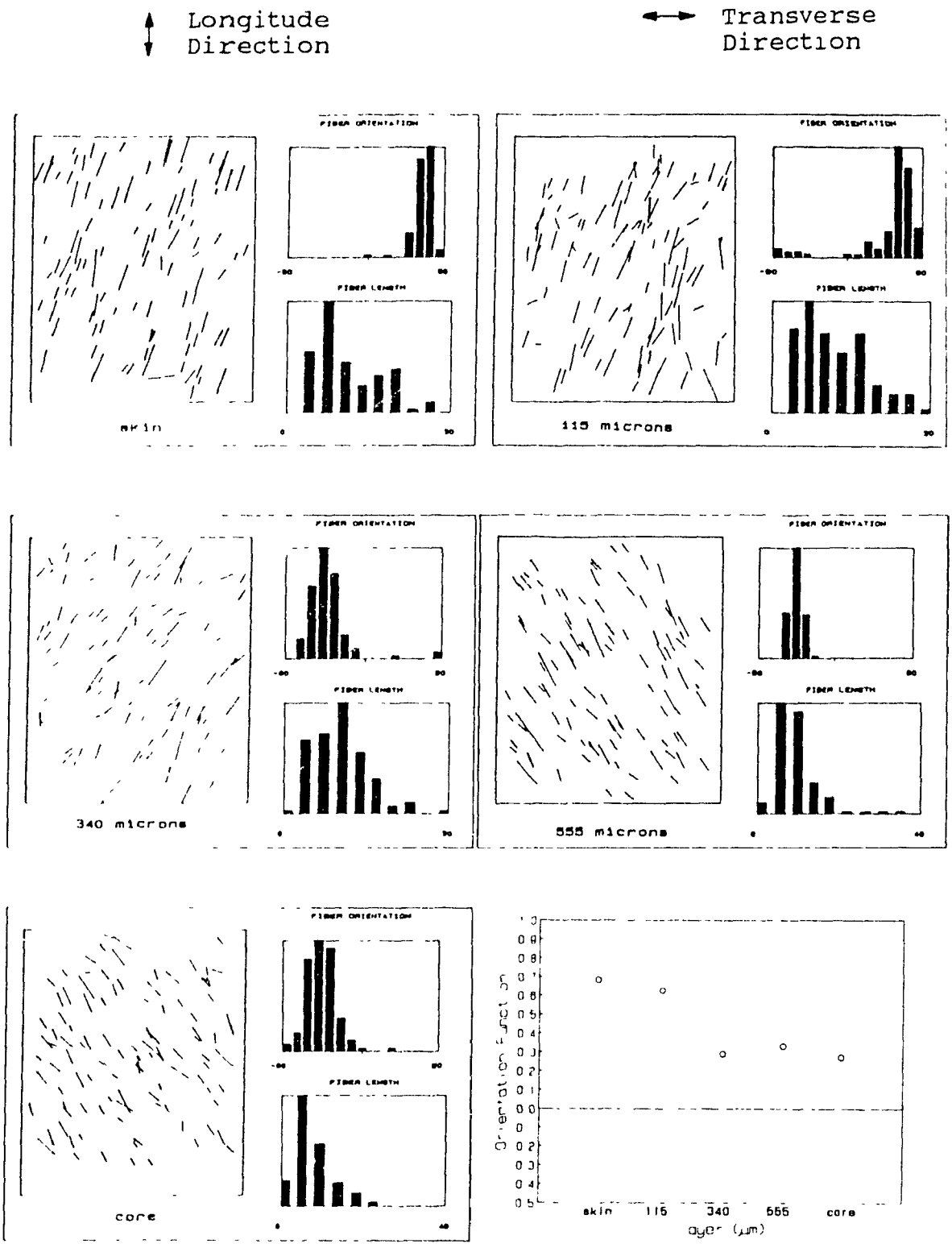

Figure 5.2. Orientation and Length Distributions for Samples Molded with Converging Sprues at 163°C (Microtome Location 2).

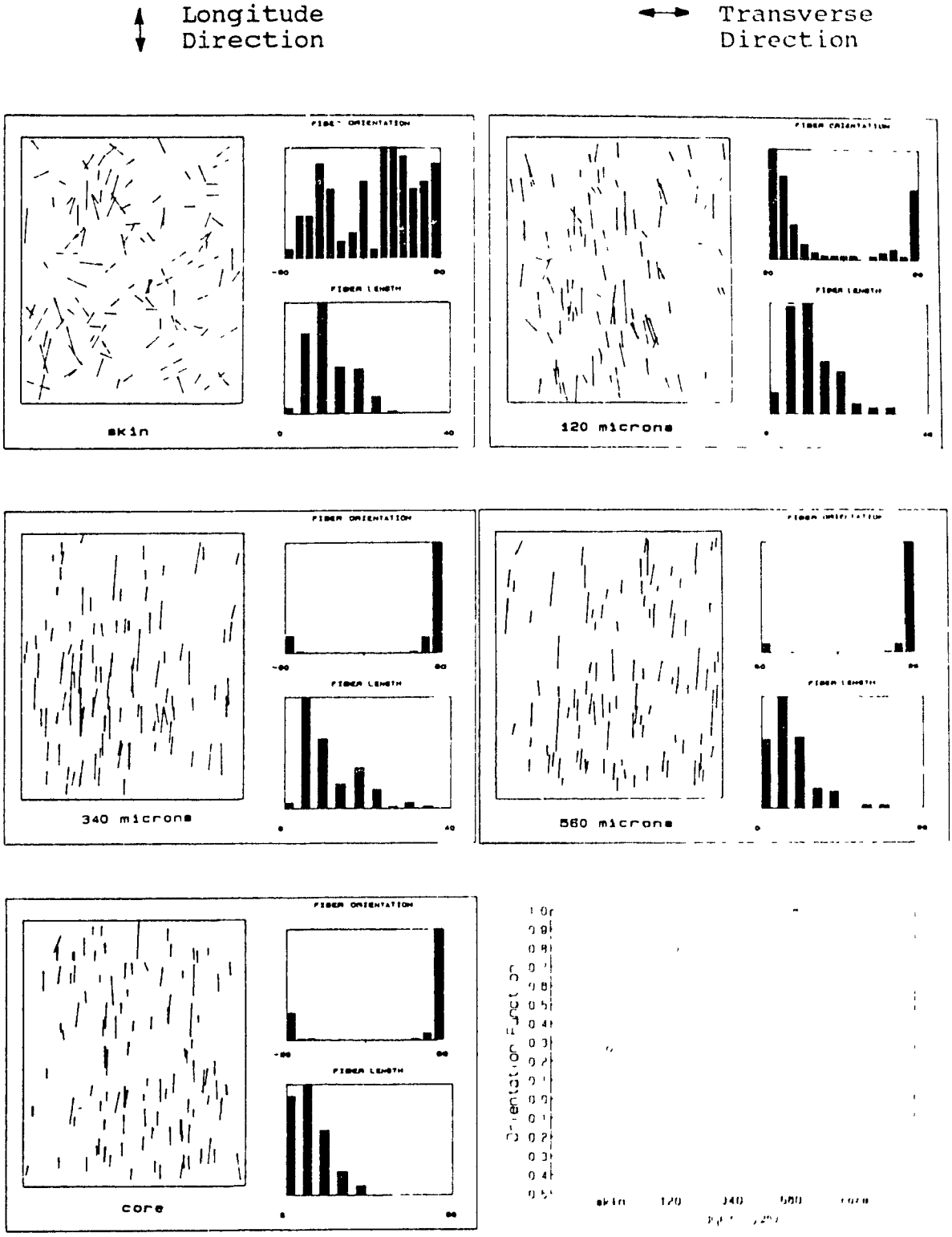

Figure 5.3. Orientation and Length Distributions for Samples Molded with Converging Sprues at 163 C (Microtome Location 3).

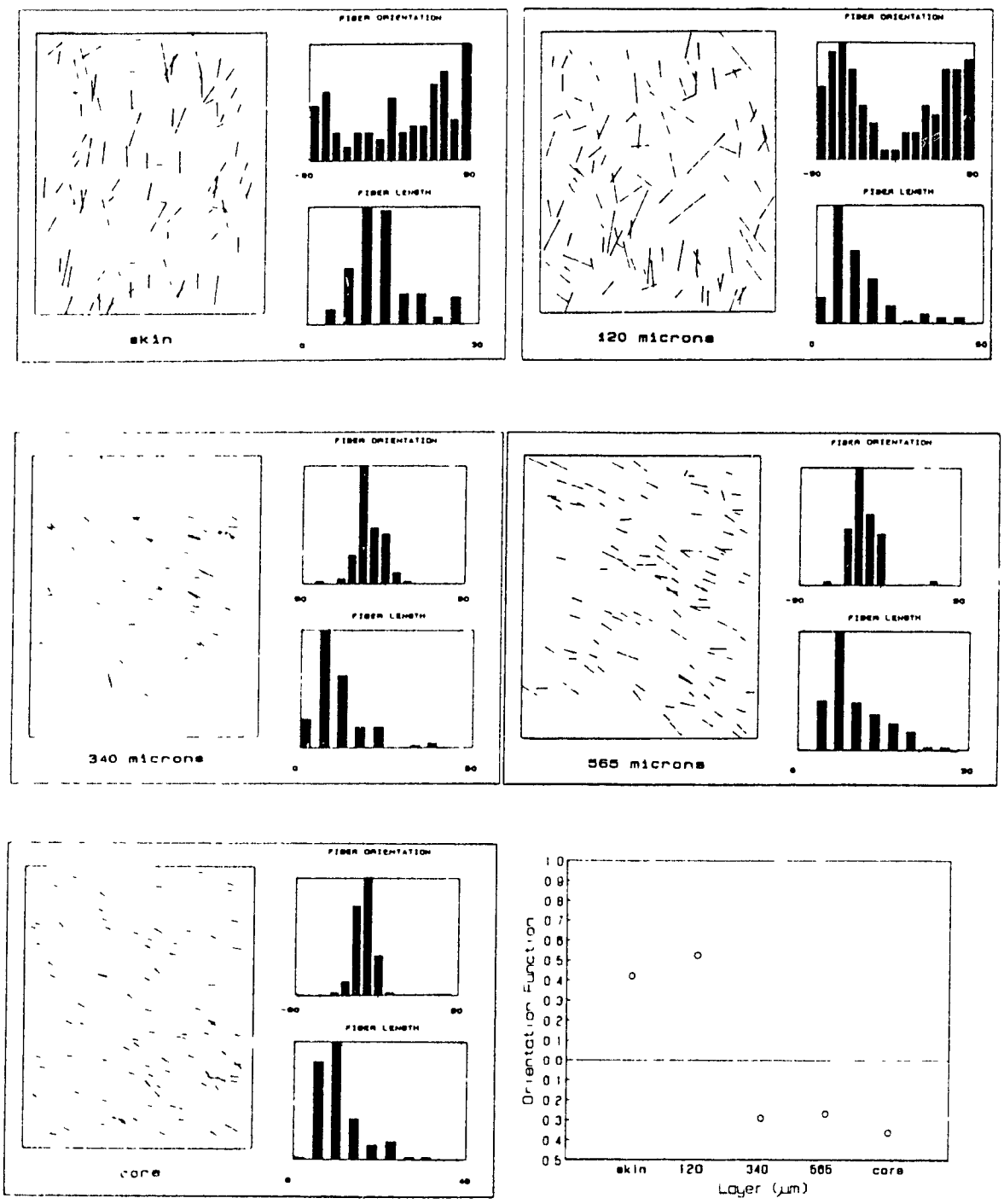

Figure 5.4. Orientation and Length Distributions for Samples Molded with Converging Sprues at 163°C (Microtome Location 4).

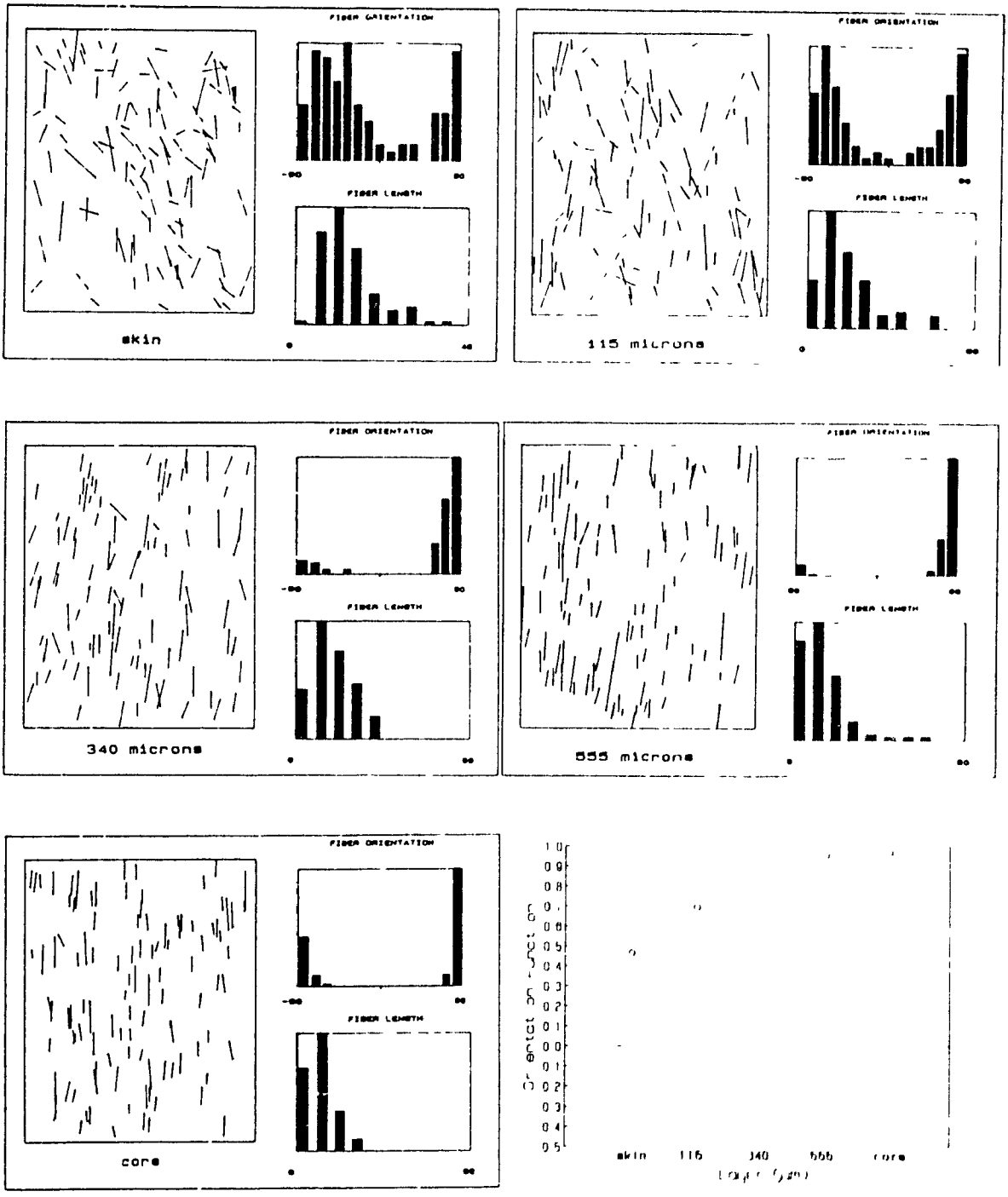

Figure 5.5. Orientation and Length Distributions for Samples Molded with Converging Sprues at 163°C (Microtome Location 5).

Longitude Direction

Transverse Direction

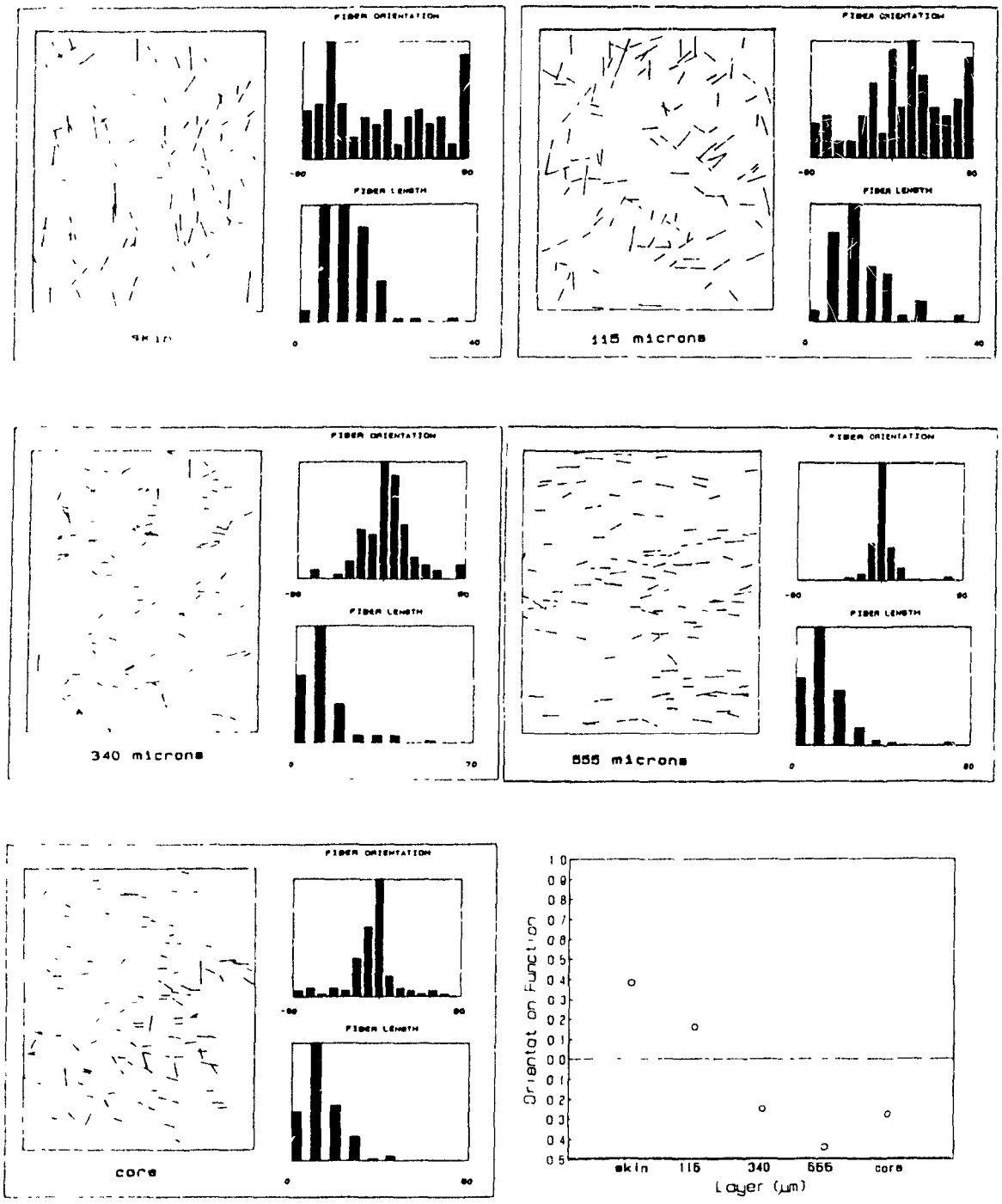

Figure 5.6. Orientation and Length Distributions for Samples Molded with Converging Sprues at 163°C (Microtome Location 6).

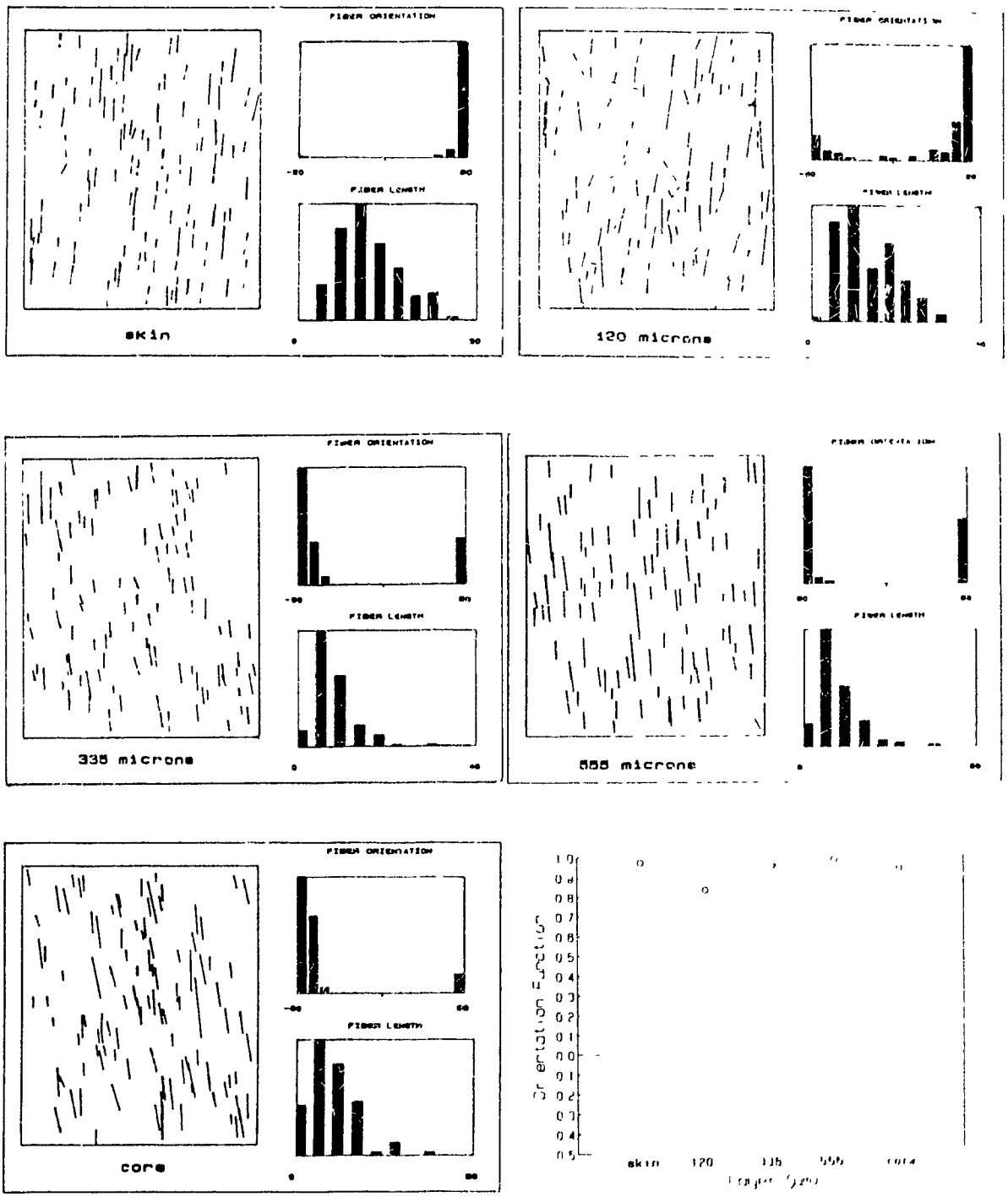

Figure 5.7. Orientation and Length Distributions for Samples Molded with Converging Sprues at 163°C (Microtome Location 7).

gradient causes orientation in the hoop direction (18). As the melt exits the sprue, it has a predominantly random fiber orientation, as shown in the orientation functions given in Figures 5.3, 5.4, and 5.5 for the skin layers. These three locations are nearest the sprue. As the melt moves away from the sprues towards the wall, the fiber orientation of the skin layer becomes stronger. This is seen in Figures 5.2 and 5.7 for the locations intermediate between the sprue and the wall. Microtome location 7 (Figure 5.7) has very strong longitudinal fiber orientation at each layer, due to the fact that this location is near a weldline where two flow fronts with longitudinal fiber orientation meet. As the fibers approach the wall, they assume an orientation parallel to the wall, as seen in Figures 5.1 and 5.6.

As the depth layers approach the core from the skin, the fibers become more oriented, as seen in the orientation function distributions. This is due to the fact that these layers have more time to achieve orientation than the layers near the skin, and are less affected by the shearing and freezing which occur at the mold surface. For virtually all locations, the orientation was constant from approximately 340 microns to the core.

Figures 5.8 to 5.10 show the orientation results for the samples molded at 204°C with converging sprues. The results are similar to those found at 163°C, except that the skin

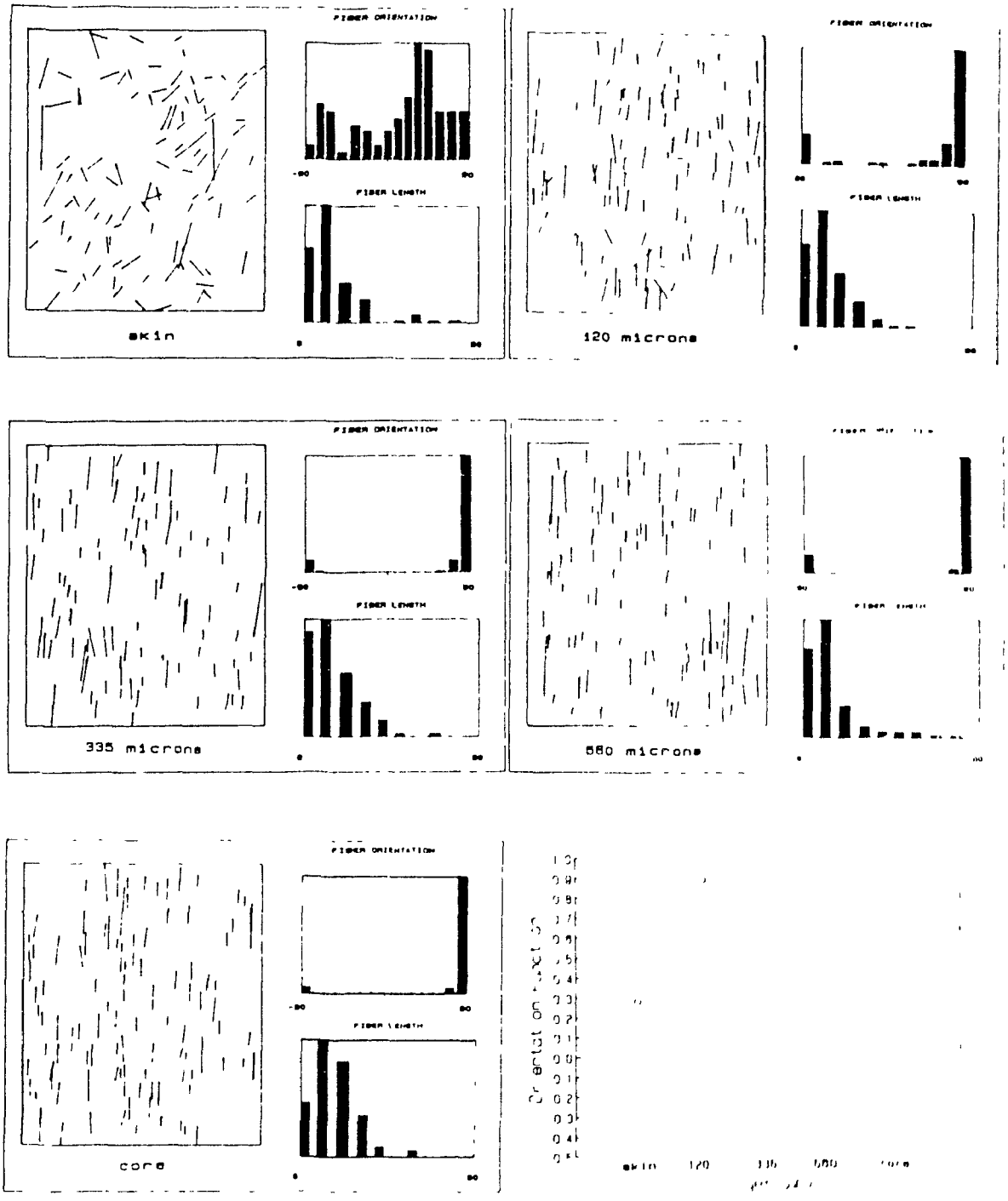

Figure 5.8. Orientation and Length Distributions for Samples Molded with Converging Sprues at 204 C (Microtome Location 3).

Longitude Direction

Transverse Direction

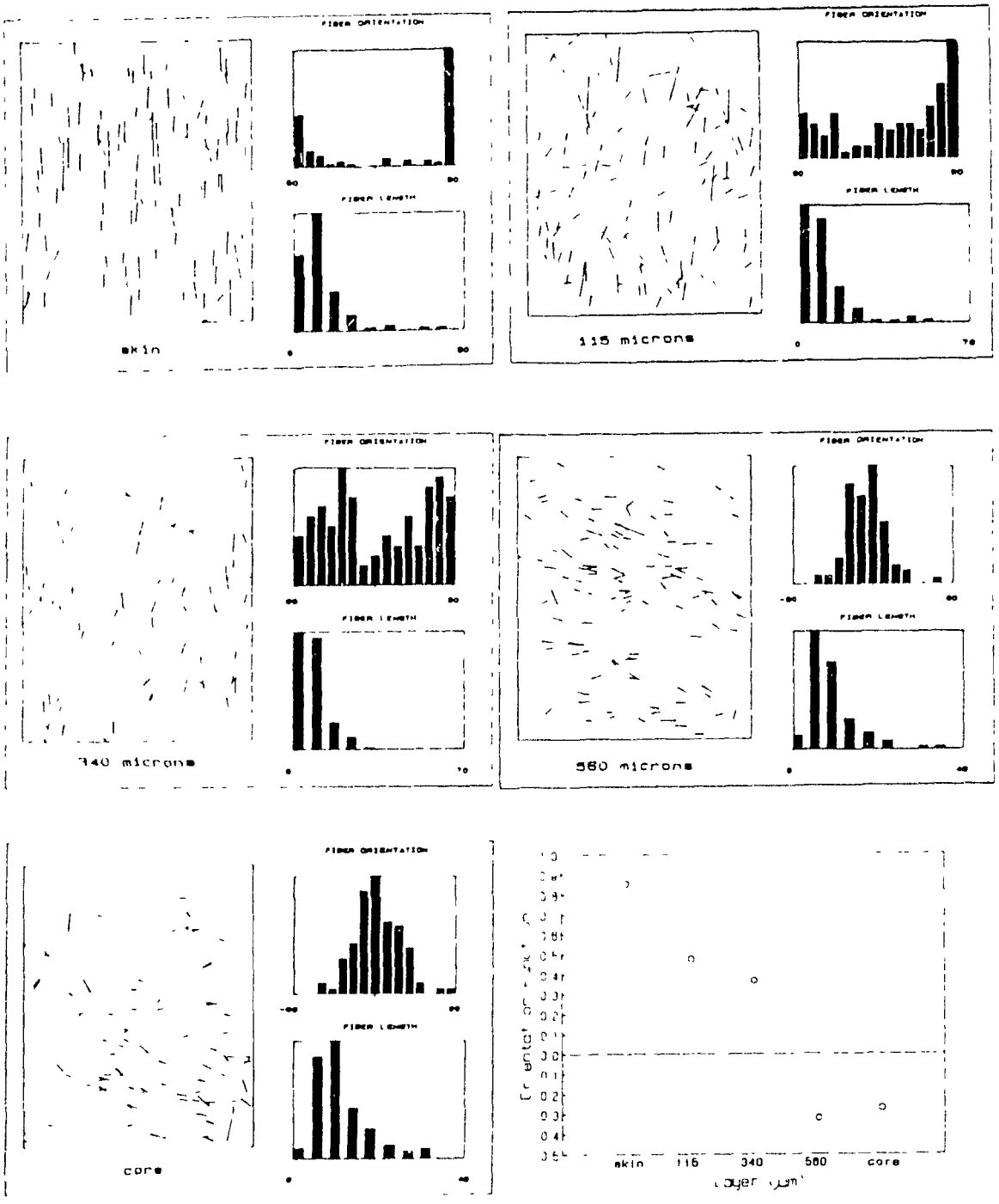

Figure 5.9. Orientation and Length Distributions for Samples Molded with Converging Sprues at 204°C (Microtome Location 4).

Longitude Direction

Transverse Direction

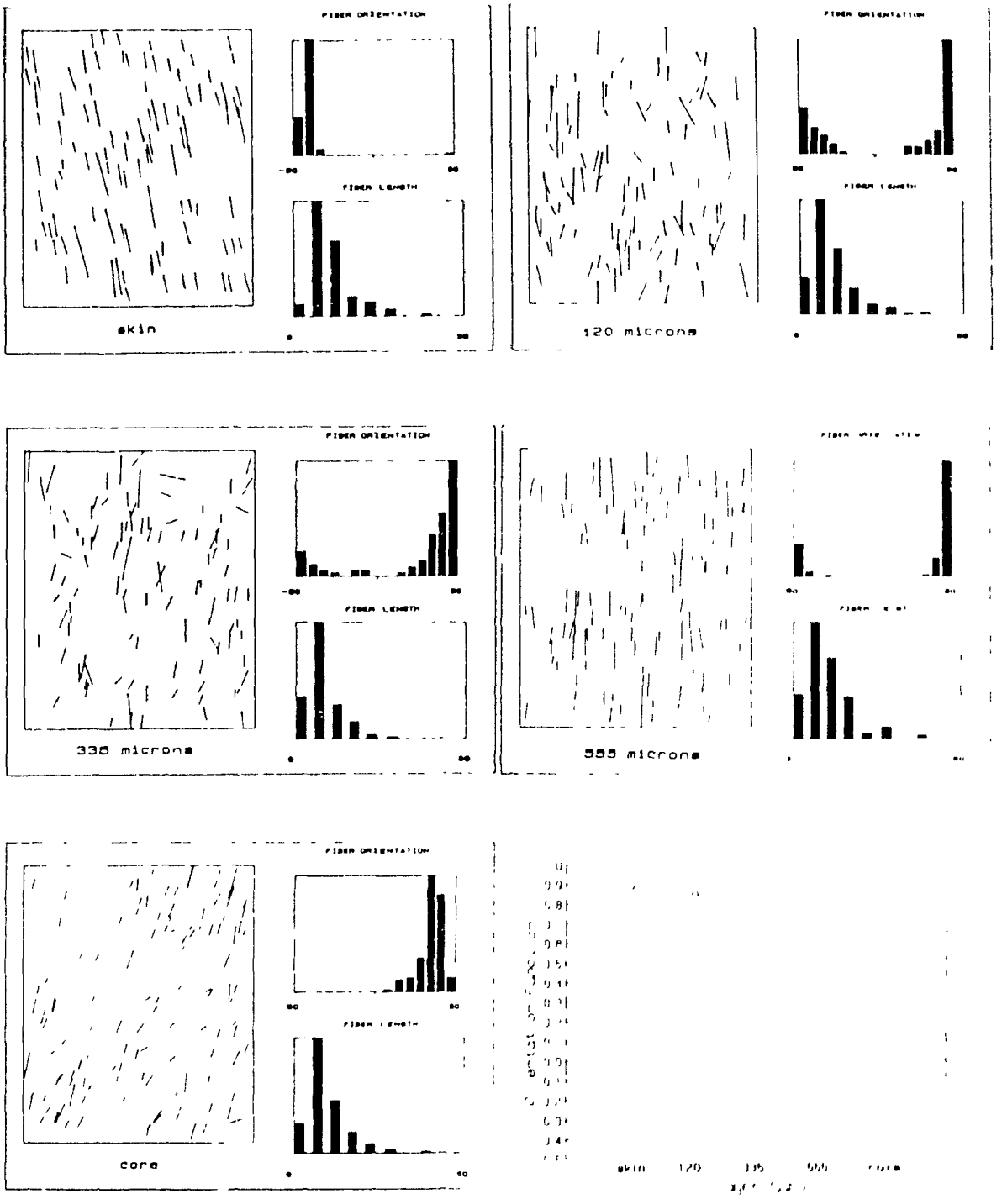

Figure 5.10. Orientation and Length Distributions for Samples Molded with Converging Sprues at 204 C (Microtome Location 5).

layer has much stronger orientation at the higher temperature. The orientation function at the skin layer is very close to 1.0 at microtome locations 4 and 5 (Figures 5.9 and 5.10), due to the fact that the material froze before the orientation induced in the sprues could change into the random configuration seen at 163°C.

The orientation and length distributions for the samples molded with straight sprues are given in Figures 5.11 through 5.13 for a molding temperature of 163°C. The results were similar to those found with converging sprues. The orientation induced in the sprues did not affect the final orientation. This was due to the deformation undergone by the material as it left the sprues and entered the mold cavity, which caused the orientation to assume a circumferential pattern, regardless of sprue design. It was this flow of the melt into the mold cavity that determined the final orientation in the sample, not the orientation induced during flow through the sprue. The fiber orientation for the samples that were molded at 204°C with straight sprues is shown in Figures 5.14 to 5.16. The effect of temperature on the orientation was small, except that the skin layer had a stronger orientation at this temperature.

The length distributions for all samples indicated that substantial fiber breakage had occurred. The fiber length was generally found to be between 6 and 20 microns, with an

Longitude Direction

Transverse Direction

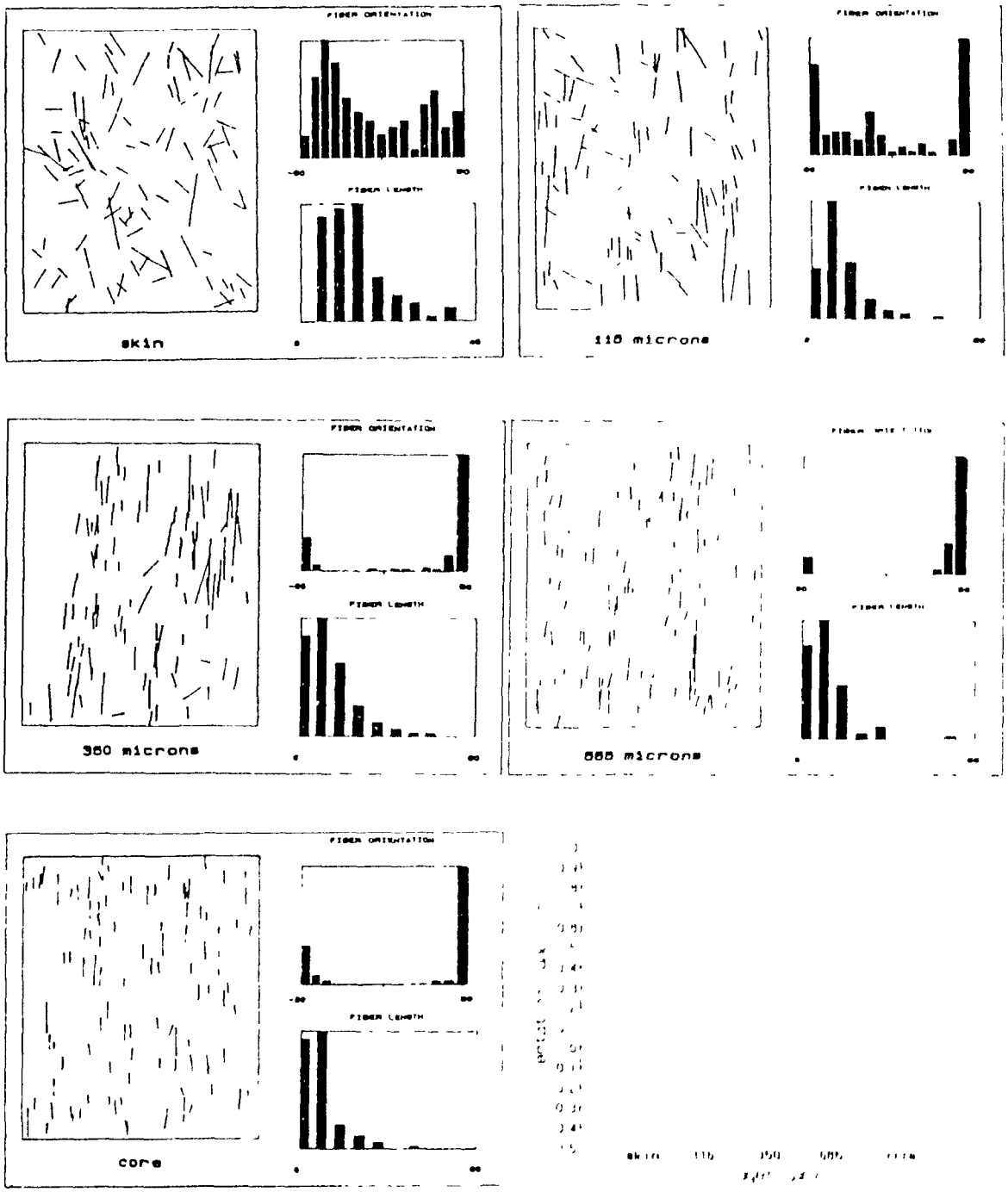

Figure 5.11. Orientation and Length Distributions for Samples Molded with Straight Sprues at 163 C (Microtome Location 3).

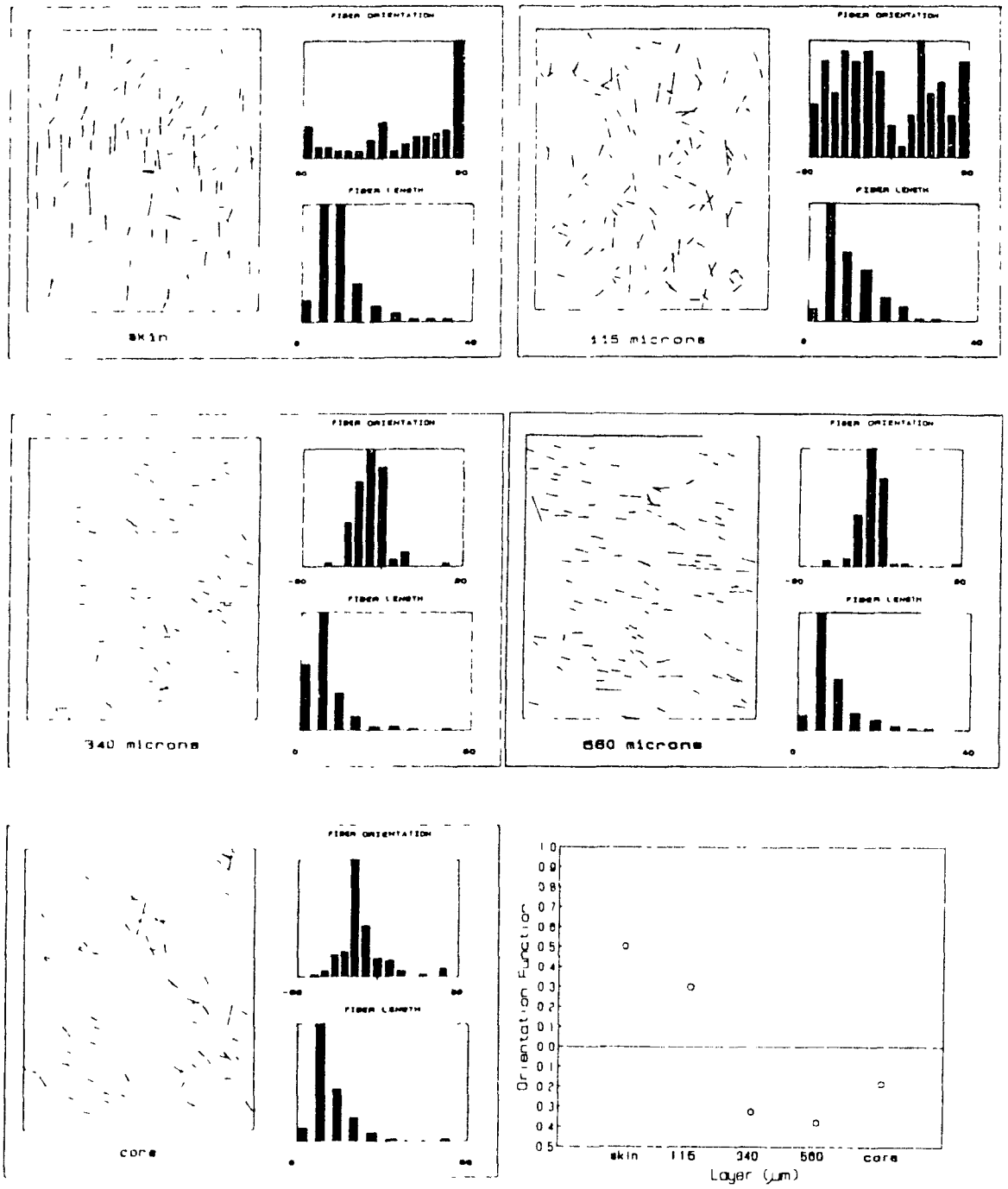

Figure 5.12. Orientation and Length Distributions for Samples Molded with Straight Sprues at 163°C (Microtome Location 4).

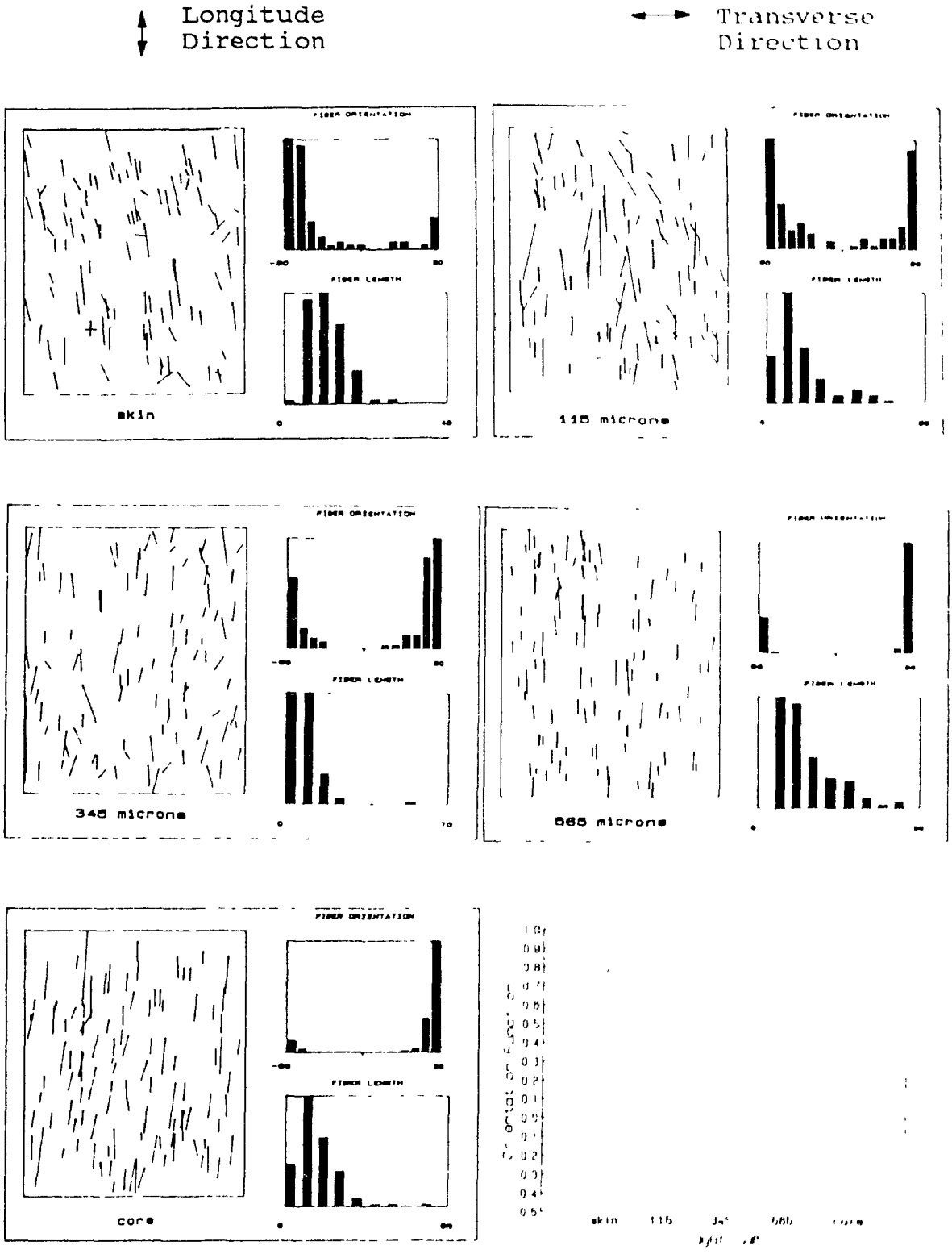

Figure 5.13. Orientation and Length Distributions for Samples Molded with Straight Sprues at 163 C (Microtome Location 5).

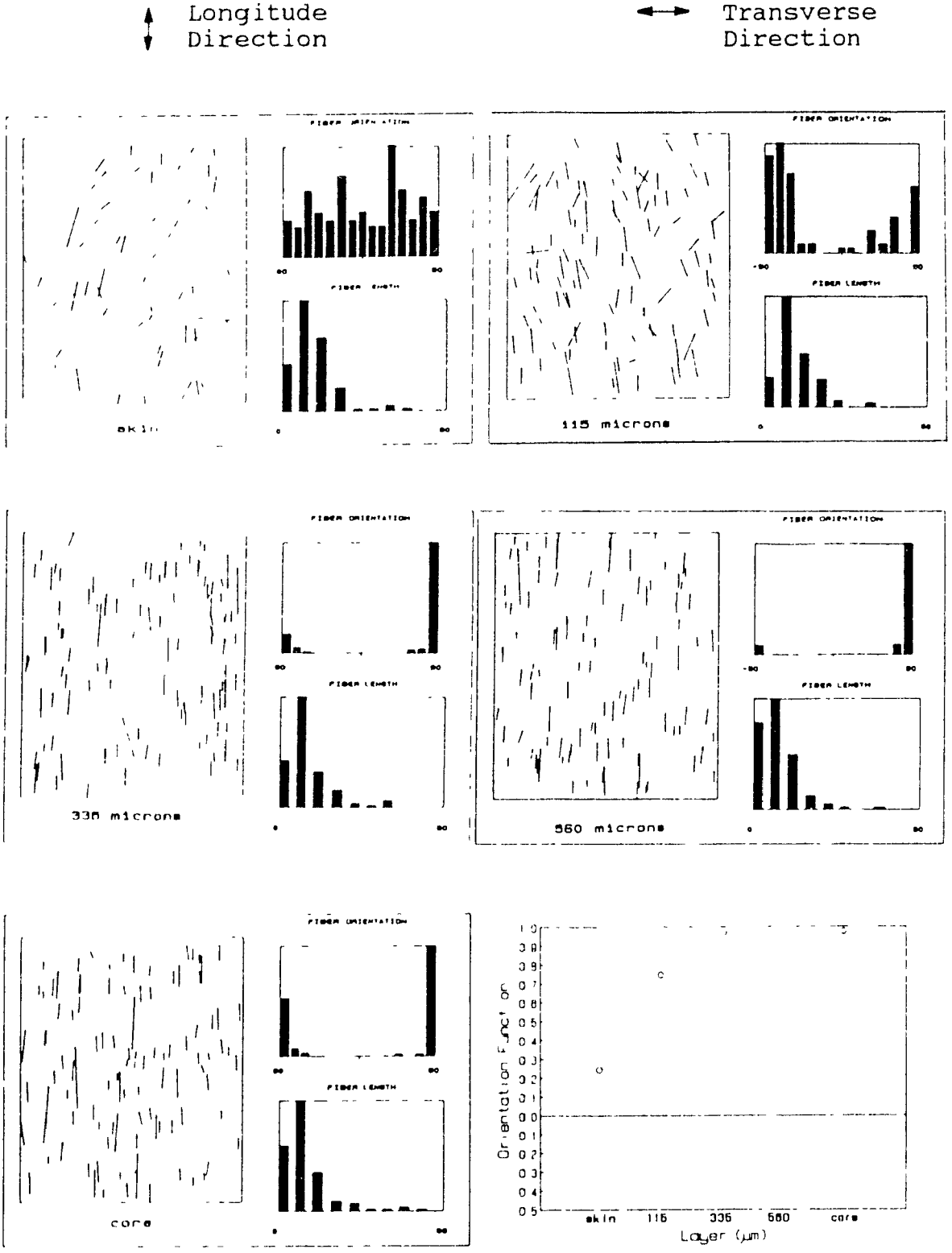

Figure 5.14. Orientation and Length Distributions for Samples Molded with Straight Sprues at 204°C (Microtome Location 3).

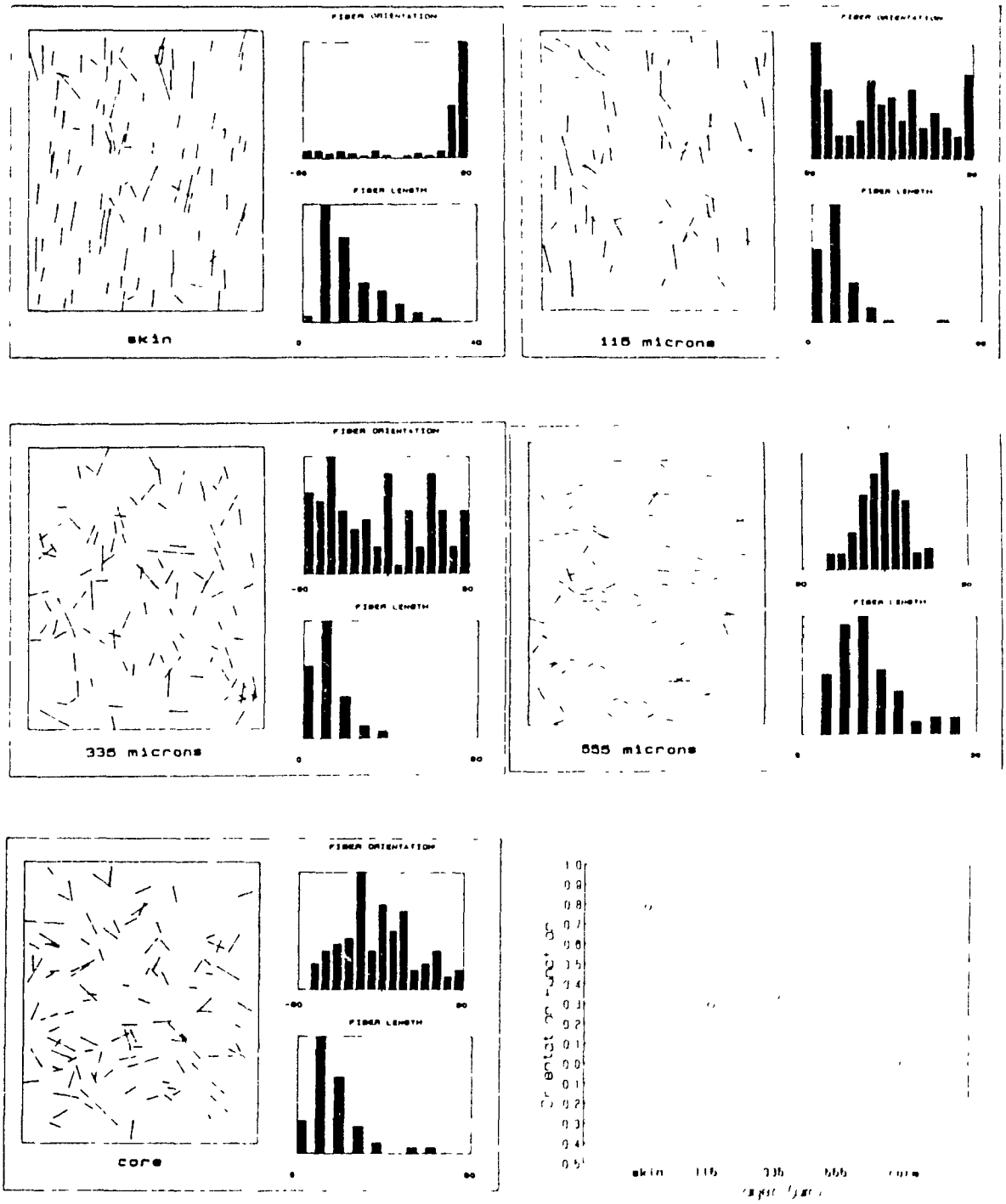

Figure 5.15. Orientation and Length Distributions for Samples Molded with Straight Spruce at 204 C (Microtome Location 4).

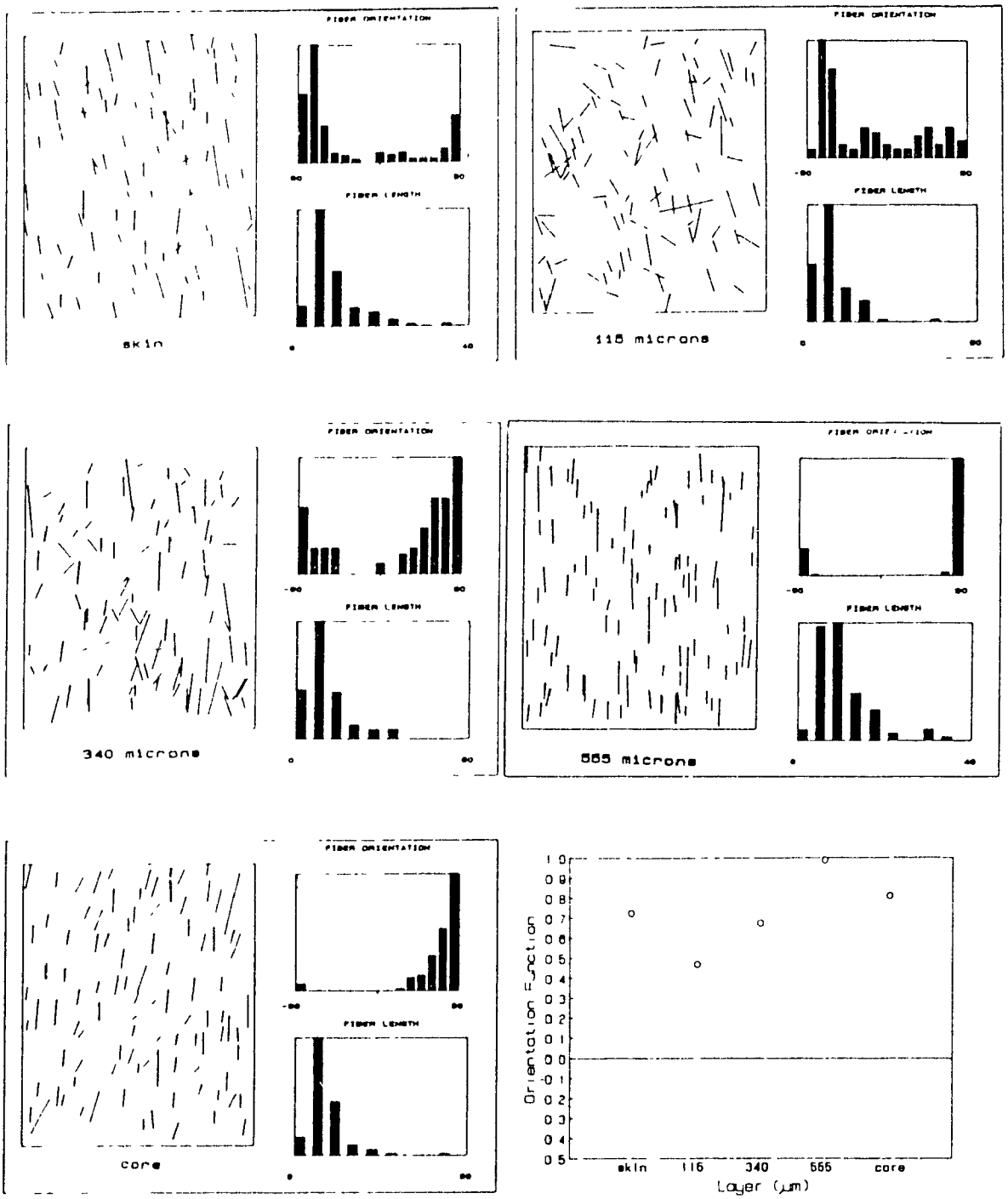

Figure 5.16. Orientation and Length Distributions for Samples Molded with Straight Sprues at 204°C (Microtome Location 5).

average of approximately 12 microns. This translates into a fiber aspect ratio of approximately 6 after molding, as compared with a ratio of 30 before molding. Transfer molding causes very strong flow, which contributes to fiber orientation but also causes significant fiber attrition.

5.1.2. Compression Molded Samples

Figures 5.17 to 5.23 present the results for the samples molded at 163°C that were prepared with "controlled milling". The orientation of the fibers is generally longitudinal (in the mill direction) for all locations and all depths. As indicated previously, the "controlled milling" process involves folding the sheet and then passing it back through the roll mills. This folding increases the thickness of the feed sheet and subsequently the strain, causing longitudinal fiber orientation (18). The orientation functions demonstrate that there is little variation from this longitudinal fiber orientation from skin to core for most layers. Figures 5.24 and 5.25 show the orientation and length distributions for samples molded at 204°C. The temperature does not alter the orientation of the fibers significantly, except at the skin layer where the orientation is very strong. The high molding temperature caused rapid freezing of the orientation at the mold surface.

The samples that were milled randomly did not exhibit strong

Longitude Direction

Transverse Direction

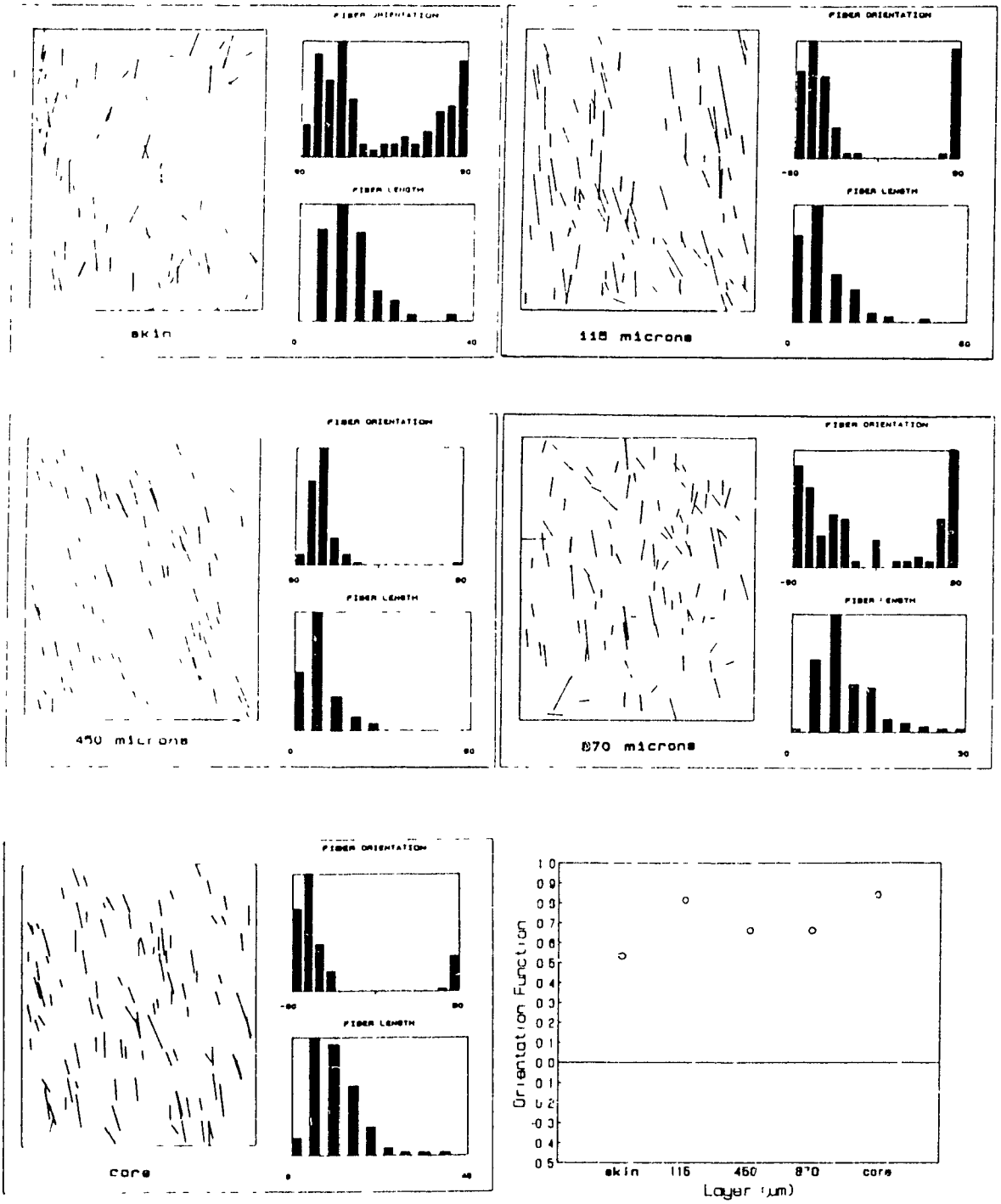

Figure 5.17. Orientation and Length Distributions for Controlled Milling Samples Molded at 163°C (Microtome Location 1).

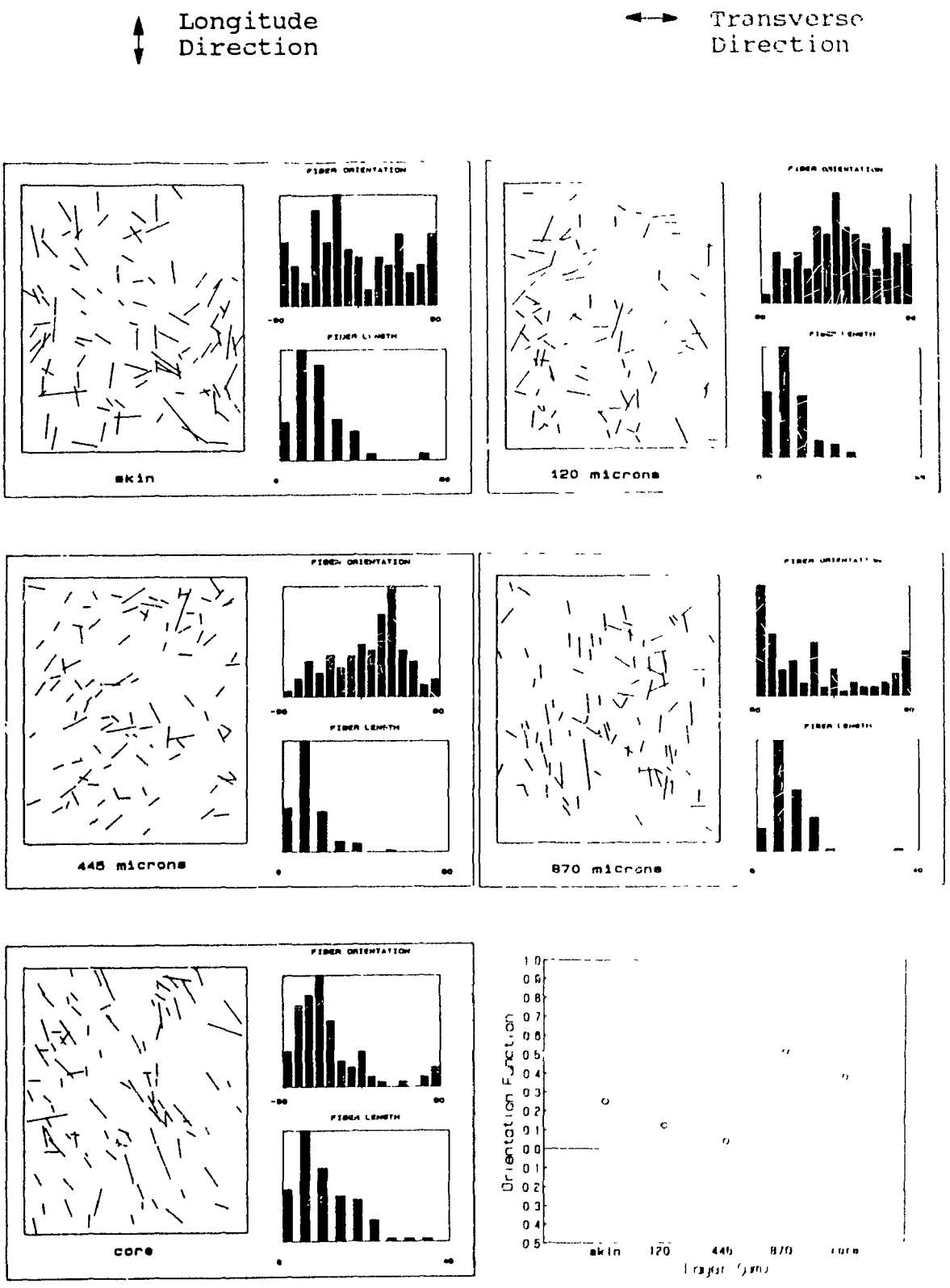

Figure 5.18. Orientation and Length Distributions for Controlled Milling Samples Molded at 163 C (Microtome Location 2).

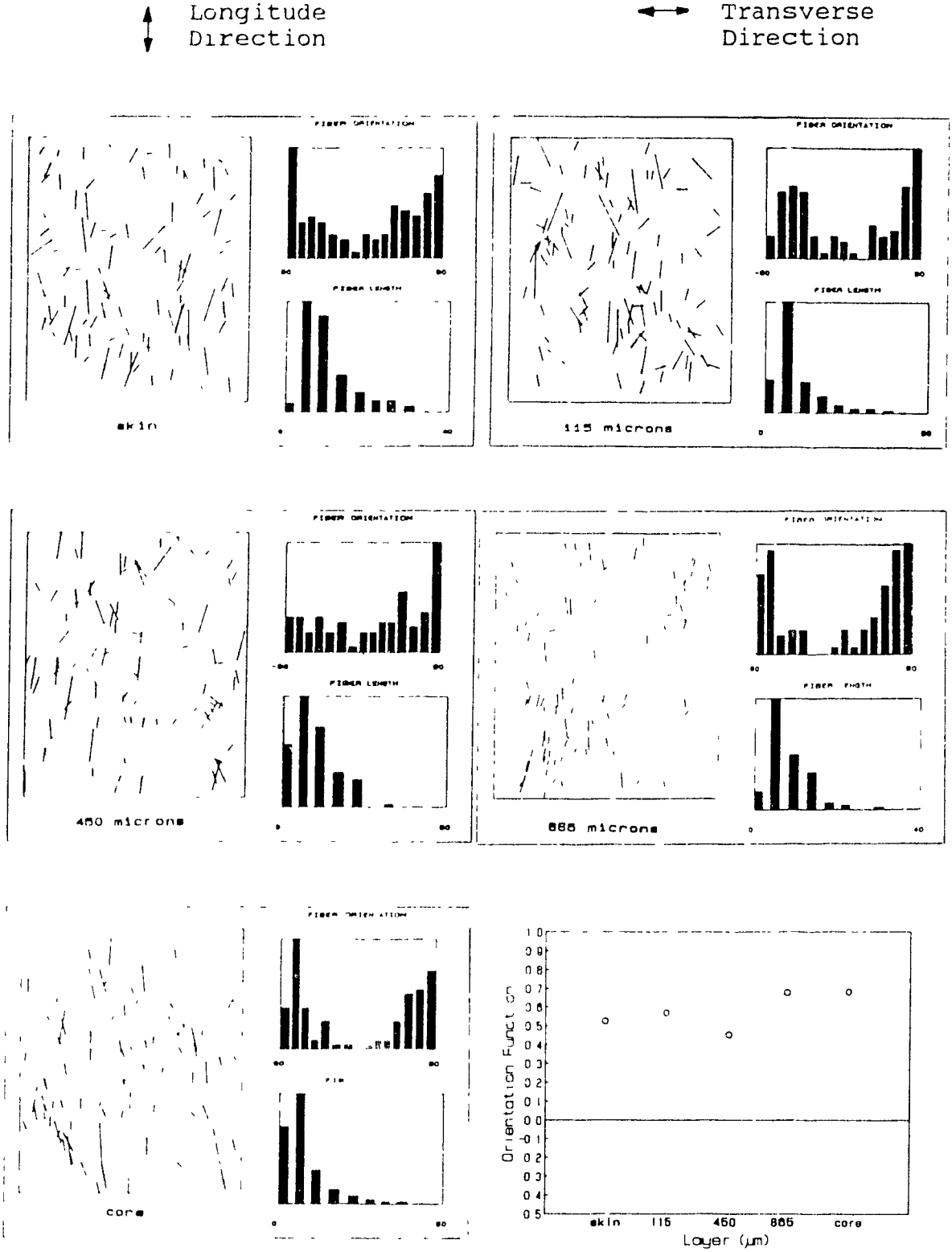

Figure 5.19. Orientation and Length Distributions for Controlled Milling Samples Molded at 163°C (Microtome Location 3).

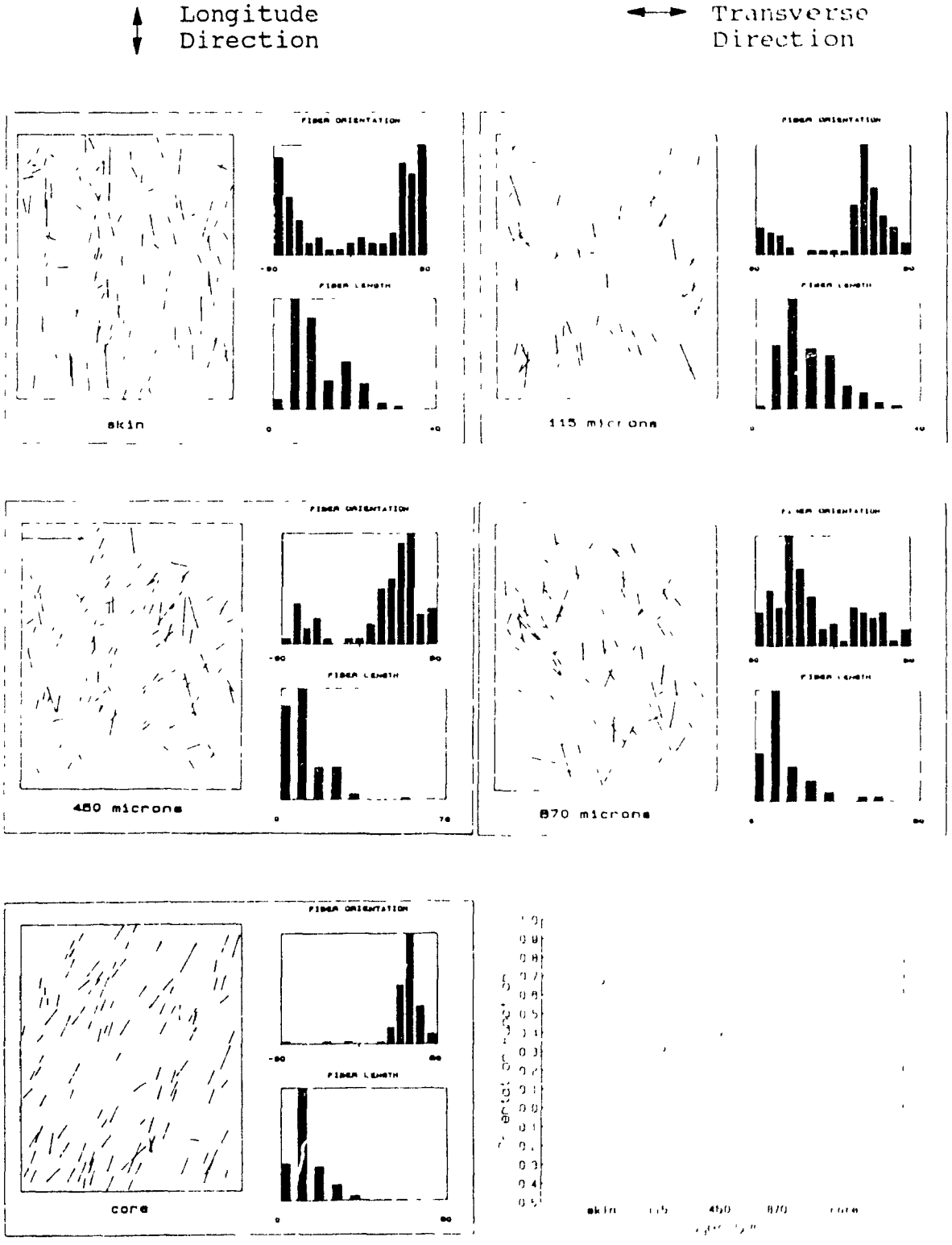

Figure 5.20. Orientation and Length Distributions for Controlled Milling Samples Molded at 163 C (Microtome Location 4).

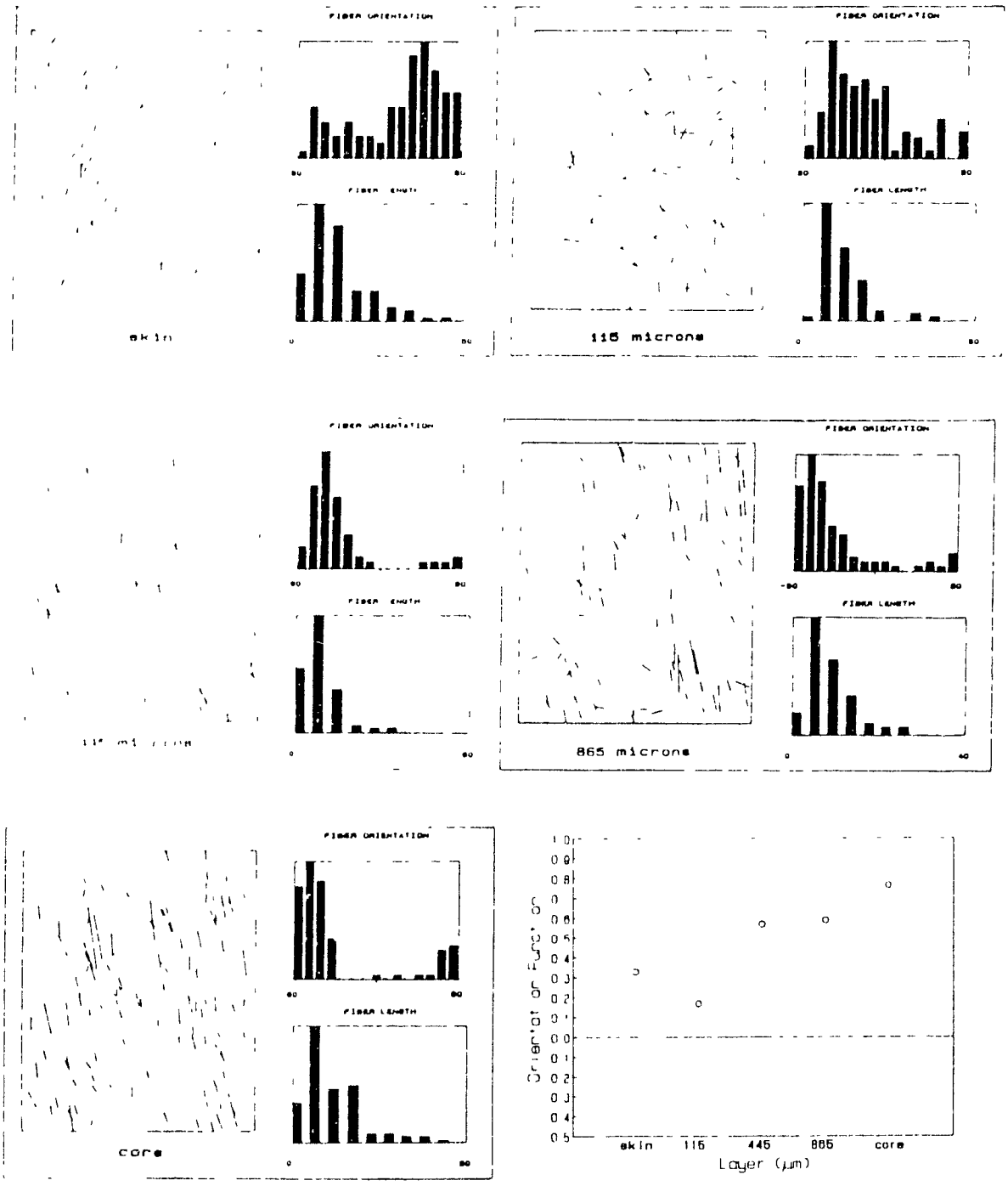

Figure 5.21. Orientation and Length Distributions for Controlled Milling Samples Molded at 163°C (Microtome Location 5).

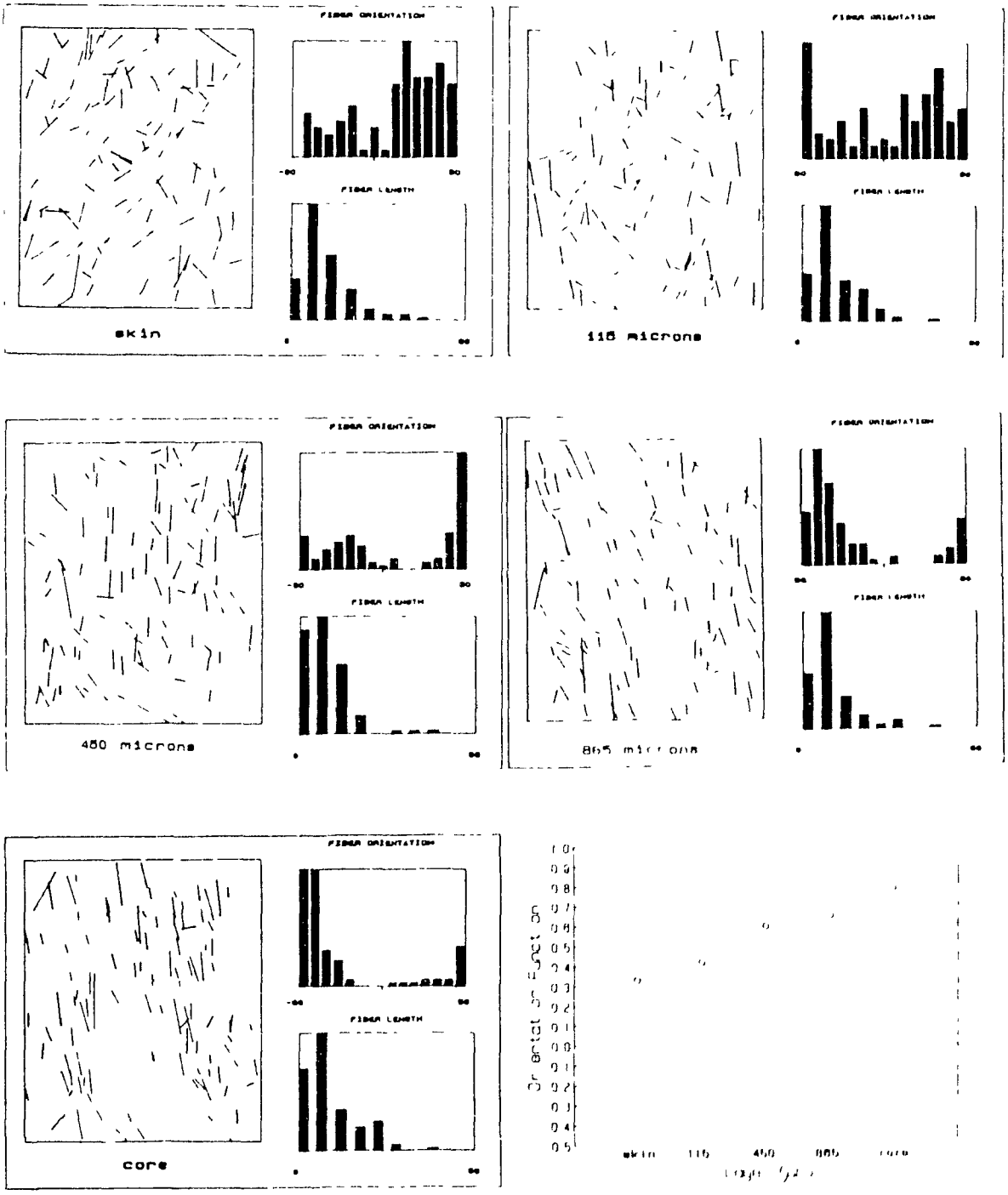

Figure 5.22. Orientation and Length Distributions for Controlled Milling Samples Molded at 163 C (Microtome Location 6).

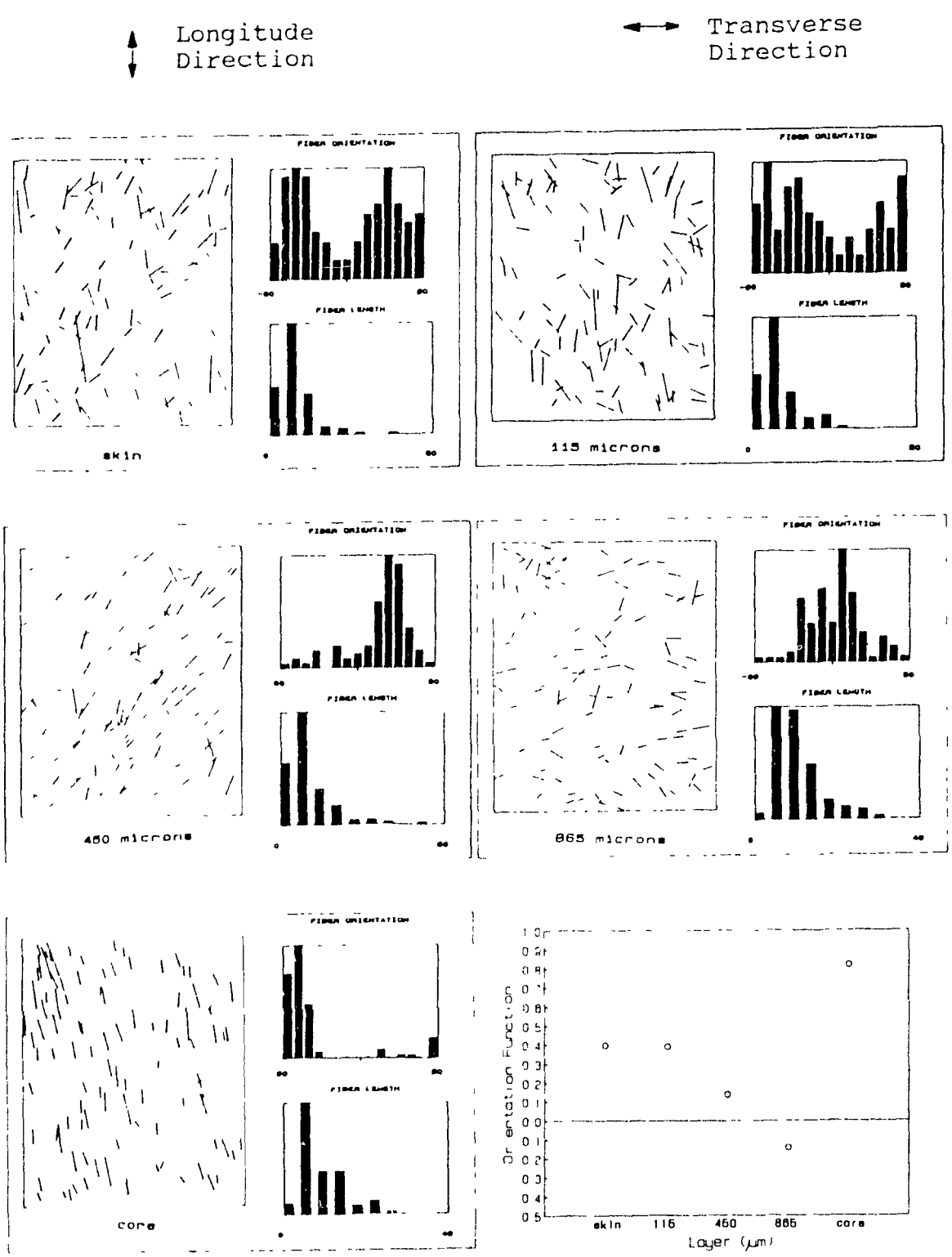

Figure 5.23. Orientation and Length Distributions for Controlled Milling Samples Molded at 163°C (Microtome Location 7).

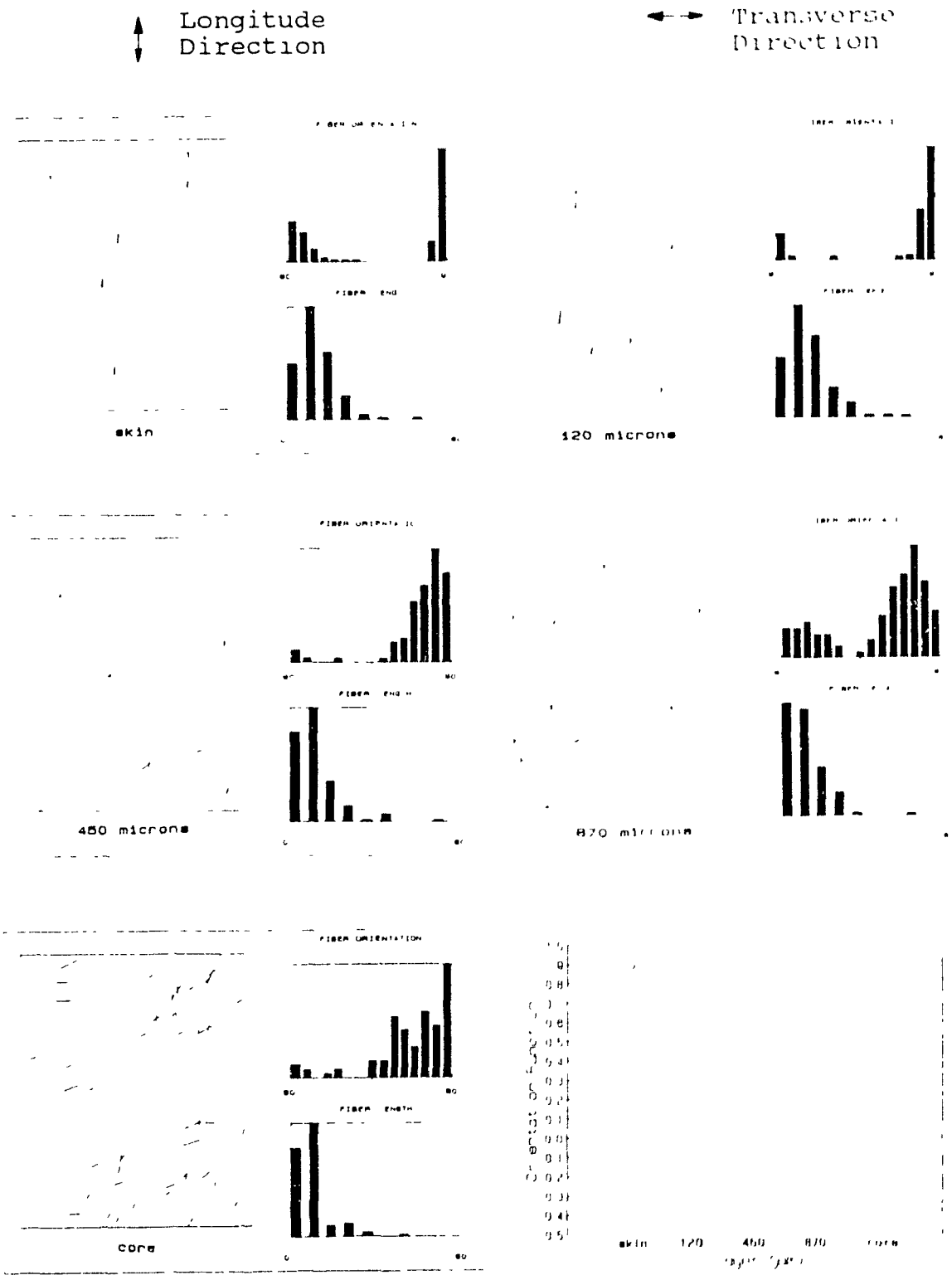

Figure 5.24. Orientation and Length Distributions for Controlled Milling Samples Molded at 204 C (Microtome Location 2).

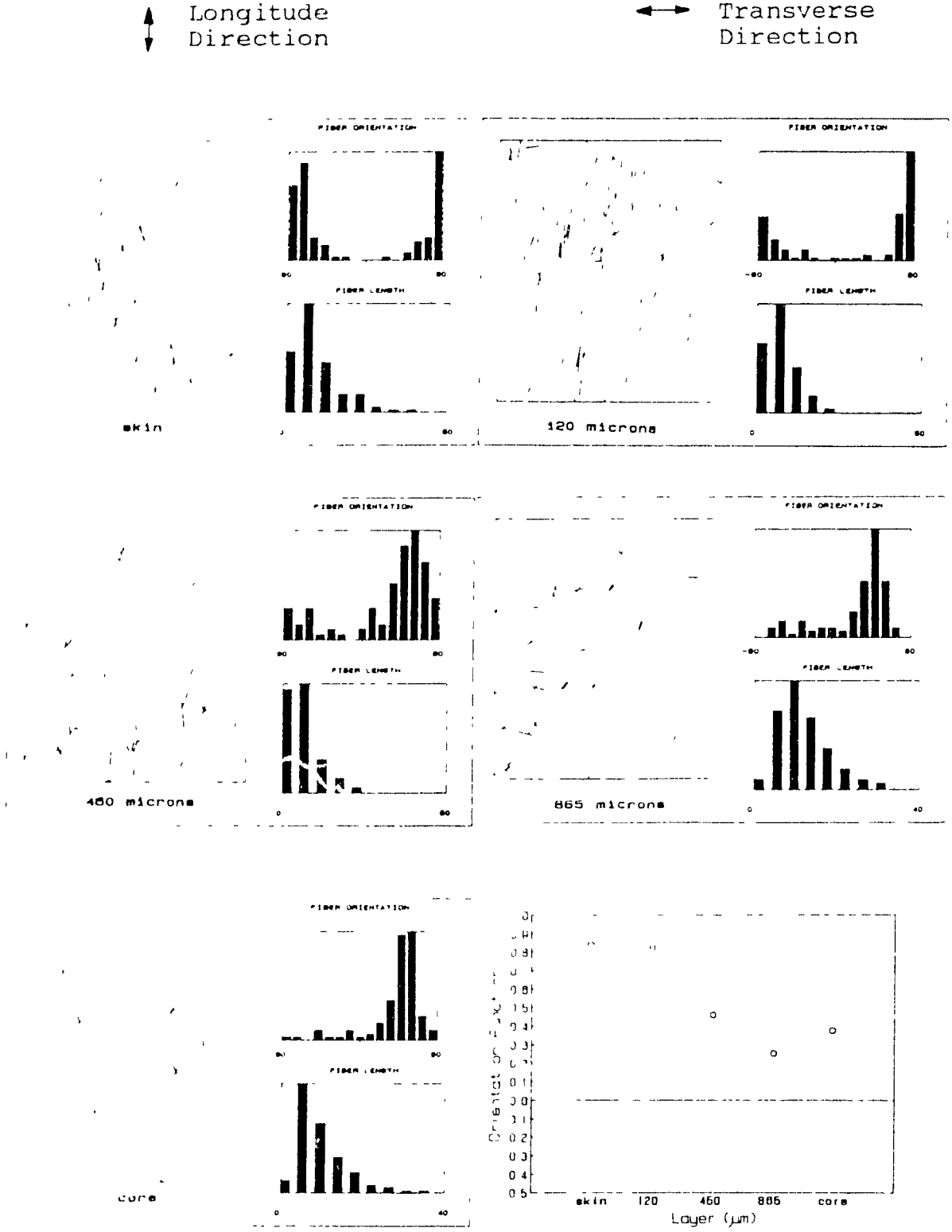

Figure 5.25. Orientation and Length Distributions for Controlled Milling Samples Molded at 204°C (Microtome Location 3).

fiber orientation. This is shown in Figures 5.26 to 5.32 for the samples molded at 163°C. Since the sheet was taken off the mill and then placed back through the rolls without folding the sheet or reducing the gap space in this procedure, all fiber orientation was achieved after the first pass through the mill (13), and no increase in the strain was achieved. Therefore, the orientation should be less pronounced than that found in the samples that underwent "controlled milling". The orientation function results show that the fiber orientation was nearly random for most layers, and while some locations did exhibit fiber orientation, it was much less substantial than that found in the sheets with "controlled milling".

The fibers suffered extensive breakage, as shown in the fiber length distributions for all samples. The fiber length was reduced to an average of approximately 12 microns. This decreased the aspect ratio of the fibers to 6. Franklin Fibers are known to be brittle and have been compared to glass fibers (12), which suffer severe breakage when milled (14). However, the fiber lengths after molding were the same for both milling procedures, even though the extra mill passes in the randomly milled composite have no effect on the fibers. This suggests that the initial mixing and milling of the composites caused the majority of the breakage, not the milling techniques used in this study.

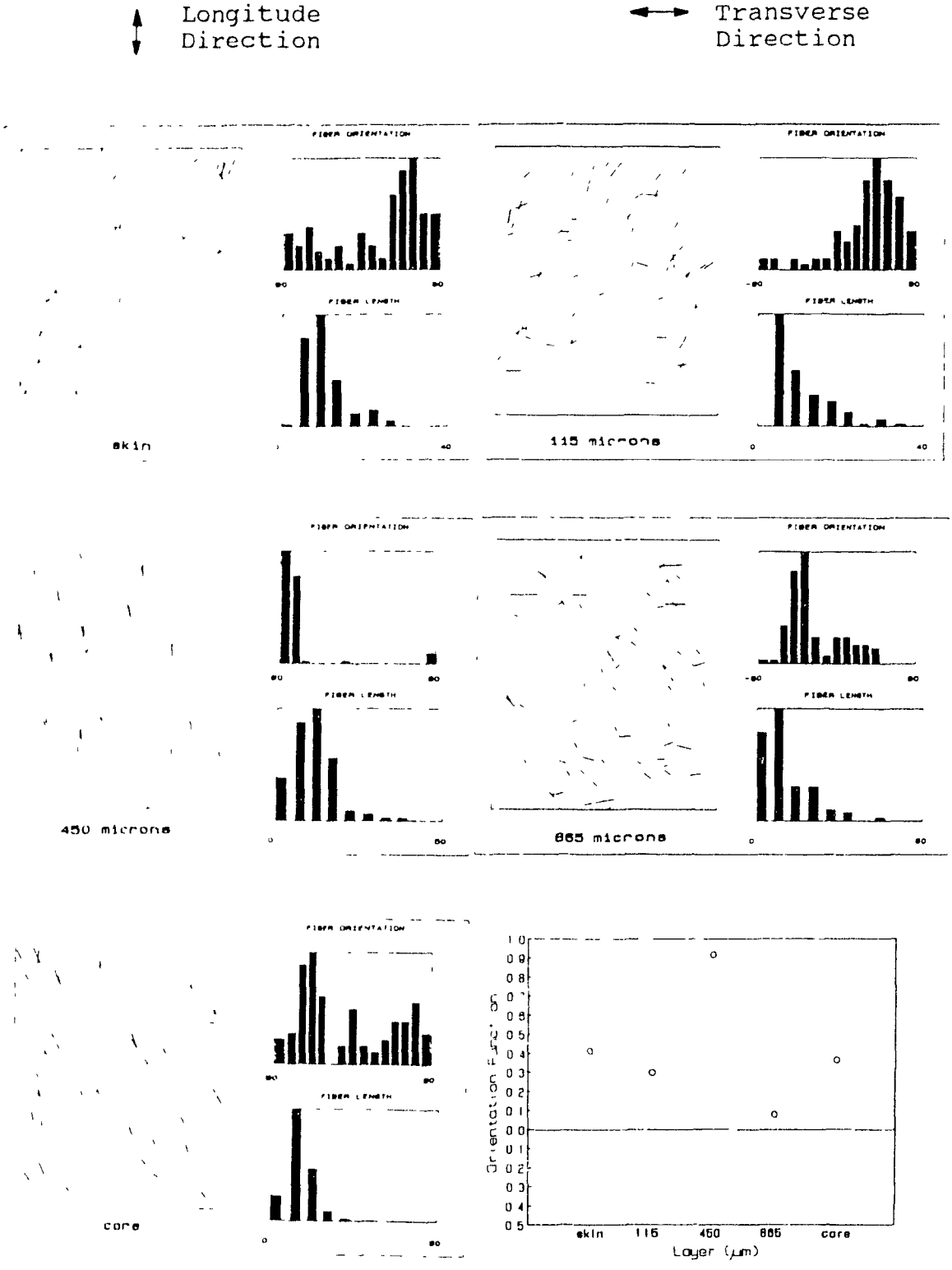

Figure 5.26. Orientation and Length Distributions for Random Milling Samples Molded at 163°C (Microtome Location 1).

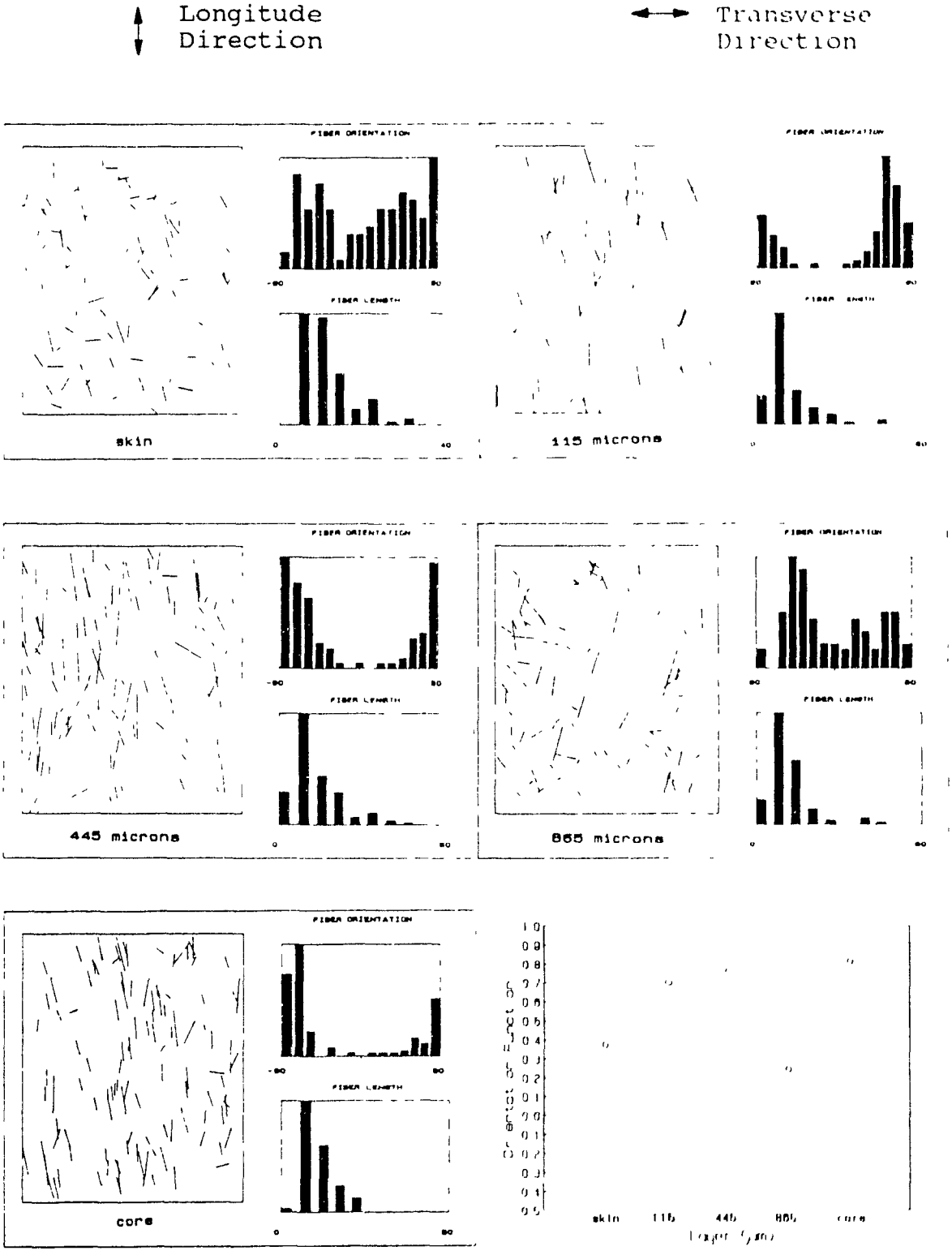

Figure 5.27. Orientation and Length Distributions for Random Milling Samples Molded at 163°C (Microtome Location 2).

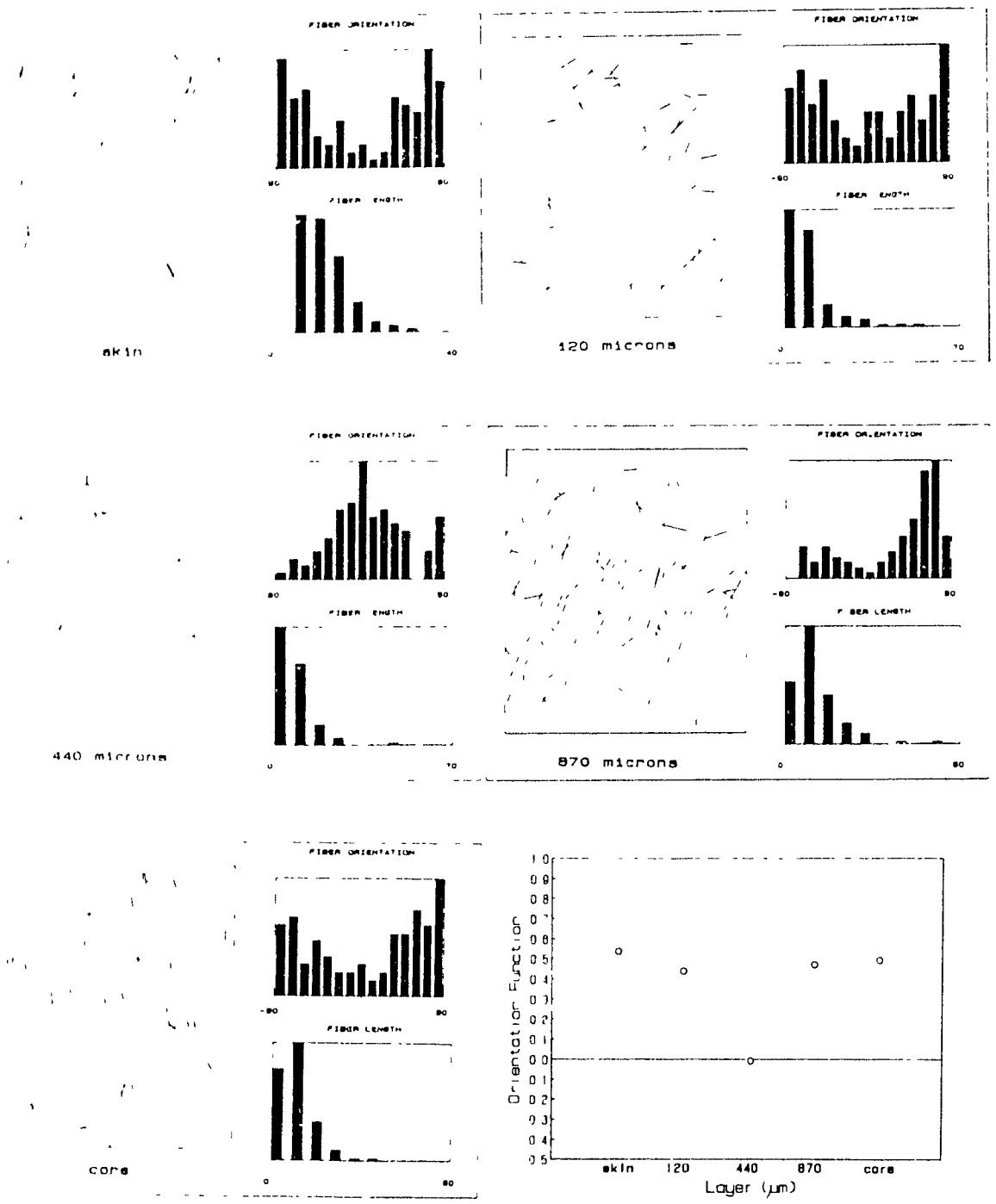

Figure 5.28. Orientation and Length Distributions for Random Milling Samples Molded at 163°C (Microtome Location 3).

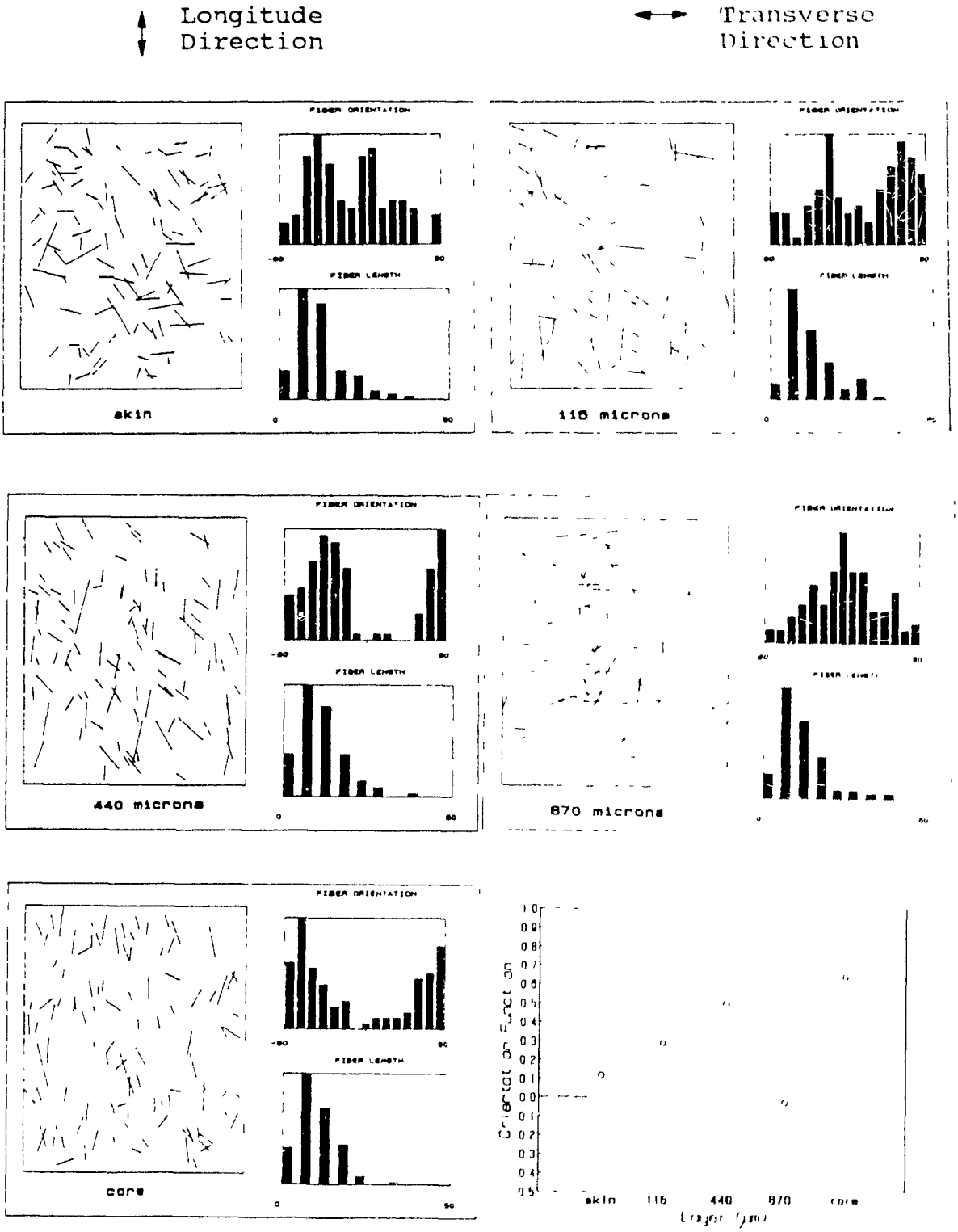

Figure 5.29. Orientation and Length Distributions for Random Milling Samples Molded at 163°C (Microtome Location 4).

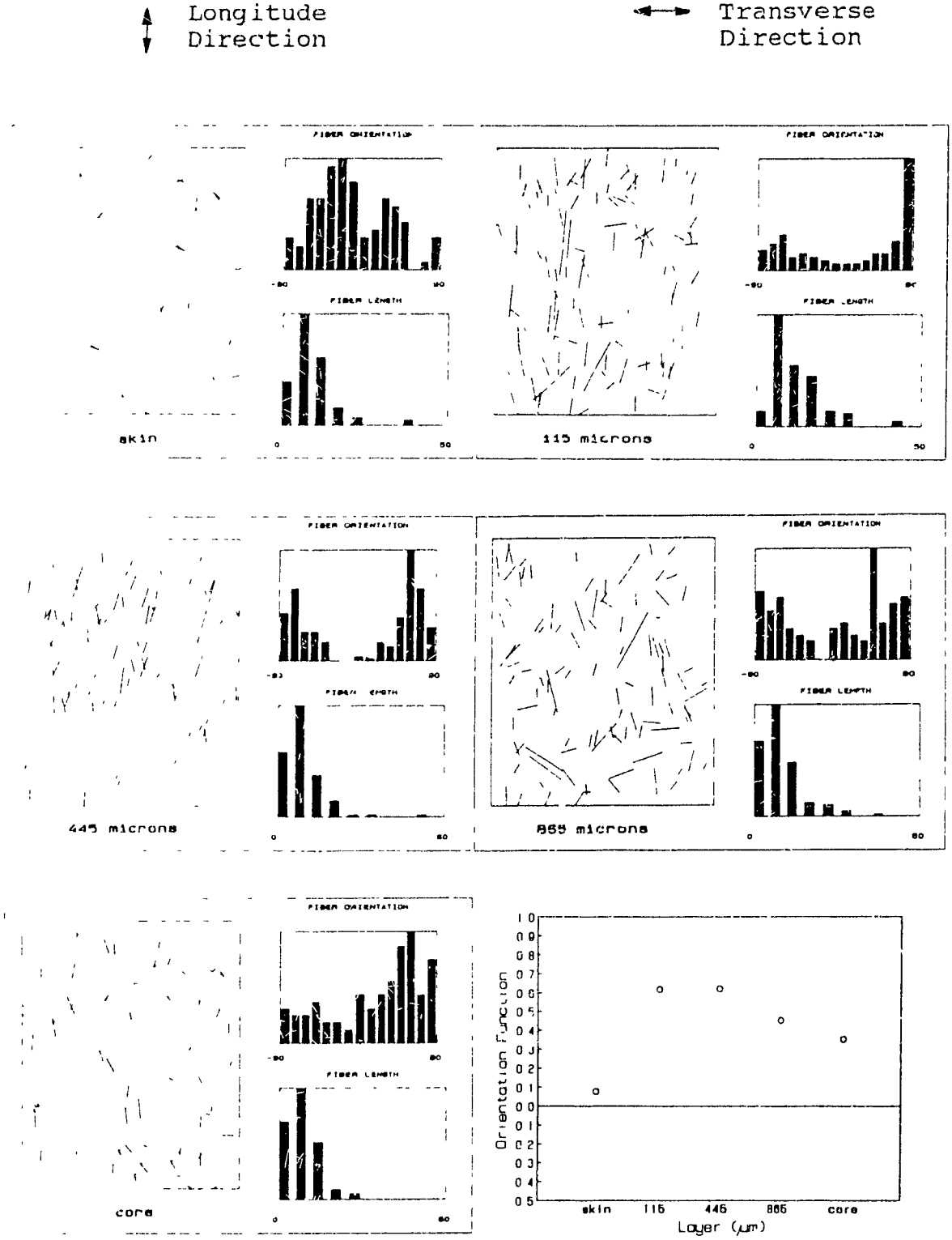

Figure 5.30. Orientation and Length Distributions for Random Milling Samples Molded at 163°C (Microtome Location 5).

Longitude Direction

Transverse Direction

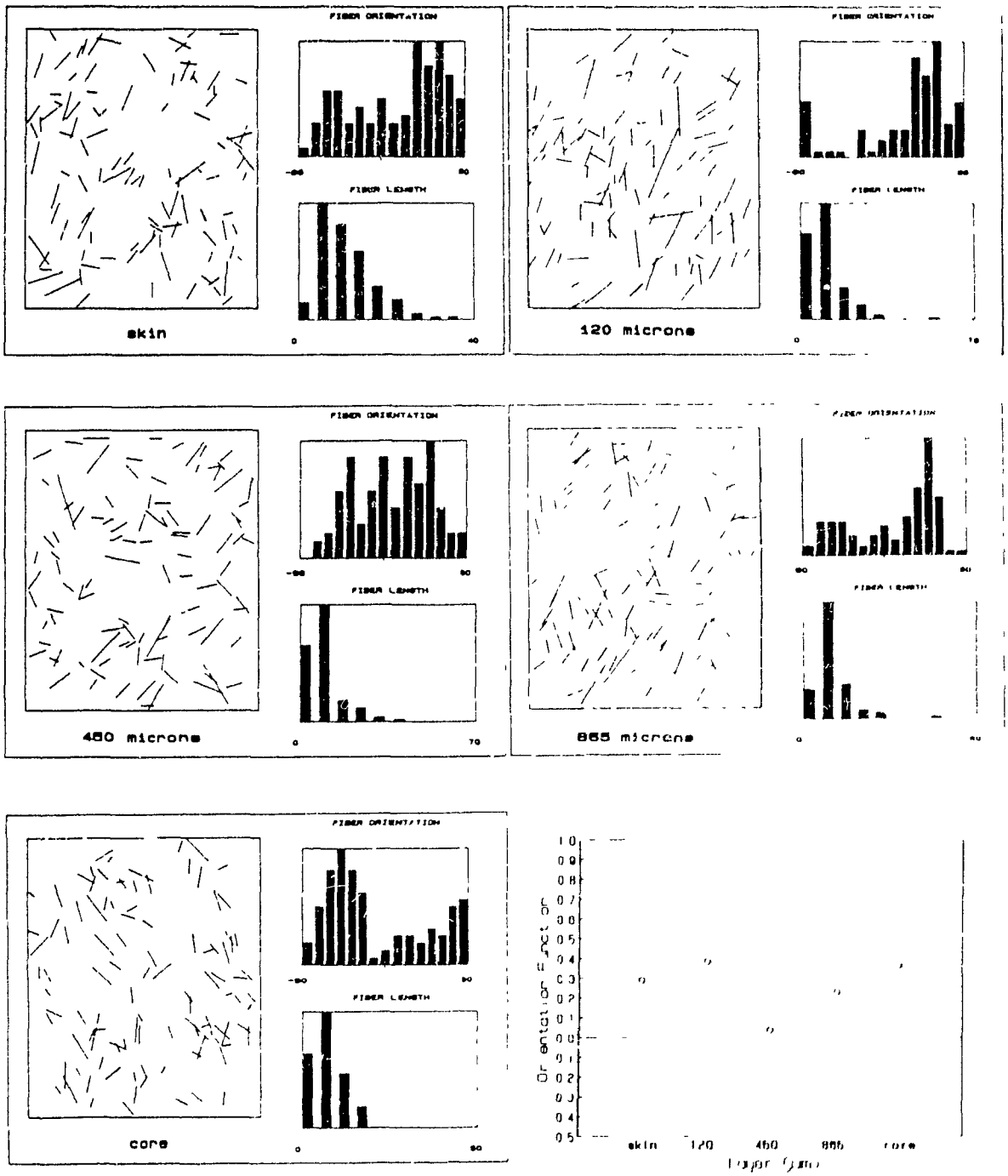

Figure 5.31. Orientation and Length Distributions for Random Milling Samples Molded at 163 C (Microtome Location 6).

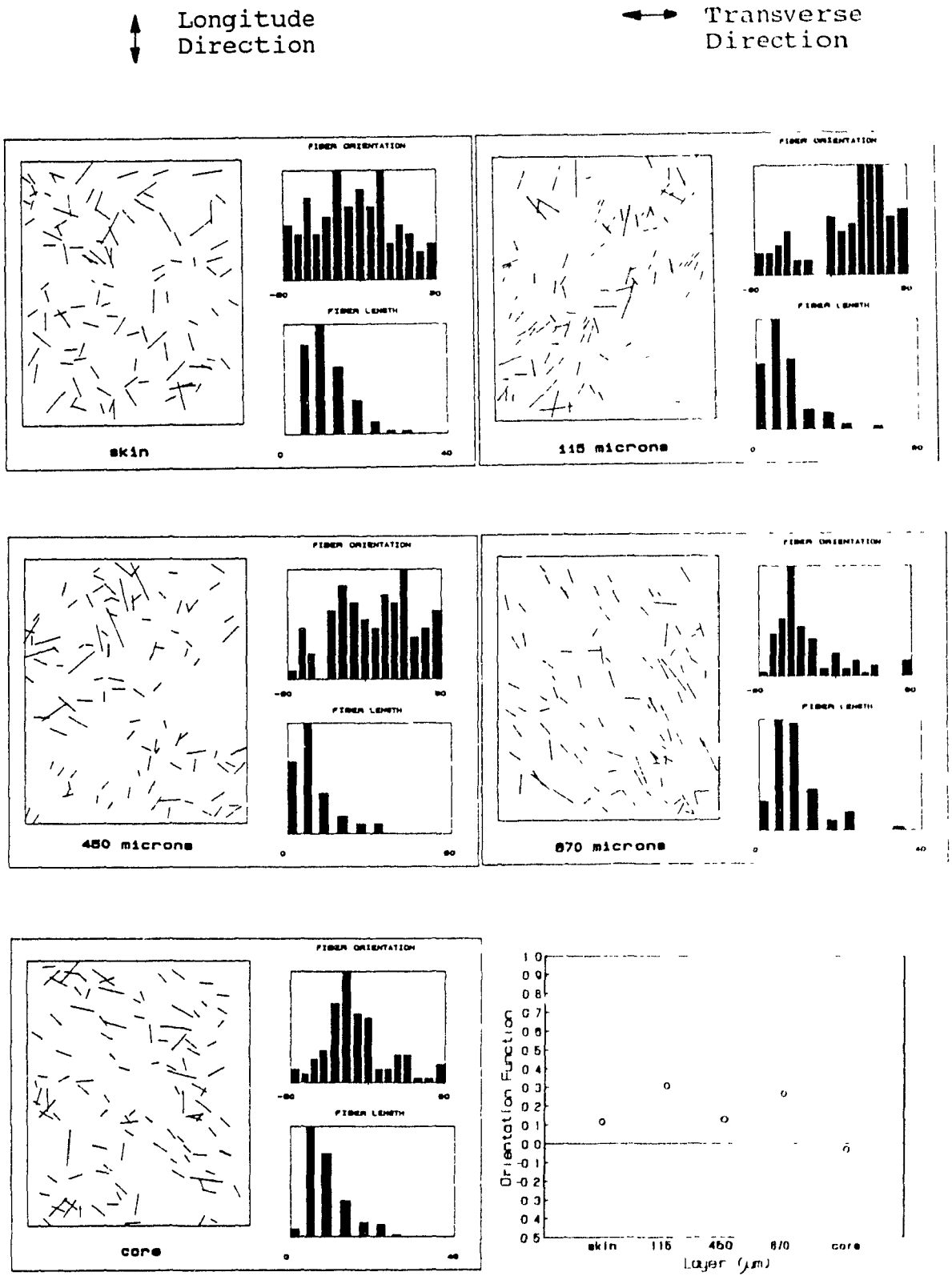

Figure 5.32. Orientation and Length Distributions for Random Milling Samples Molded at 163 C (Microtome Location 7).

5.1.3. Comparison Between Transfer and Compression Molding

The transfer molded samples exhibited strong anisotropic and non-homogeneous fiber orientation for all sprue designs. The orientation of the fibers in the compression molded samples was dependent on the milling procedure. For samples with "controlled milling", the fiber orientation was longitudinal, anisotropic, but homogeneous. The samples that were randomly milled generally exhibited random, isotropic, and homogeneous fiber orientation. The orientation found in the compression molded samples was more consistent from skin to core and from location to location than the orientation in the transfer molded samples. For both molding procedures, an increase in temperature had little effect on fiber orientation, except at the skin layer. Fiber breakage was substantial for both transfer and compresion molding.

5.2. Tensile Test Results

The results from the tensile testing, which measured tensile strength, elongation at break, and Young's modulus, are presented in this section. Bartlett's test was used to find a pooled variance for each type of sample, so a single standard deviation is given for each sample and each type of test.

5.2.1. Transfer Molded Samples

The results for the samples molded with converging sprues at a temperature of 163°C are presented in Figure 5.33. The observed behavior at 163°C indicated that, statistically, there was no difference between tensile strengths and elongations at break at virtually every location. The orientation results indicated substantial variation in fiber orientation from location to location, but this did not result in differences in tensile strength or elongation at break. This could be due to the very small size of the fibers, specifically after processing, which was shown in the fiber length distributions in the previous section. As well, the fiber concentration was only 2% by volume, and may have been too low to cause an appreciable difference between locations with different fiber orientations.

The Young's modulus is more sensitive to fiber orientation than tensile strength or elongation at break (18) and did show a statistical variation with test location. The greatest modulus value was seen at tensile location 4, where the fibers are oriented in the test direction (longitudinal fiber orientation), and the lowest values occured at locations 3, 5, and 6 where the orientation was perpendicular to the direction of test (transverse fiber orientation).

The results for the samples molded with converging sprues at

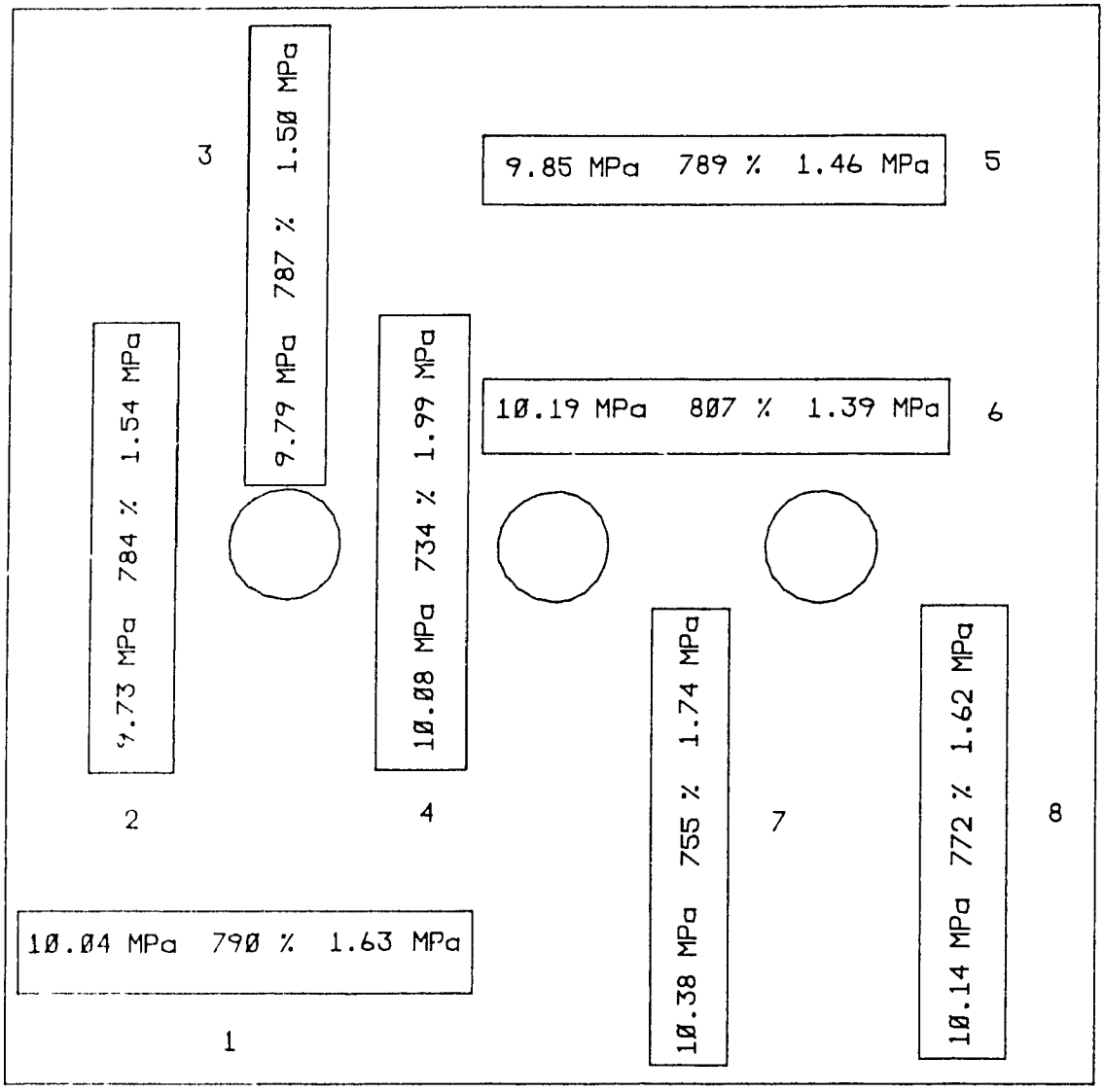

Figure 5.33. Tensile Test Results for Samples Molded with Converging Sprues at 163°C.

204°C are shown in Figure 5.34. The strength and elongation at break were generally lower than the values at 163°C. This was expected since an increase in temperature usually results in a reduction in cross-linking efficiency and a decrease in properties (17, 23). The Young's modulus did not change significantly and, at some locations, increased slightly. An increase in anisotropy in the tensile strength and elongation at break was found at this temperature.

Figure 5.35 gives the tensile test results for samples molded with straight sprues at 163°C. The results were similar to those found for the samples that were transfer molded with converging sprues at this temperature. The tensile strength and elongation at break did not vary with location, so the straight sprue had no effect on these tensile properties. The Young's modulus did show anisotropy.

An increase in molding temperature to 204°C did cause a variation in properties, as shown in Figure 5.36. There was significant anisotropy in tensile strength, elongation at break, and Young's modulus. The Young's modulus at location 3 was higher than at location 4, even though the orientation results indicated that the fiber orientation at locations 3 and 4 were transverse and longitudinal, respectively. This did not correspond with theory or with the previous results, and this abnormality was not due to a change in fiber orientation.

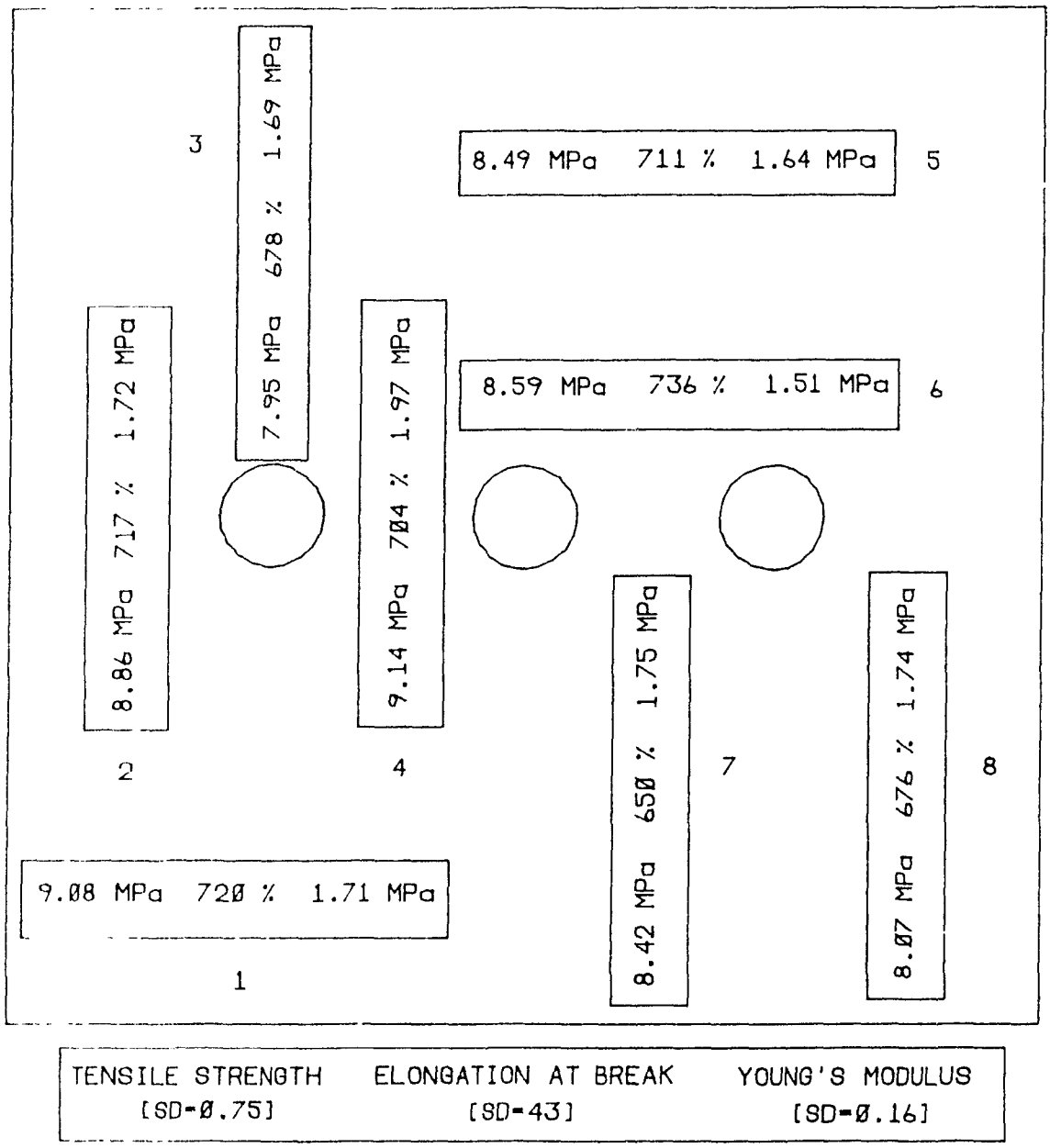

Figure 5.34. Tensile Test Results for Samples Molded with Converging Sprues at 204°C.

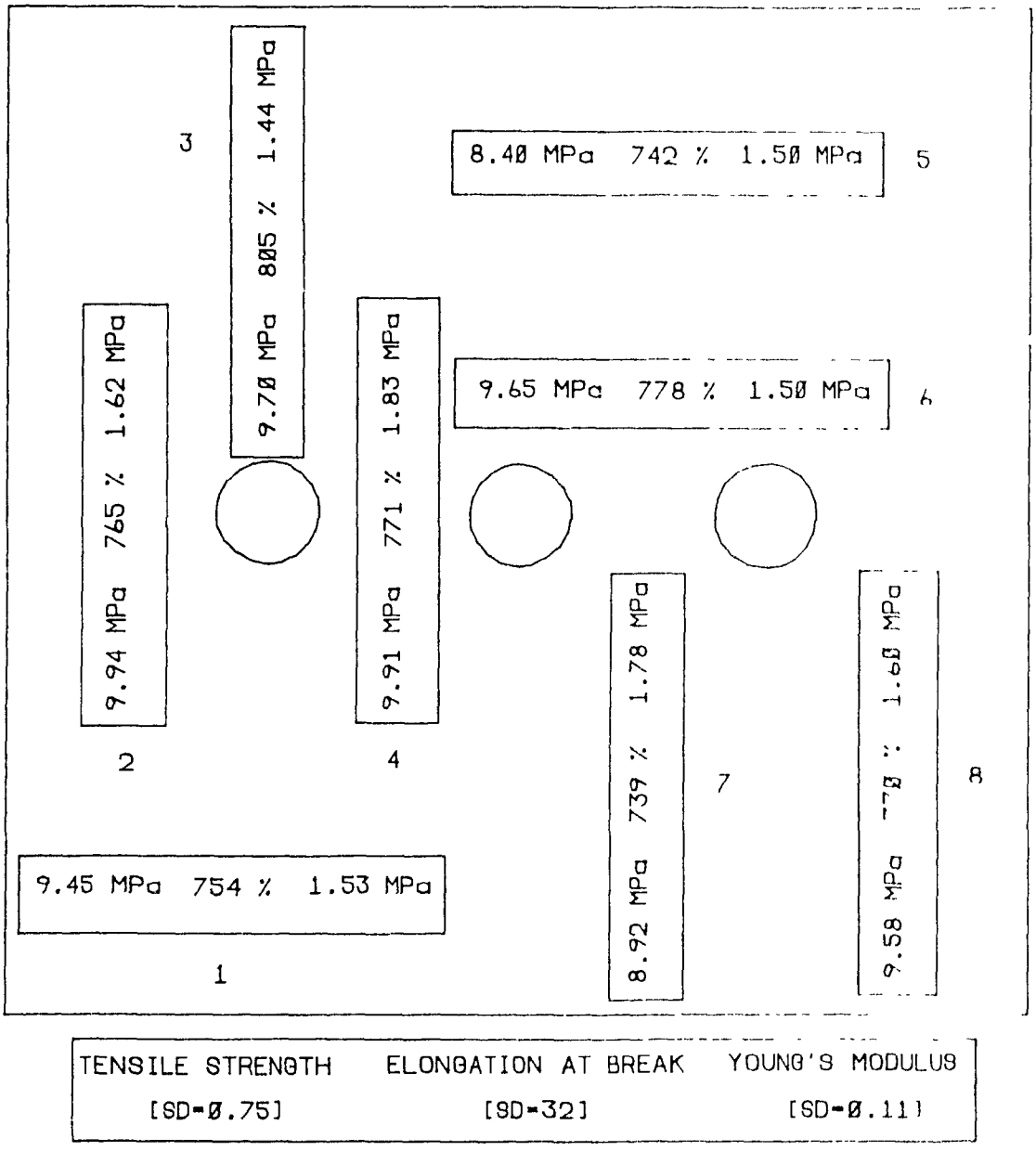

Figure 5.35. Tensile Test Results for Samples Molded with Straight Sprues at 163°C.

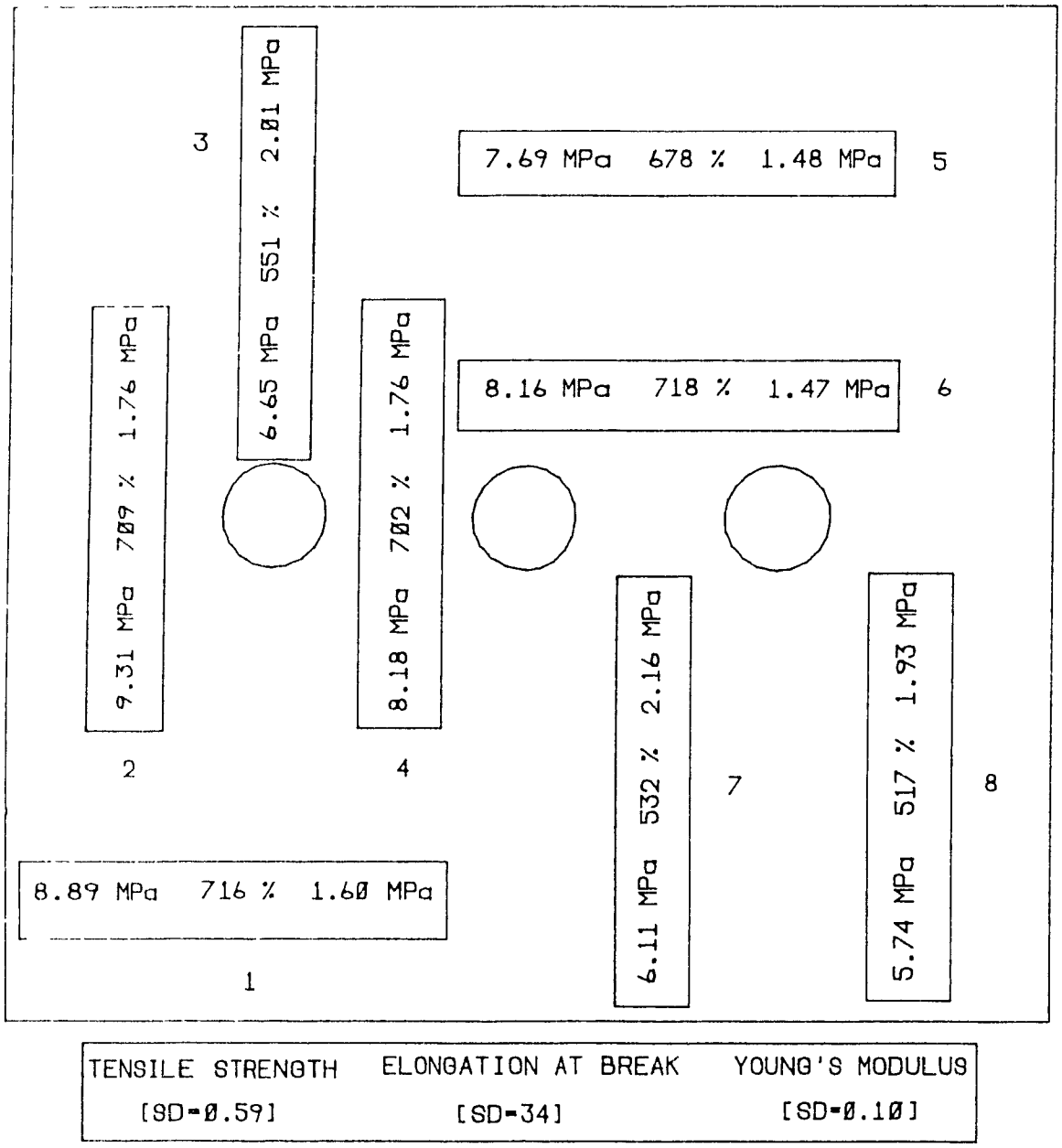

Figure 5.36. Tensile Test Results for Samples Molded with Straight Sprues at 204°C.

A dynamic mechanical analysis was performed to determine whether a difference in curing may have caused the observed behavior in the Young's modulus. Two rectangular sections, one taken from tensile location 3 for a sample molded at 163 °C and the other from a similar location at 204 °C, were analyzed. The dynamic mechanical analysis was performed using flexure of the samples at a strain of 64 microns, peak to peak, frequencies of 1, 10, and 30 Hz, and a heating rate of 1 °C/min. The mechanical loss angle (tan δ), storage modulus (E'), and loss modulus (E") are shown in Figures 5.37, 5.38, and 5.39, respectively, for the sample molded at 163 °C. From approximately 185°C to 195°C, slippage of the sample occurred, and the data points in this range were omitted. However, the Figures indicate that a smooth continuation of the curve appears likely in this area. Figures 5.40, 5.41, and 5.42 show these properties for the sample molded at 204 °C. The curves at this temperature are continuous and smooth from 185°C to 195°C, so it may be presumed that this was also the case for the sample molded at 163°C.

The increase in E' for both samples at approximately 200 °C indicates that neither sample was fully cured at this point. However, the very large increase in tan δ at 200°C for the sample molded at 204°C shows that a variation in the state of cure between the two samples had occurred. Tan δ is the ratio of E" to E', so an increase in tan δ means either an increase in E" or a decrease in E'. Since E" is the viscous component

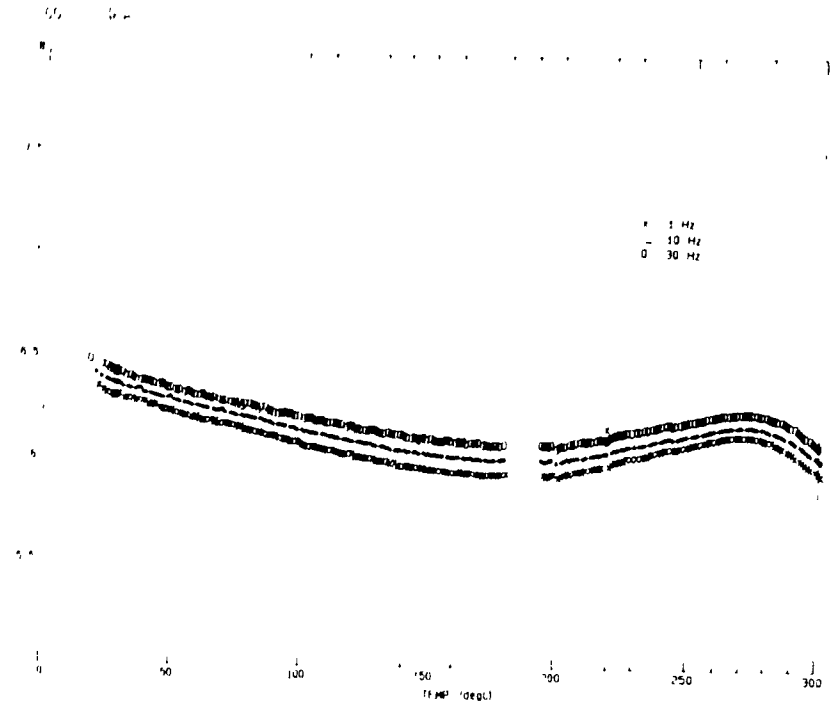

Figure 5.37. E' for Sample Molded at 163°C.

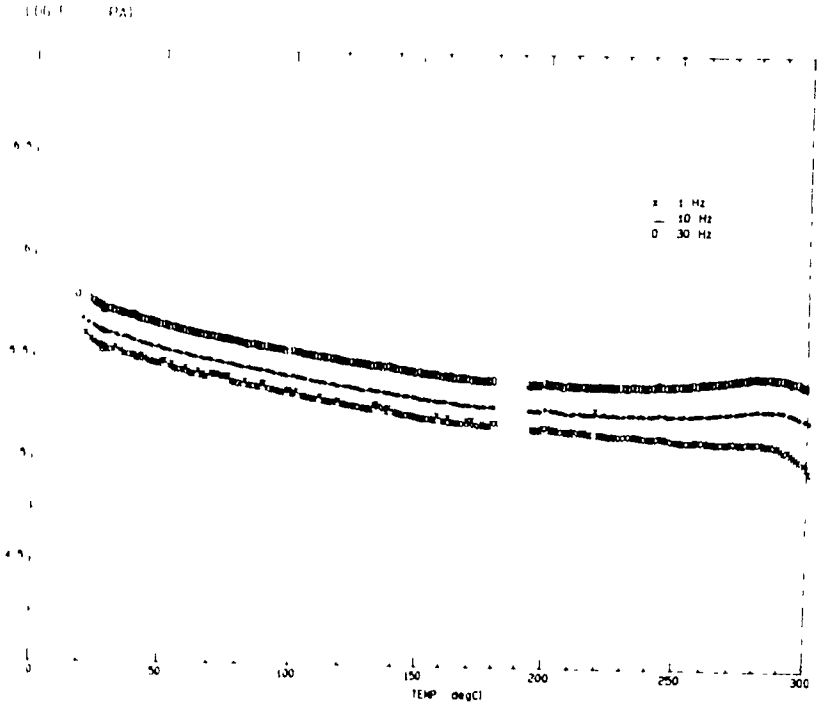

Figure 5.38. E" for Sample Molded at 163°C.

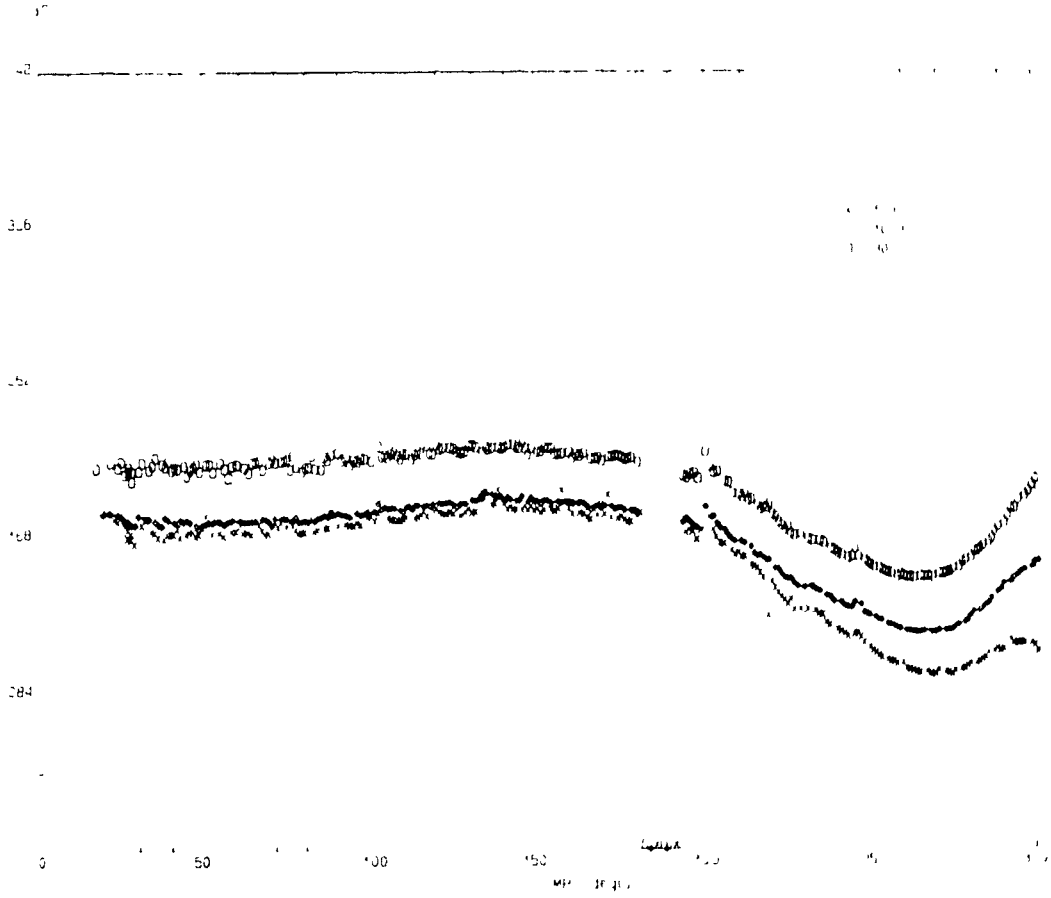

Figure 5.39. Tan δ for Sample Molded at 163°C.

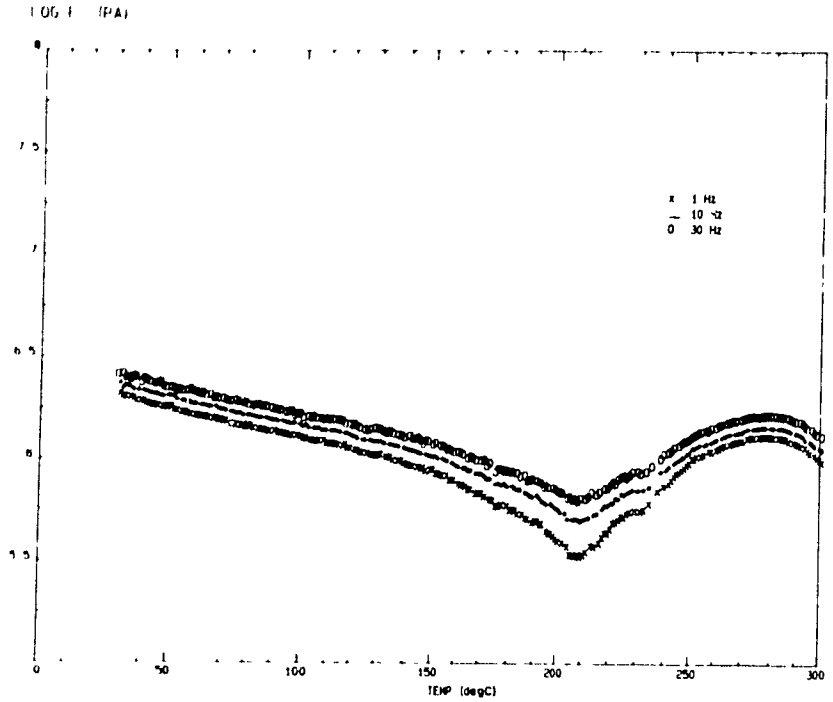

Figure 5.40. E' for Sample Molded at 204°C.

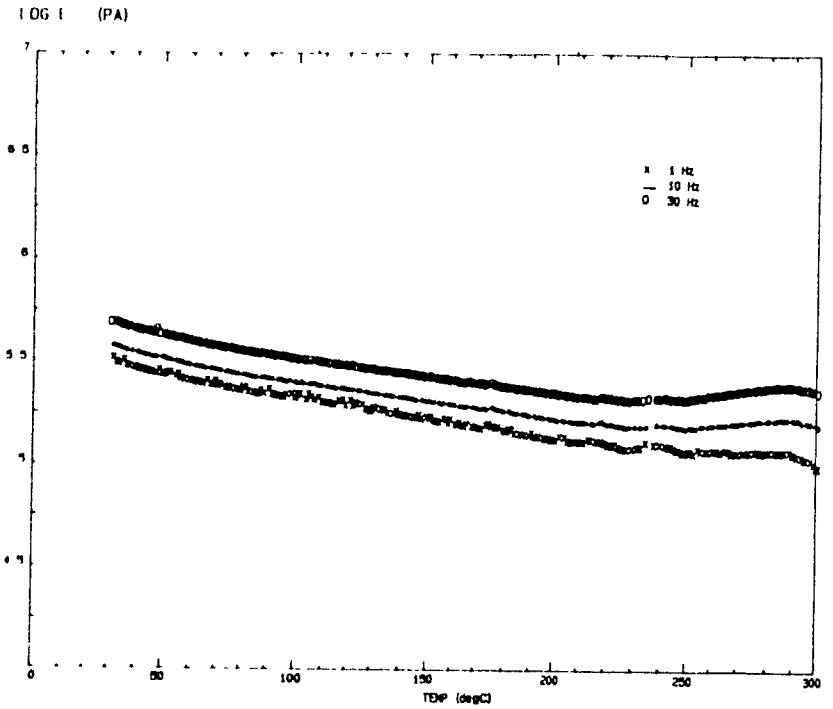

Figure 5.41. E" for Sample Molded at 204°C.

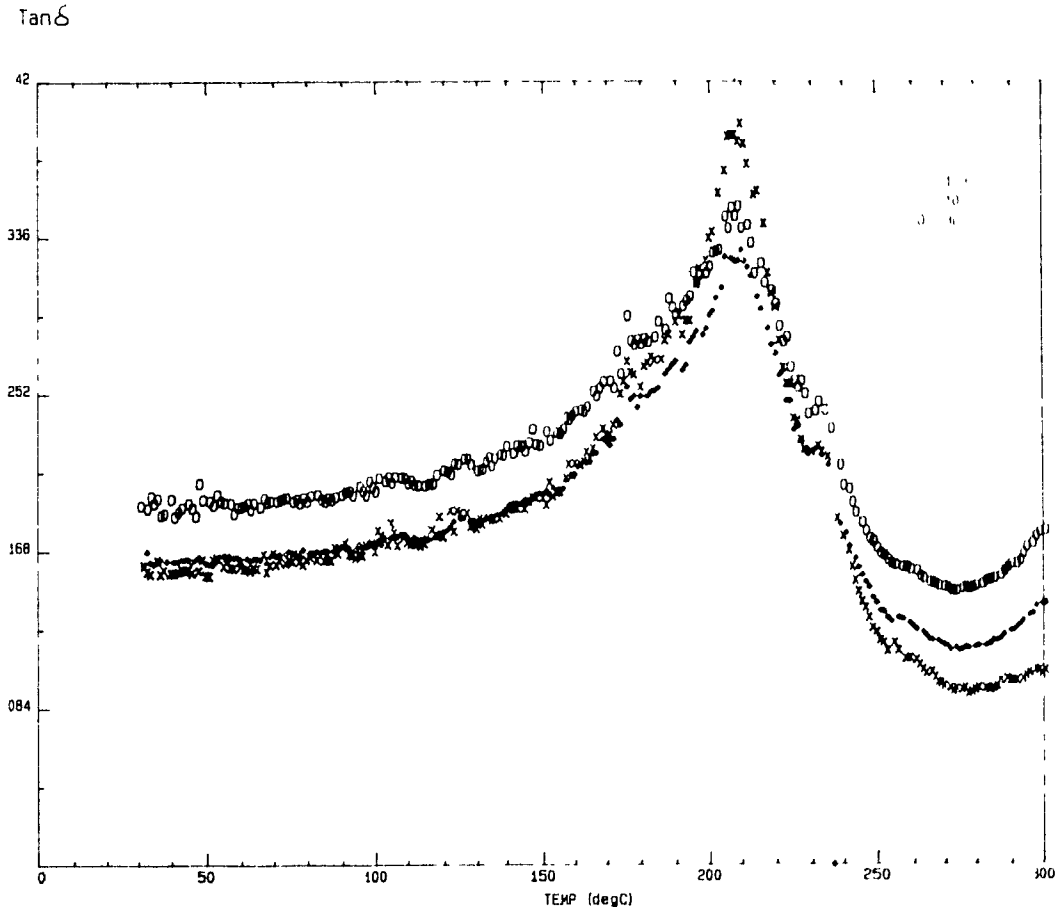

Figure 5.42. Tan δ for Sample Molded at 204 C.

and E' is the elastic component, the increase in tan δ at 204°C indicates that the composite is less elastic. Premature vulcanization, or scorch, is a likely possibility since a scorched sample exhibits poor elasticity, decreased elongation and strength, and increased stiffness. These are all seen for the sample molded at 204°C at location 3, as well as locations 7 and 8. This suggests that the temperature was not constant throughout the mold.

5.2.2. Compression Molded Samples

The samples that underwent "controlled milling" exhibited homgeneous tensile properties. This is shown in Figure 5.43 for a molding temperature of 163°C. There was no statistical variation from location to location for strength, elongation at break, or Young's modulus. This isotropy was also seen at 204°C, as shown in Figure 5.44. An increase in mold temperature caused a decrease in tensile strength and elongation at break, but did not significantly effect the Young's modulus.

Figure 5.45 presents the tensile results for samples that underwent "random milling" and were molded at 163°C. No statistical variation of properties occurred between locations.

The samples that were milled using the "controlled milling"

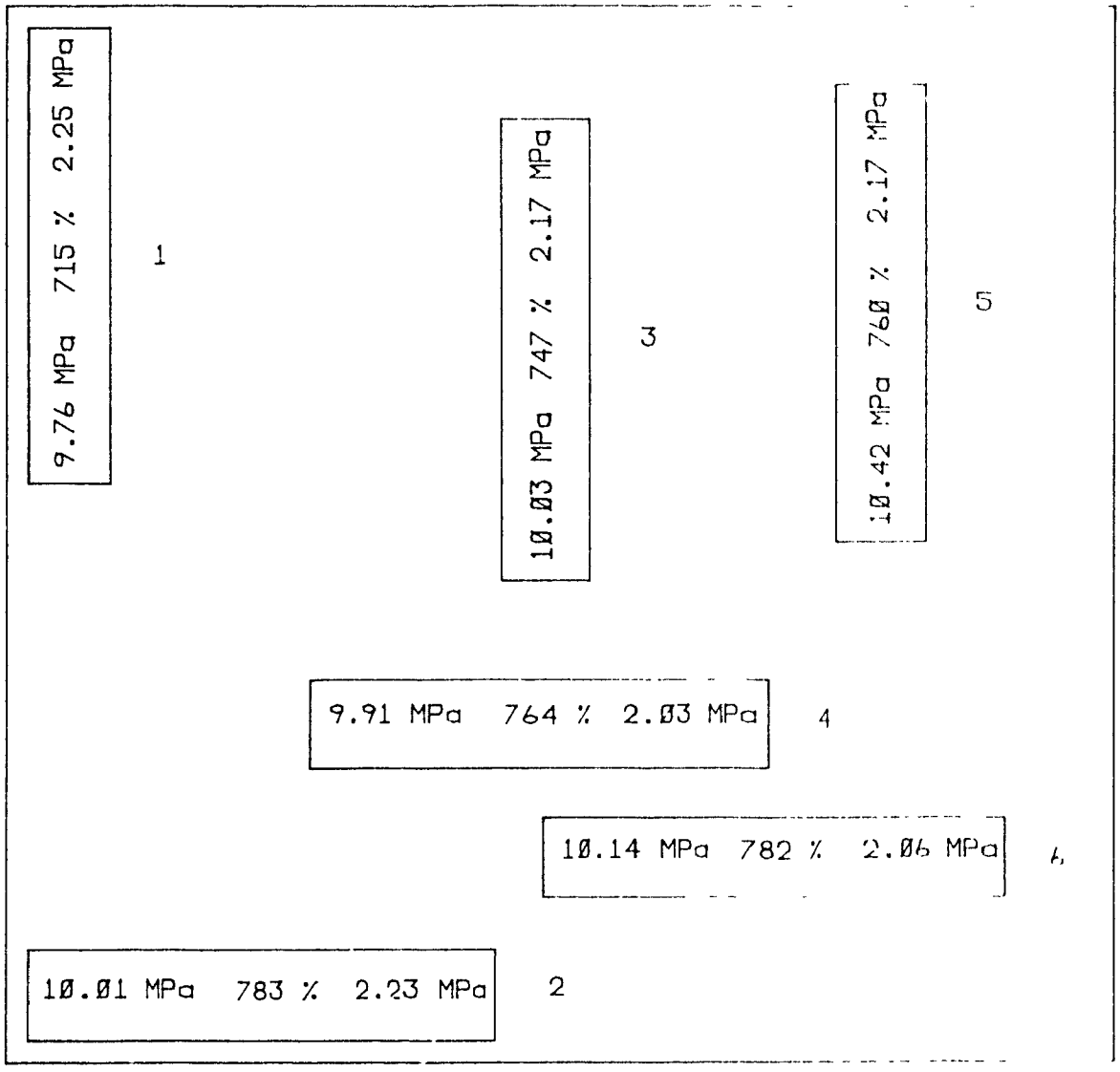

Figure 5.43. Tensile Test Results for Controlled Milling Samples Molded at 163°C.

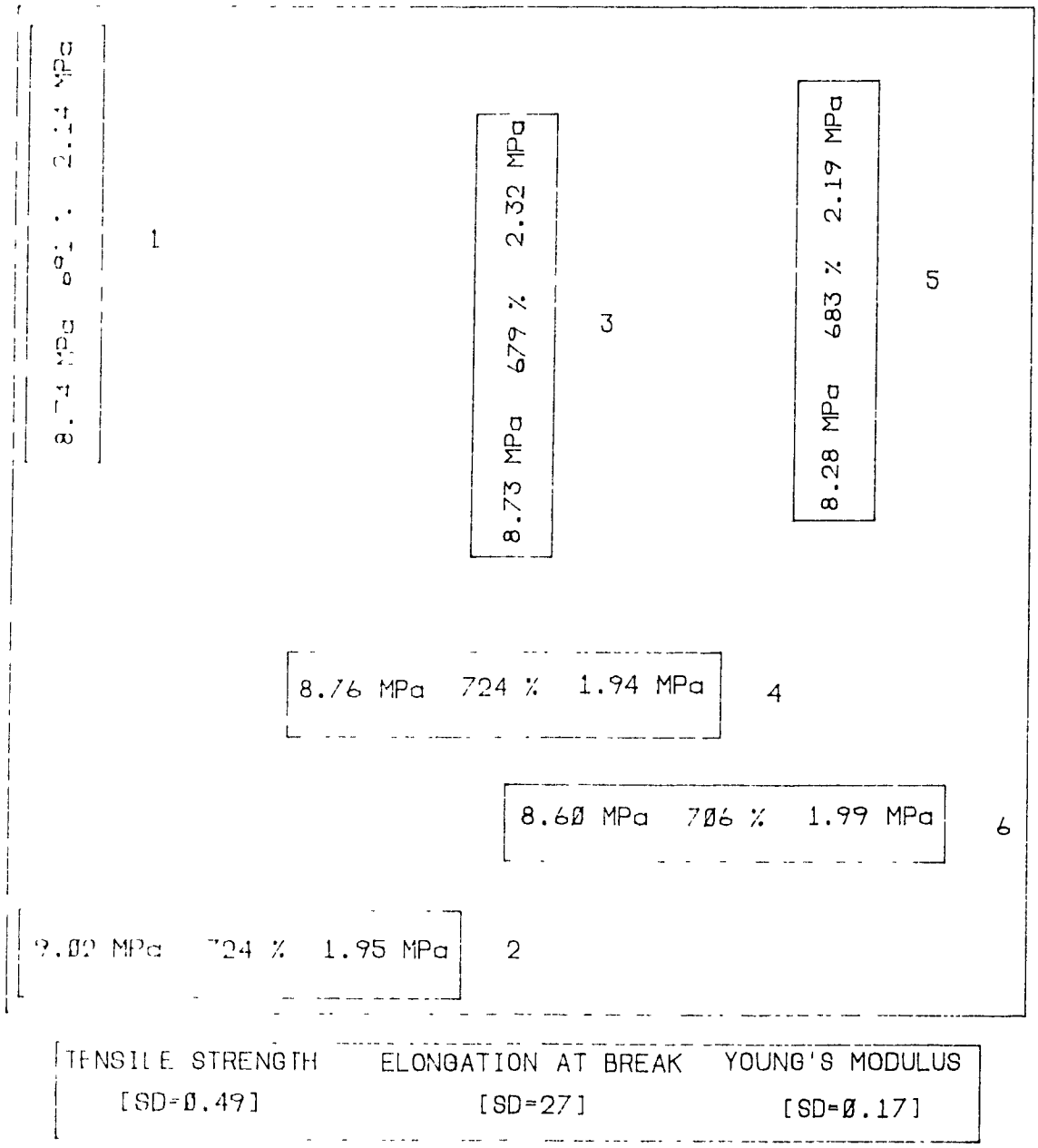

Figure 5.44. Tensile Test Results for Controlled Milling Samples Molded at 204°C.

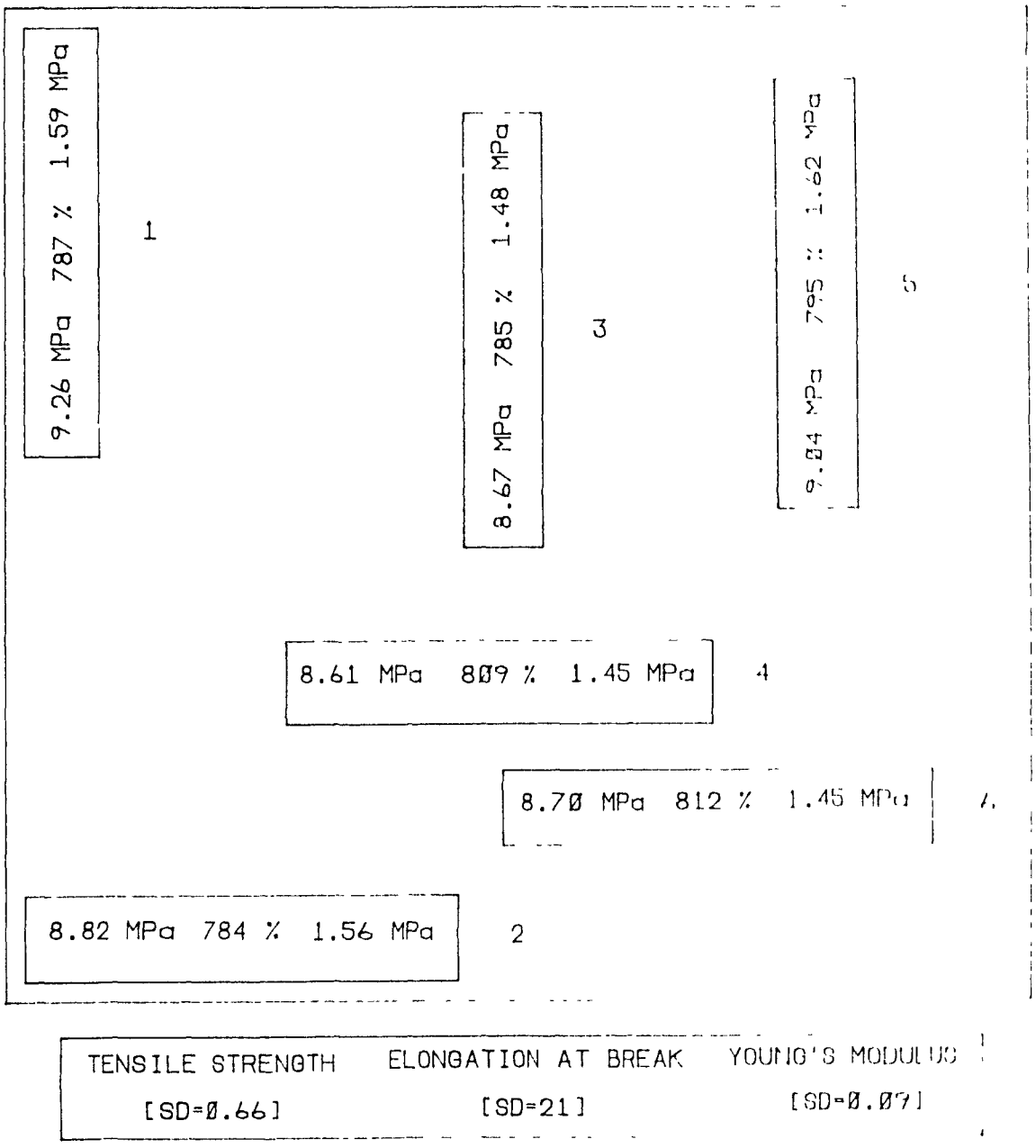

Figure 5.45. Tensile Test Results for Random Milling Samples Molded at 163°C.

technique had greater tensile strength and Young's modulus than those that were randomly milled. The tensile strength and Young's modulus attain their highest values when the fibers are oriented longitudinally, and the "controlled milling" process caused longitudinal fiber orientation. The elongation at break was not strongly affected by the milling procedure. These observations were seen at both molding temperatures.

5.2.3. Comparison Between Transfer and Compression Molding

The tensile strength and elongation at break were generally similar for all transfer molded samples and the compression molded samples with "controlled milling", at a molding temperature of 163°C. The Young's modulus was greater for the compression molded samples with "controlled milling", even when compared to the transfer molded locations with strong longitudinal orientation. The orientation results showed that the compression molded samples had a more uniform orientation from skin to core than the transfer molded samples. As well, the orientation in the compression molded samples with "controlled milling" was more homogeneous over the entire sample, whereas the orientation in the transfer molded plaques varied considerably throughout the sample. Therefore, the orientation was much more likely to be consistent from one end of the tensile test specimen to the other in the compression molded samples, and, for the samples with

"controlled milling", this orientation was longitudinal. The compression molded samples with "random milling" had modulus values similar to those found in the transfer molded locations with transverse fiber orientation. At 204°C, the trends were similar.

It is expected that the anisotropy in mechanical properties would be greater for transfer molded samples than compression molded samples due to the strong flow in the transfer molding process. A means of determining anisotropy is by comparing the longitudinal and transverse moduli within a sample (22). The ratio of the longitudinal Young's modulus to the transverse Young's modulus gives the anisotropy ratio.

Anisotropy ratios for compression and transfer molded samples were determined. For the compression molded samples, locations 1 and 2 were compared, as they are perpendicular to each other, as are locations 3 and 4, and 5 and 6. For the transfer molded samples, the fiber orientation results were used to determine the locations with longitudinal orientation (tensile specimens 4 and 7) and transverse orientation (tensile specimens 3, 5, and 6). These were then compared to each other. For both types of moldings, an overall average was found. The results are presented in Table 5.1.

The average ratios indicate that the anisotropy is greater for the transfer molded samples, as expected. It should be

Table 5.1. Anisotropy Ratios for Molded Samples.

Compression Molded Samples

Condition	1/2	3/4	5/6	Average
Controlled Milling, 163°C	1.01	1.07	1.05	1.04
Controlled Milling, 204°C	1.10	1.20	1.10	1.13
Random Milling, 163°C	1.01	1.07	1.12	1.05
Random Milling, 204°C	1.02	1.06	0.95	1.01

Transfer Molded Samples

Condition	4/3	7/5	4/6	Average
Converging Sprues, 163°C	1.33	1.19	1.43	1.32
Converging Sprues, 204°C	1.17	1.07	1.20	1.15
Diverging Sprues, 163°C	1.28	1.05	1.30	1.21
Diverging Sprues, 204°C	1.12	1.21	1.14	1.16
Straight Sprues, 163°C	1.27	1.19	1.22	1.23
Straight Sprues, 204°C	0.88	1.46	1.20	1.18

noted that while anisotropy did exist in the Young's moduli for the transfer molded samples, it was not substantial, especially when compared to short fiber reinforced composites, as shown in Table 1.2.

5.2.4. Comparison Between Experimental Data and Theoretical Predictions

The Halpin-Tsai equations are commonly used to predict the Young's modulus in the longitudinal and transverse directions for different types of reinforcement. Table 5.2 gives the Halpin-Tsai predictions for Young's modulus for continuous cords, particulate fillers, and short fibers, using the parameters found in the tested composite. The equation numbers correspond to those found in the Literature Review (Chapter 3). The predictions are then compared to the values obtained for the samples that were transfer molded with converging sprues at 163°C.

The results indicate that none of the equations adequately predicted the Young's modulus. As expected, the short fiber prediction is the best, but it still is not accurate. The assumptions made in the equation are that the fibers are well oriented in the test direction, have a uniform length, are regularly spaced, and are well bonded. In the composite, many of these criteria are not met. However, this would tend to cause the predicted result to be greater than the experimental

Table 5.2. Comparison Between Halpin-Tsai Modulus Predictions and Experimental Values.

Reinforcement	Fiber Orientation	Equation Number*	Modulus (MPa)
Continuous cord (Calculated)	L	1	3580
	T	2	0.88
Particulate filler (Calculated)	-	3	0.88
Short Fiber (Calculated)	L	4	1.05
	T	5	0.88
Franklin Fiber** (Experimental)	L	-	1.99
	T	-	1.50

L = Longitude direction
T = Transverse direction

* Refers to the numbers given the equations in the Literature Review (Chapter 3).

** Values taken from transfer molded samples (converging sprues, 163°C, tensile locations 4 and 3, respectively).

The following values were used in the equations:

$E_f = 1.79 \times 10^5$ MPa
$E_m = 0.83$ MPa
$\phi_f = 0.02$
$\phi_m = 0.98$
L/D = 6 (after molding)

value, instead of the opposite. The most likely reason that the theory does not accurately predict the modulus is the nature of the whisker reinforcement. Whiskers have superior strength properties, so that even a low volume fraction of fibers will still cause substantial modulus improvement. With short fibers, a much higher volume fraction is needed, so the equation underpredicts the modulus at the low fiber concentration used in this project. Therefore, a modified equation which would take into account the special properties of the whiskers would produce a more realistic prediction.

The Young's modulus of a sample with a known fiber orientation between 0 and 90° may be predicted by use of Equation (7). This equation was used to predict the Young's modulus of a transfer molded tensile specimen with a core orientation angle of -54° and a θ of 36°, where θ is the difference between the angle of the fibers and 90°. The results are shown in Table 5.3. This was the only location chosen for comparison because the others generally exhibited longitudinal or transverse fiber orientation. The predicted modulus is greater than the experimental value, due to the non-homogeneity of the fiber orientation. The composite must have unidirectional fiber orientation in order to obey Equation (7), and the orientation of the fibers in the molded composites used in this study was not unidirectional throughout the specimen. The variation in fiber orientation from skin to core resulted in an overprediction of the composite modulus by Equation (7).

Table 5.3. Prediction of Young's Modulus for Composite with Fiber Orientation Angle θ.

Tensile Test Specimen	Orientation Angle	θ	Predicted Mod (MPa)	Experimental Mod (MPa)
1	-54°	36°	1.79	1.63

The following values were used in the equation:

E_1 = 1.99 MPa
E_t 1.50 MPa

5.2.5. Effect of Franklin Fibers on Tensile Properties

The tensile properties of the unreinforced rubber are given in Table 4.1. When these are compared to the tensile results that have been reported, it can be seen that the addition of Franklin Fibers causes an increase in tensile strength and Young's modulus, without significantly influencing the elongation at break. The increase in Young's modulus is expected for fibrous reinforcement, but the increase in tensile strength and the behavior of the elongation at break are typical of the effects of particulate filler reinforcement. This suggests that whisker reinforcement acts as a combination of particulate filler and short fiber reinforcements. The above effects are observed at low fiber loadings.

5.3. Tensile Set Results

The tensile set is a measure of the elastic recovery of a material after enduring a constant strain. It is defined as:

$$\epsilon = \frac{L - L_0}{L_0} \qquad (9)$$

where L is the distance between bench marks after the sample has been stretched to a set elongation, held there for ten minutes, and then removed from the grips and relaxed for ten minutes. L_0 is the initial distance between bench marks. Bartlett's test was used to determine a single standard

deviation for each sample.

5.3.1. Transfer Molded Samples

The tensile set results for the samples molded with converging sprues at 163°C are presented in Figure 5.46. The lowest set values were found at locations 3, 5, and 6 where the fiber orientation is transverse. The highest values were at positions 2 and 4 where the fibers were oriented longitudinally. The set value will be zero for fully elastic recovery, therefore, the more elastic the material, the lower the set. When the fibers are longitudinally oriented, they control the deformation, and their effect on properties decreases as their orientation becomes more transverse (8). Also, when the fibers are oriented in the direction of the stress (longitudinal fiber orientation), they restrict the ability of the material to recover and return to its original configuration. Therefore, longitudinal fiber orientation results in a decrease in elasticity and an increase in tensile set. The results indicate lower set values at locations with transverse fiber orientation and higher set values at locations with longitudinal fiber orientation.

The results for samples molded at 204°C with converging sprues are shown in Figure 5.47. The results were similar to those found at 163°C. The values were generally higher at this temperature, due to the decreased efficiency in cross-linking.

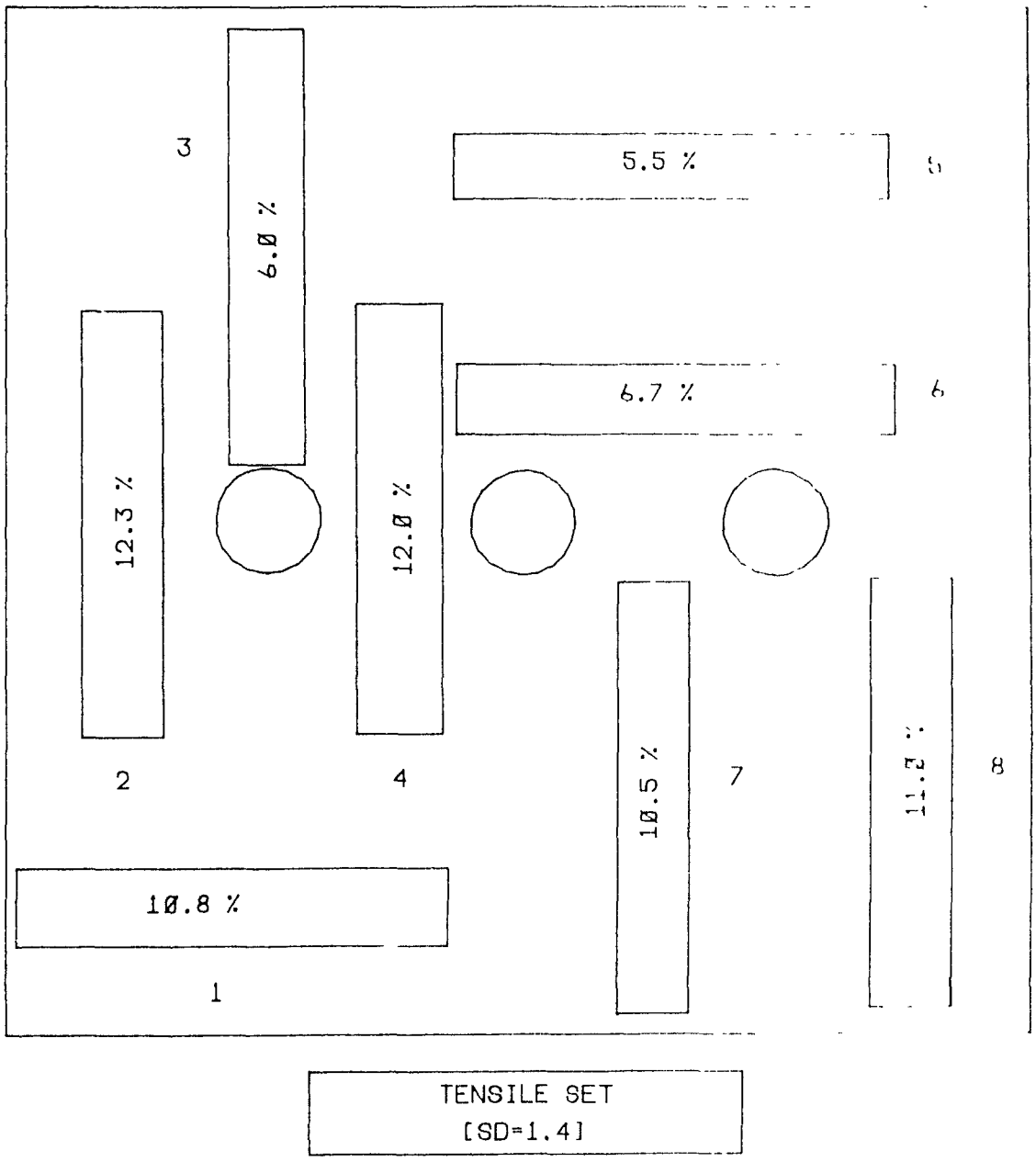

Figure 5.46. Tensile Set Results for Samples Molded with Converging Sprues at 163°C.

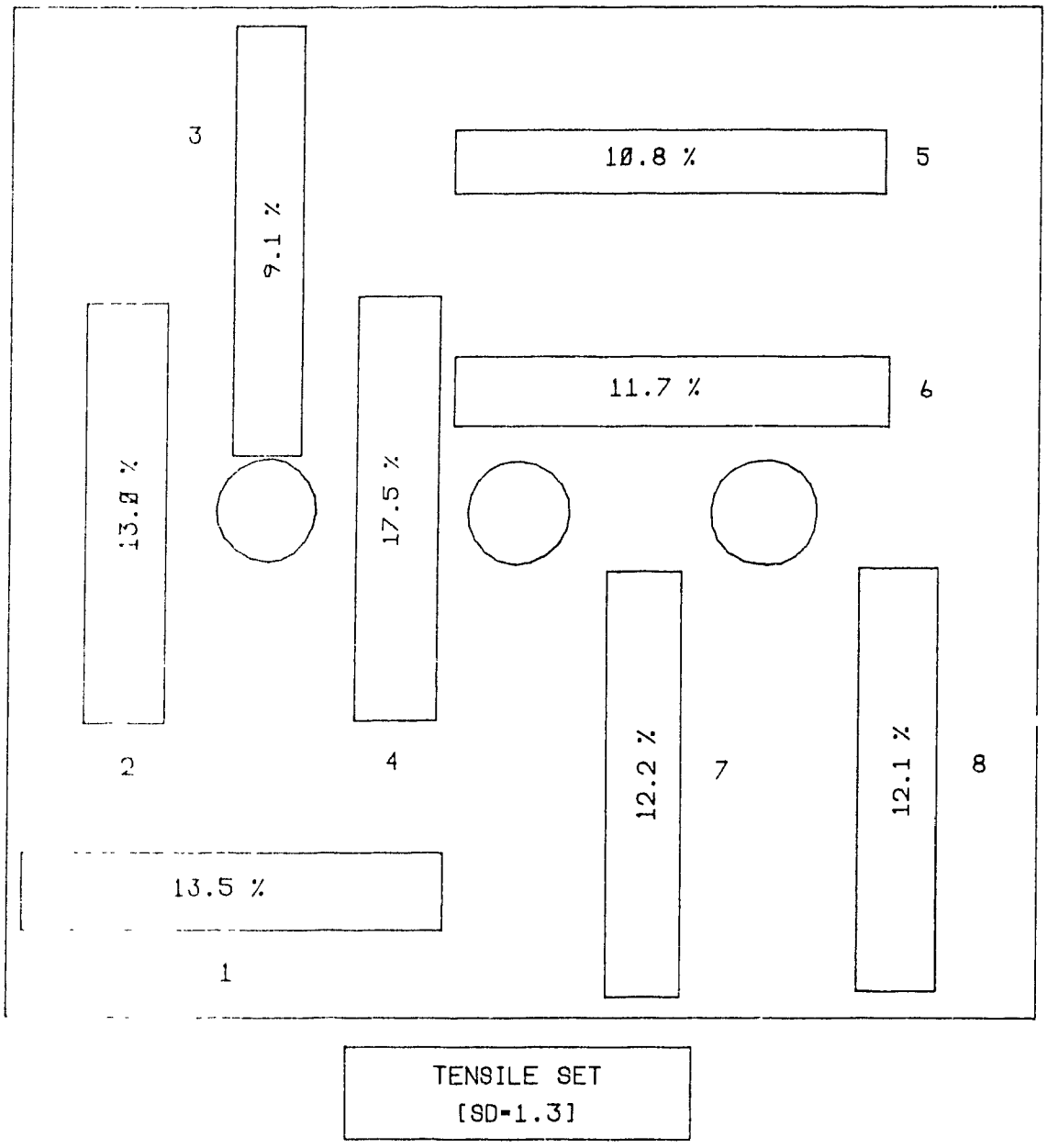

Figure 5.47. Tensile Set Results for Samples Molded with Converging Sprues at 204°C.

Figures 5.48 and 5.49 present the results for samples molded with straight sprues at 163°C and 204°C, respectively. The variation of set with orientation and temperature which was observed with converging sprues was also seen with straight sprues. A change in sprue design did not alter the orientation of the fibers; so, no variation in tensile set was achieved with a different sprue design.

5.3.2. Compression Molded Samples

The samples that were prepared with the "controlled milling" procedure and molded at 163°C showed some anisotropy in the tensile set, as shown in Figure 5.50. At 204°C, the anisotropy was reduced, as seen in Figure 5.51. The set values were higher at the higher molding temperature, as expected.

Figure 5.52 gives the results for the samples that underwent random milling and were molded at 163°C. The set values were lower than those found in the samples with controlled milling, due to the random orientation of the fibers.

5.3.3. Comparison Between Transfer and Compression Molding

The set values were more anisotropic for the transfer molded samples, due to the greater anisotropy in the fiber orientation. The highest set values were found for the

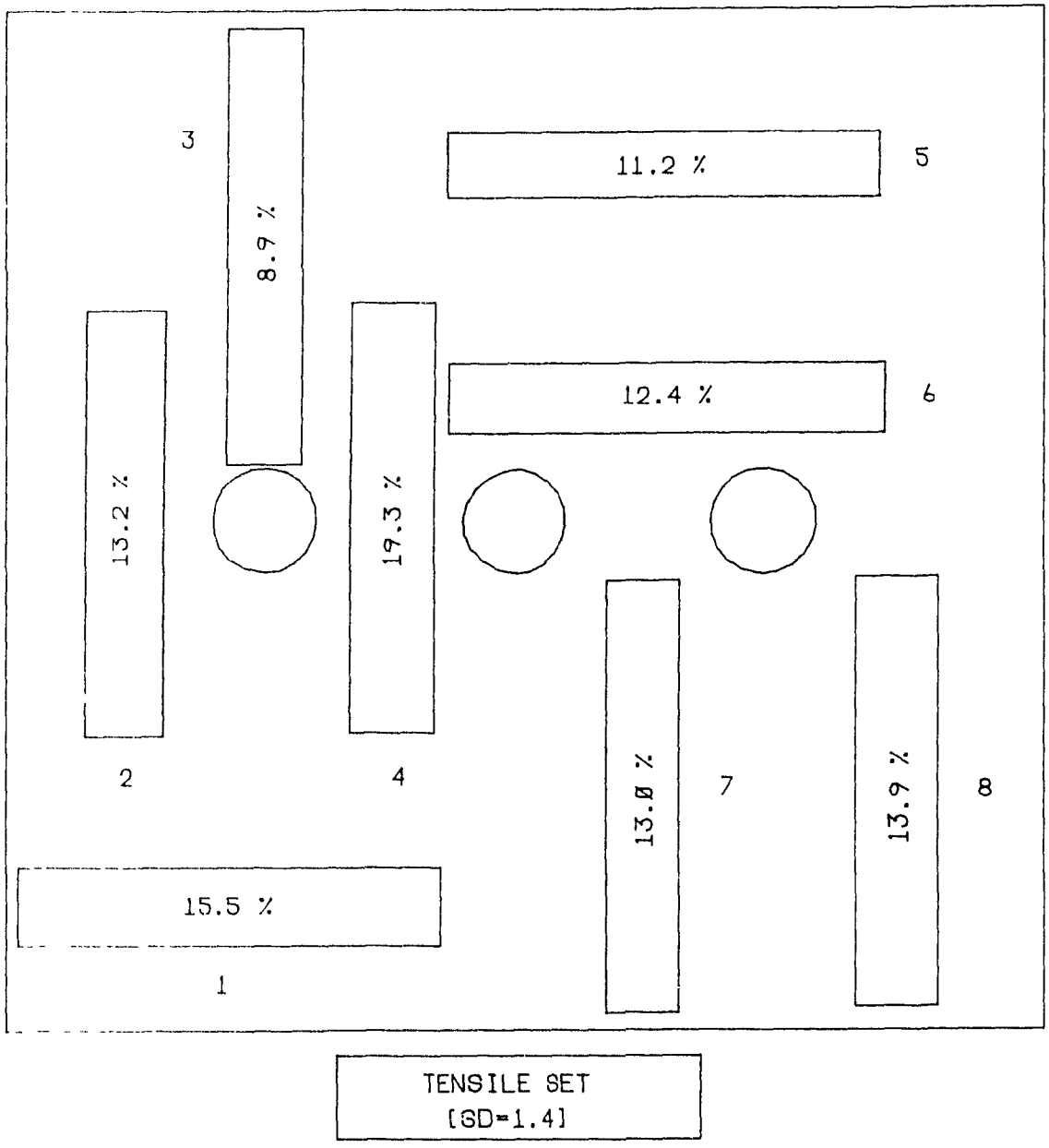

Figure 5.48. Tensile Set Results for Samples Molded with Straight Sprues at 163°C.

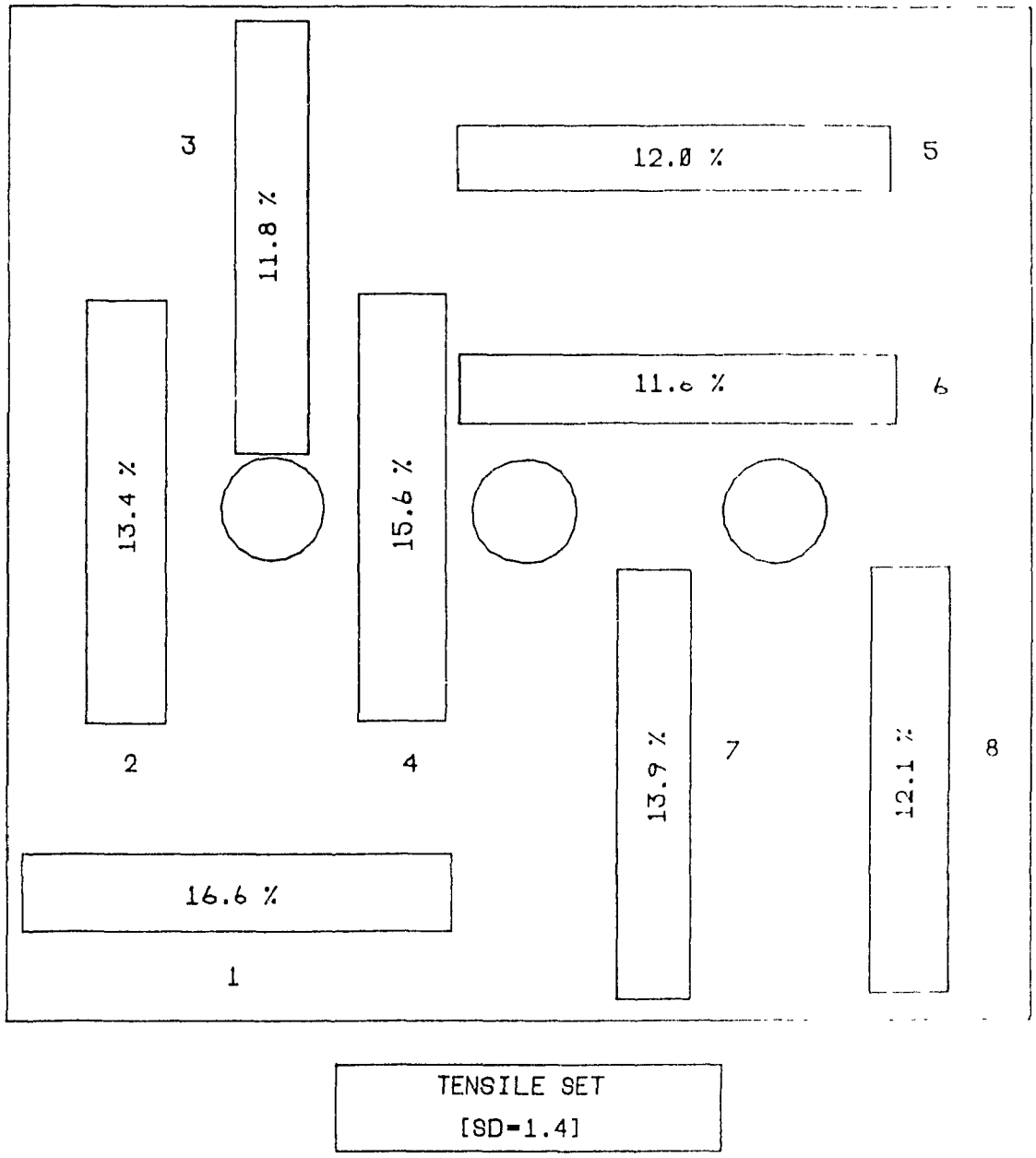

Figure 5.49. Tensile Set Results for Samples Molded with Straight Sprues at 204°C.

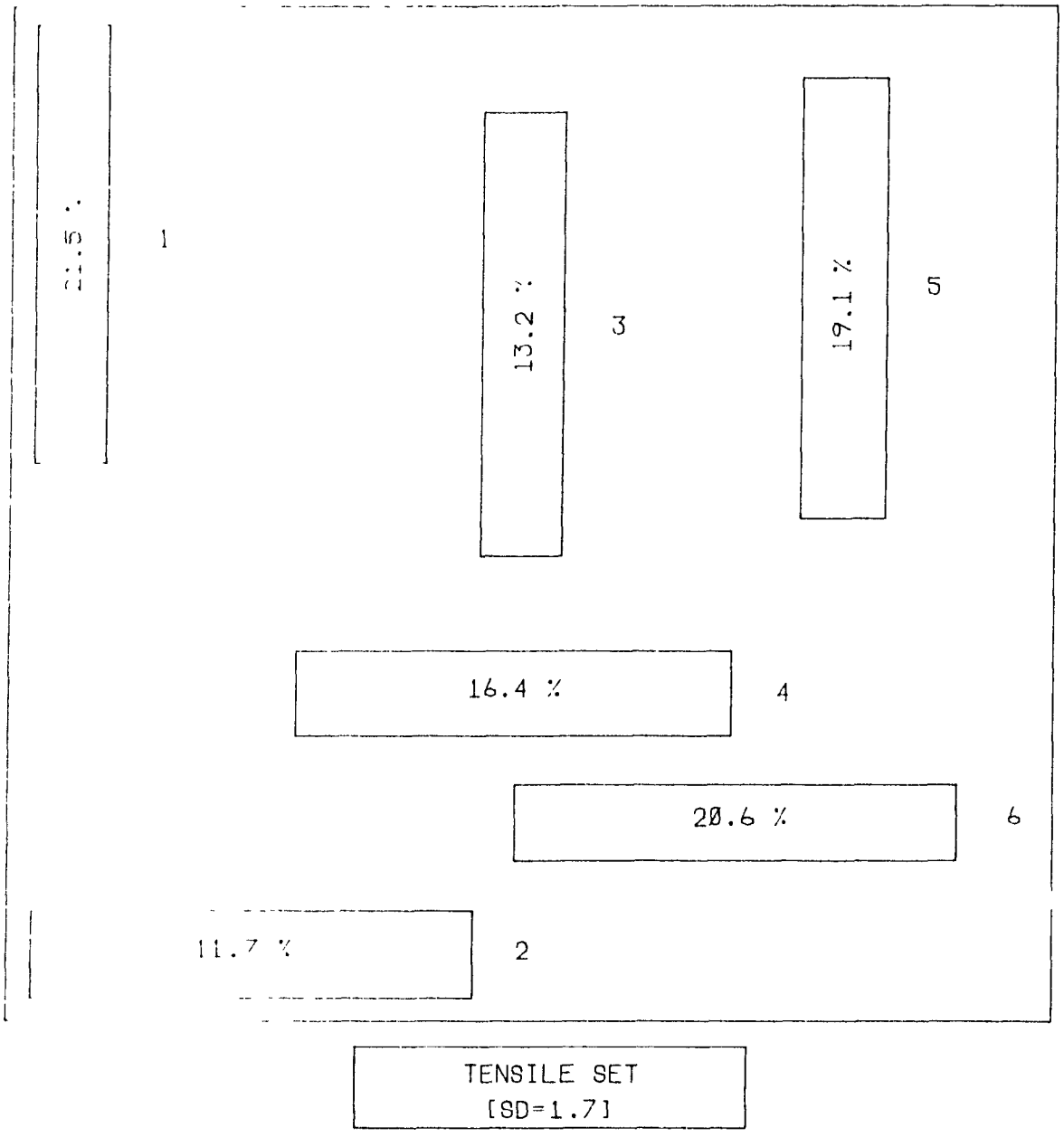

Figure 5.50. Tensile Set Results for Controlled Milling Samples Molded at 163°C.

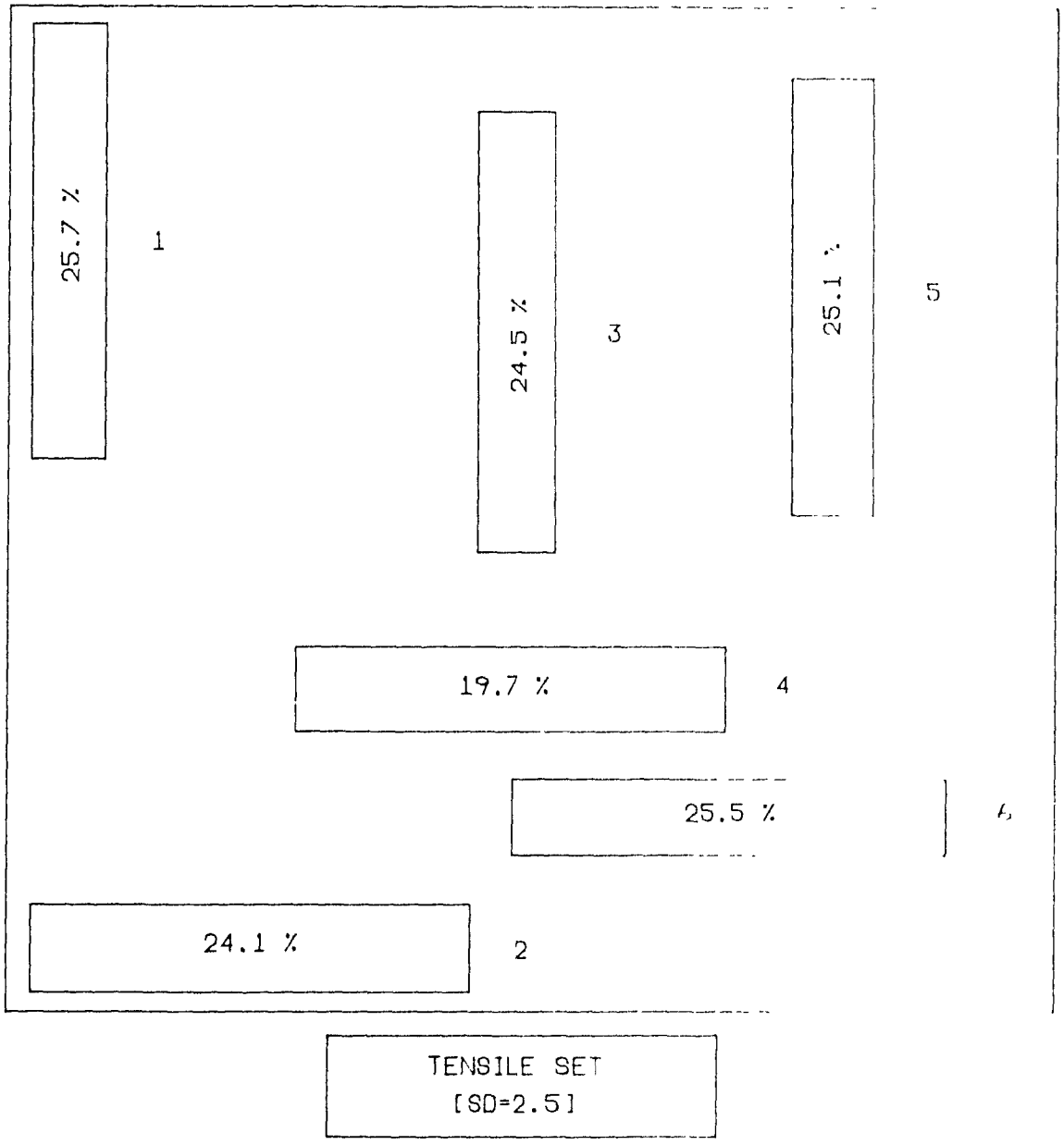

Figure 5.51. Tensile Set Results for Controlled Milling Samples Molded at 204°C.

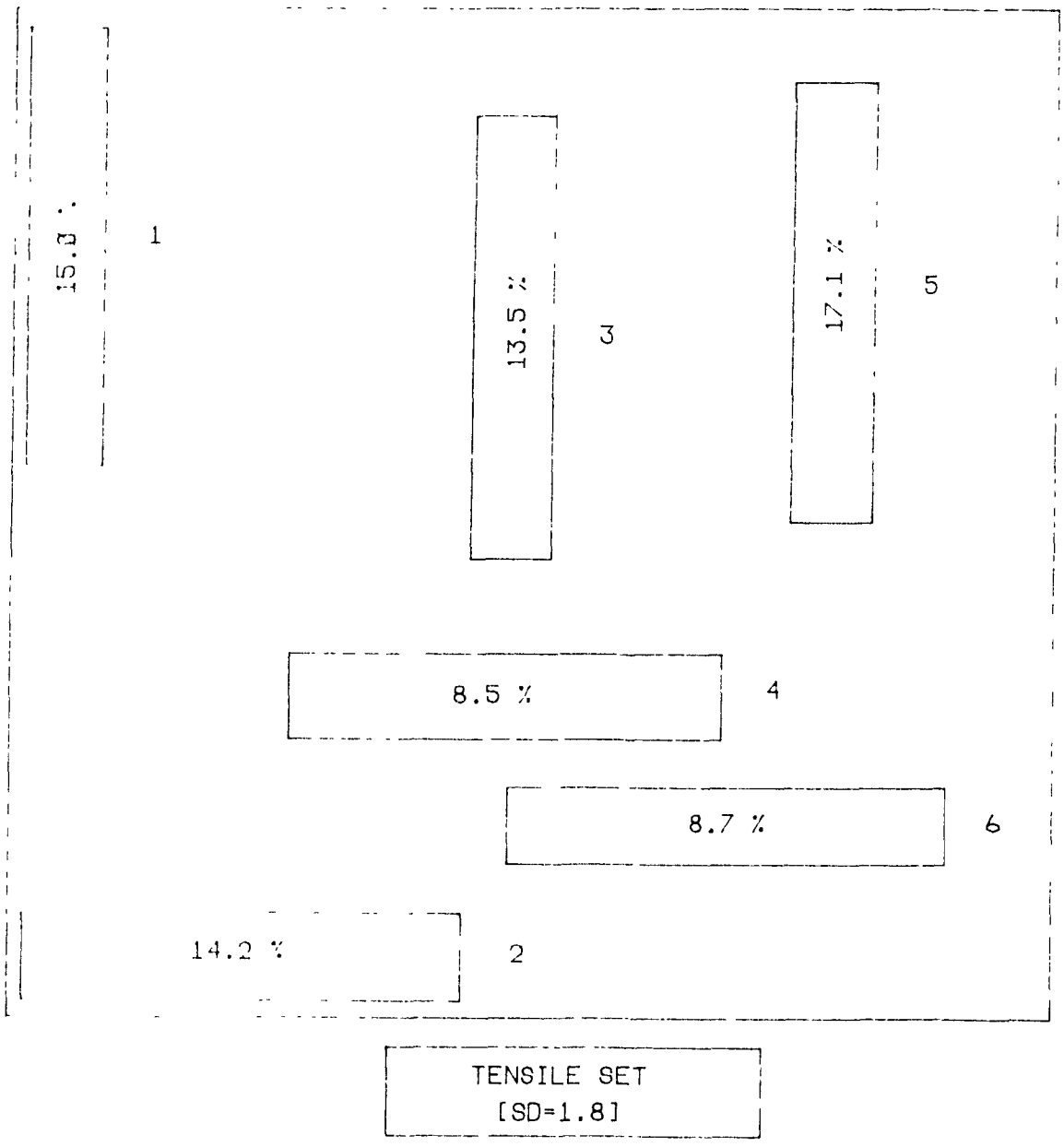

Figure 5.52. Tensile Set Results for Random Milling Samples Molded at 163°C.

compression molded samples with controlled milling which had uniform longitudinal fiber orientation. The tensile set was highly dependent on the fiber orientation. An increase in molding temperature caused an increase in the set for both molding procedures.

6. CONCLUSIONS AND RECOMMENDATIONS

6.1. Conclusions

This project has shown that whisker-reinforced silicone rubber composites can be molded using compression and transfer molding. It was also shown that manipulation of processing parameters provides a mechanism of controlling fiber orientation and tensile properties. An image analysis system, developed in the laboratory, was helpful in obtaining a rapid and accurate evaluation of the fiber orientation and length distributions in the samples.

The orientation of the fibers is anisotropic and non-homogeneous for the transfer molded samples. The fibers exhibit circumferential orientation at the core, regardless of sprue design or temperature. The milling procedure influenced the fiber orientation in the compression molded samples. The fiber orientation is anisotropic and homogeneous for the samples prepared with "controlled milling", regardless of temperature. The samples that were prepared with "random milling" yield random fiber orientation at both temperatures.

Significant fiber attrition occurred for both molding procedures. The initial fiber length of 30 microns was reduced to a final length of approximately 12 microns. The 12 micron average length was found in all samples, regardless

of molding procedure or milling technique. This suggests that the initial mixing of the fibers was responsible for the severe fiber breakage.

The tensile strength and elongation at break are isotropic for the transfer molded samples and are independent of sprue design. The Young's modulus is anisotropic, and is greatest at locations with longitudinal fiber orientation. The compression molded samples with "controlled milling" exhibit greater tensile strength and Young's modulus than those with "random milling". All tensile properties are homogeneous and isotropic within the compression molded samples. An increase in molding temperature causes a decrease in strength and elongation for all molded samples. The Young's modulus is not affected by an increase in temperature. The compression molded samples with "controlled milling" have the greatest Young's moduli due to their homogeneous longitudinal fiber orientation. Differences in the state of cure may occur at an increased mold temperature for the transfer molded samples. The tensile set is sensitive to fiber orientation and temperature, for all molded samples.

The Halpin-Tsai equations do not accurately predict the Young's modulus of the composites. This is due to the inherent differences in dimensions and properties between whiskers and other forms of reinforcement. Substantial modulus improvement may be realized with whisker reinforcement

at a much lower volume fraction than is required with short fiber or particulate reinforcement. Theoretical predictions for the Young's modulus of a composite with the fibers oriented at an angle between 0 and 90° do not agree with the experimental results due to the non-homogeneity of the fiber orientation within the samples.

6.2. Recommendations for Future Work

The fiber loading used in this project was very low, and may not have given optimum property improvement. Using several different fiber loadings would increase the understanding of how fiber concentration affects mechanical properties and would allow the user of this composite to find the optimum fiber loading to obtain the desired property values.

It would be helpful to change the design of the transfer molding operation so that the mold is placed vertically below the sprue. This might cause more uniform fiber orientation. The three different sprue designs could then be compared to see what type of fiber orientation resulted.

The amount of peroxide curing agent was kept constant in the samples, even when the curing temperature was changed. It would be useful to change the amount of peroxide to see if this effects the properties.

It would be of interest to determine the manner in which the composites failed in tension. This could be achieved by viewing the fractured tensile specimens with a scanning electron microscope. An analysis of the mode of failure of the composites would aid in determining the effect of the reinforcement.

Some discrepancies occurred in the high temperature transfer molding, perhaps due to differences in cure from location to location. It would be useful to do a complete study of the state of cure throughout the sample to verify this. As well, a dynamic mechanical analysis of the composite may be helpful in developing a broader understanding of the Franklin Fiber-silicone rubber system.

REFERENCES

1. P.J. Flory, Principles of Polymer Chemistry, Cornell University Press, Ithaca, New York, 1971, Chap. 11.

2. H.S.-Y. Hsich, R.J. Ambrose, Injection and Compression Molding Technology of Elastomers, Marcel Dekker Inc., New York, New York, 1987, Chap. 5.

3. E.L. Warrick, O.R. Pierce, K.E. Polmanteer, J.C. Saam, Rubber Chem. Technol., 52, 437 (1979).

4. M.G. Noble, Vanderbilt Rubber Handbook, R.T. Vanderbilt Corp., 1978, 216.

5. P.K. Pal, S.K. De, Rubber Chem. Technol., 55, 1370 (1982).

6. D.K. Setua, S.K. De, Rubber Chem. Technol., 56, 808 (1983).

7. L.A. Goettler, K.S. Shen, Rubber Chem. Technol., 56, 619 (1983).

8. L.A. Goettler, Handbook of Elastomers, Marcel Dekker Inc., New York, New York, 1988, Chap. 7.

9. J.C. Halpin, J. Comp. Mater., 3, 732 (1969).

10. S. Abrate, Rubber Chem. Technol., 59, 384 (1986).

11. Specifications from United States Gypsum Company, Chicago, Illinois.

12. J. Menough, Rubber World, 192 (1), 14 (1985).

13. S.R. Moghe, Rubber Chem. Technol., 49, 1160 (1976).

14. E.A. Dyzura, A.L. Serebro, N.D. Kiryushina, Int. Polym. Sci. and Technol., 13 (3), 8 (1986).

15. C.L. Tucker, Injection and Compression Molding Technology of Elastomers, Marcel Dekker Inc., New York, New York, 1987, Chap. 7.

16. A.I. Isayev, A.D. Azari, Rubber Chem. Technol., 59, 868 (1986).

17. M.A. Wheelans, Rubber Chem. Technol., 51, 1023 (1978).

18. L.A. Goettler, R.I. Leib, A.J. Lambright, Rubber Chem. Tecnnol., 52, 838 (1979).

19. A.Y. Coran, K. Boustany, P. Hamed, Rubber Chem. Technol., 47, 396 (1974).

20. J.E. O'Conner, Rubber Chem. Technol., 50, 945 (1977).

21. A.Y. Coran, K. Boustany, P.Hamed, J. Appl. Polymer Sci., 15, 2471 (1971).

22. P.C. Li, L.A. Goettler, P. Hamed, J. Elastomers and Plastics, 10, 59 (1978).

23. W.W. Paris, J.R. Dillhoefer, W.C. Woods, Rubber Chem. Technol., 55, 494 (1982).

24. Results of testing performed by the Lord Corporation, Cary, North Carolina.

25. M.J. Bozarth, J.W. Gillespie, Jr., R.L. McCullough, Polymer Composites, 8 (2), 74 (1987).